USAAVLABS TECHNICAL REPORT 65-51

ANALYSIS AND CORRELATION OF HELICOPTER ROTOR BLADE RESPONSE IN A VARIABLE INFLOW ENVIRONMENT

Ser-50405

By

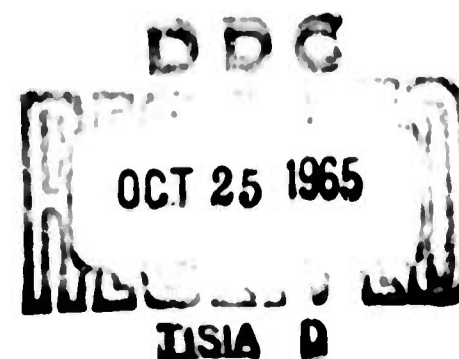R. G. Carlson
K. D. Hilzinger

September 1965

U. S. ARMY AVIATION MATERIEL LABORATORIES
FORT EUSTIS, VIRGINIA

CONTRACT DA 44-177-AMC-87(T)

SIKORSKY AIRCRAFT DIVISION
UNITED AIRCRAFT CORPORATION

BLANK PAGES
IN THIS
DOCUMENT
WERE NOT
FILMED

This report has been reviewed by the US Army Aviation Materiel Laboratories and is considered to be technically sound. The report is published for the exchange of information and the stimulation of ideas.

ANALYSIS AND CORRELATION OF
HELICOPTER ROTOR BLADE
RESPONSE IN A VARIABLE
INFLOW ENVIRONMENT

SER-50405

by

R. G. Carlson
K. D. Hilzinger

Prepared by
Sikorsky Aircraft Division
United Aircraft Corporation
Stratford, Connecticut

for

U. S. ARMY AVIATION MATERIEL LABORATORIES
FORT EUSTIS, VIRGINIA

SUMMARY

An investigation was undertaken to determine the extent to which presently available analytical methods can be used to evaluate rotor blade air loads and helicopter rotor dynamic response. The Cornell Aeronautical Laboratory (CAL) variable inflow analysis developed under Contract DA 44-177-TC-198 was combined with the Sikorsky blade aeroelastic analysis. Appropriate trim conditions were developed and used to apply the combined analysis to the H-34 and HU-1A aircraft. Extensive test data have been obtained for these aircraft. These data were used for a correlation study to evaluate the accuracy of the analysis. Flight conditions considered were steady-state level flight at airspeeds up to 113 knots.

This correlation study showed that the combined analysis gave significant improvement in accuracy over previous analytical techniques using constant inflow. The definition of higher harmonic participation, notably the blade root-shear forces making up the airframe excitation, was substantially better than that obtained using constant inflow. In general, the improvement in correlation of air loads and moments was greater at low airspeeds than at higher airspeeds where variable inflow has less effect. The variable inflow analysis did not produce peak-to-peak stress values matching the good correlation obtained using a constant inflow analysis at the high speed conditions used for blade design. Although fairly good correlation with test data was obtained, further improvement can be made. The most significant area for improvement appears to be in air-load definition, particularly in inflow definition. A further refined inflow analysis combined with the Sikorsky aeroelastic analysis should provide improved air loads and moment values.

The analysis proved to be readily applicable to both the HU-1A and H-34 aircraft. In addition, the analysis is finding application in the design of future aircraft now under consideration.

FOREWORD

CONTENTS

ILLUSTRATIONS

SYMBOLS

A Aerodynamic load, lb, inch-lb

A_O Collective pitch, deg

A_1 Cosine component of cyclic pitch, deg

a_k Lift curve slope

a_{nn} Thrust moment matrix coefficient, inch-lb/deg

B_1 Sine component of cyclic pitch, deg

b Number of blades

b_k Blade semi-chord, in

$b(\psi)$ Intercept of thrust moment blade pitch azimuth line, inch-lb

C Blade chord, in

C_O Section drag coefficient

C_L Section lift coefficient

C_M Section pitching moment coefficient

C_N Lag damper coefficient, lb-in sec/radian

C_{nq} Element of aerodynamic damping matrix, lb sec/in

D Blade drag, lb

e Blade offset, in

E Modulus of elasticity, lb/in^2

E_n Cosine component of edgewise bending slope, radian

F_o Applied force, lb

F_n Sine component of edgewise bending slope, radian

F_z Steady vertical hub force, lb

gw   Aircraft gross weight, lb

i   Blade radial station

I   Area moment of inertia, in^4

I_k Blade plunging motion, in/sec

L   Length of beam, blade lift, in, lb

L_{Fus} Lift of fuselage, lb

L_{rotor} Rotor drag vertical component, lb

$m(\psi)$ Slope of thrust moment blade pitch line, inch-lb/deg

$M_n{}^E$ Cosine component of edgewise bending moment, inch-lb

$\overline{M}_n{}^E$ Sine component of edgewise bending moment, inch-lb

M_{xx} Steady hub rolling moment, inch-lb

M_{yy} Steady hub pitching moment, inch-lb

n   Harmonic of revolution

P   Number of mode

PM   Blade aerodynamic pitching moment, inch-lb

q   Harmonic of flapping velocity

r   Blade segment radial location, in

R	Rotor radius, in
$S_0{}^E$	Steady edgewise root shear, lb
$S_0{}^F$	Steady flatwise root shear, lb
$S_1{}^F$	First harmonic cosine flatwise root shear, lb
$\bar{S}_1{}^F$	First harmonic sine flatwise root shear, lb
t	Time, sec
TM_0	Steady thrust moment, inch-lb
TM_1	First harmonic cosine component of thrust moment, inch-lb
$\widehat{TM}_1$	First harmonic sine component of thrust moment, inch-lb
U_p	Normal component of blade segment total velocity, in/sec
$(v_q)_i$	Harmonic of blade segment velocity, in/sec
V	Forward speed, in/sec
V_i	Rotor induced velocity, in/sec
$\bar{x}$	Radial location of resultant thrust vector, in
$(y_q)_i$	Blade displacement, in
α	Blade section angle of attack, deg
α_t	Angle of tip path plane, deg
α_s	Shaft inclination, deg
β	Flapping angular velocity, radians/sec
β_0	Steady coning, radians
Γ	Bound circulation, in^2/sec

$\theta(\psi)$ Blade impressed control angle at azimuth ψ, deg

ζ Blade edgewise slope, deg

σ Wake geometric coefficient, $^1/\text{in}$

ψ Azimuth position, deg

Ω Rotor angular velocity, radian/sec

$\Delta(\ )$ Change in parameter indicated

$(\ )^S$ Sine component

$(\ )^C$ Cosine component

$(\ )^R$ Real part

$(\ )^I$ Imaginary part

INTRODUCTION

There is a real need in the helicopter industry for an aeroelastic analysis capable of predicting accurately the dynamic behavior of a rotor system. Such an analysis is necessary to give the industry a reliable method with which to evaluate and refine blade designs. This research program for a "Coordinated Aeroelastic Research Program for Helicopter Rotor Systems" was undertaken for the United States Army Aviation Materiel Laboratories under Contract No. DA 44-177-AMC-87(T) to determine to what extent the dynamic behavior of a rotor can be predicted by application of analytical methods presently available. A variable inflow analysis, developed by Cornell Aeronautical Laboratories (CAL) to give better definition of rotor inflow, was combined with the Sikorsky Aircraft aeroelastic analysis, suitably modified to accept variable inflow and to incorporate additional improvements. This analysis is a fully coupled flatwise-edgewise-torsional analysis based on an extension of Myklestad's method for rotating beams. The availability of both air-load and blade moment data from flight tests of both the H-34 and HU-1A aircraft (References 1, 6, 9, and 10) provided a basis for correlation of the analytical results. Since these two aircraft have significantly different rotor systems, both aircraft were considered in order to demonstrate the ability of the analysis to evaluate varied types of rotors and to obtain comparative data for correlation of different rotors.

This report contains the results of this program. The validity of the modified Myklestad analysis, which forms the basis of the Sikorsky aeroelastic analysis. is first substantiated. The procedures required to carry out this aeroelastic analysis, the method of incorporating the variable inflow analysis, and the modifications made to the analysis are then explained. Results are given for a study of flight test data to determine what parameters are important in the analysis, and to determine what flight conditions should be used as a basis for evaluating the analysis. Comparisons between test data and the analysis for these cases are presented. Several additional modifications are made to the analysis in an attempt to provide improved air-load definition through the introduction of additional flexibility

effects in the calculations. The effects of these modifications are presented. These results are analyzed to evaluate the ability of the analytical procedure to predict dynamic response and to provide recommendations for further improvements.

SUBSTANTIATION OF METHODS

A. BACKGROUND OF ANALYSIS

Results of earlier correlation studies for the Sikorsky blade aeroelastic analysis have been discussed in References 5, 11, and 12. Comparisons of analysis (using constant inflow) with flight test data indicated that calculated performance and one-half peak-to-peak flatwise blade stresses gave good agreement with flight measured values at higher airspeeds. Satisfactory correlation was achieved for both articulated rotor helicopters (Sikorsky H-34 and S-61) and rigid-rotor helicopters (Lockheed CL-475). However, it was also found that the assumption of constant induced velocity imposed serious limitations on the analysis. Reference 4 concluded that better definition of induced velocity was required in order to: (1) predict higher harmonic air loads and blade stresses with greater accuracy at all airspeeds; (2) correlate one-half peak-to-peak blade stresses below 100 knots; and (3) determine analytically inflight fuselage vibration levels at all airspeeds.

Under this program, CAL's variable inflow analysis (Reference 3) has been combined with the Sikorsky aeroelastic analysis (References 5 and 12) to provide better definition of induced velocity and associated higher harmonic air loads. The question that remained for substantiation was whether the method of blade analysis would now adequately define higher harmonic blade bending moments and shears corresponding to these higher harmonic air loads. To provide this substantiation, Sikorsky Aircraft proposed to demonstrate adequacy of the present blade analysis method by comparing responses of the uncoupled non-rotating analysis with deflections, slopes, moments, and shears as determined by an independent closed-form analytic solution for sinusoidal inputs. Selection of a nonrotating beam analysis for substantiation was based upon the following:

1. There was no known closed-form exact solution for predicting the vibratory response of a rotating beam.

2. A nonrotating beam comparison would place greater demands on the Sikorsky blade analysis method, since higher harmonic forced response at a particular

3

frequency requires participation of a greater number of modes than for the corresponding rotating beam case.

The problems of predicting the higher frequency response of a rotating beam were recognized early by Sikorsky Aircraft in the development of the Sikorsky blade aeroelastic analysis. The decision was made to use a method based upon direct inverse solution of the blade dynamic equations, rather than a normal mode type solution. This provides the advantage of full participation of the higher modes(to as many degrees-of-freedom as considered), in contrast to a method which considers only limited mode participation. The normal mode approach does offer certain advantages of simplification of the mathematical formulation which can result in savings in computer time. However, for accuracy the direct solution approach, used by Sikorsky Aircraft in this study, should equal or surpass the normal mode approach.

B.   ANALYTICAL COMPARISON OF METHODS

A test problem was set up for determining the adequacy of the present Sikorsky blade analysis method for predicting higher harmonic blade response. A uniform pinned-free beam with mass, stiffness and length properties which approximate those of the H-34 main rotor blade was chosen. The beam is subjected to uniformly distributed oscillatory loadings at frequencies of one per rev [203 cycles per minute (cpm)] , six per rev (1218 cpm), and eleven per rev (2233 cpm). Objective of the analysis is to compare responses of the uncoupled nonrotating Sikorsky blade analysis with corresponding deflections, slopes, moments, and shears as determined by an independent closed-form analytic solution.

The independent closed-form analytic solution, Appendix I, was derived from the classical Bernoulli-Euler nonhomogeneous differential equation for transverse vibration of a nonrotating beam. Solution of the equation gave resulting steady-state harmonic deflections, slopes, moments, and shears for the uniformly loaded pinned-free beam.

4

Independent closed-form equations (45), (46), (47), and (48) were next programmed for the IBM 7090 computer. Solutions were obtained for p = 203, 1218, and 2233 cpm.

For comparison, the Sikorsky blade aeroelastic analysis was run in the computer with identical input under corresponding nonrotating conditions. Here, Ω (rotor angular velocity) was made equal to zero, as was blade twist in order to decouple flatwise and edgewise motions. In contrast to a closed-form solution, the blade for the aeroelastic analysis may not be treated as a continuous structure but must be subdivided into discrete segments. Twenty-four blade segments were selected.

Results of the comparison are presented in Figures 1 and 2, which give plots of dynamic response of the blade as determined by both analyses. Shown are resulting deflections, moments, and shears for sinusoidal unit-load excitation at frequencies of 203, and 2233 cpm respectively. The first five modes for the nonrotating beam have natural frequencies of 153, 496, 1040, 1765, and 2700 cpm. These are helpful in the following discussion and interpretation of results.

Response of the beam to 1/rev. excitation (203 cpm) is shown in Figure 1. This frequency is about 50 cpm above the first bending mode, about 300 cpm below the second mode. As expected, the deflection curve is first mode in character. Close agreement is noted between analyses for resulting steady-state harmonic response of deflections, moments, and shears.

High frequency or eleven per rev (2233 cpm) vibratory response is plotted in Figure 2. In this case frequency of response is bounded by the fourth mode at 1765 cpm and the fifth mode at 2700 cpm. The resulting deflection response curve exhibits some degree of fifth-modal response. For this case, good agreement was also noted between the two analyses, not only for deflections but for higher derivative bending moments and shears as well.

Similar correlation was found for an excitation frequency of 1218 cpm. The results show that the analysis is capable of

5
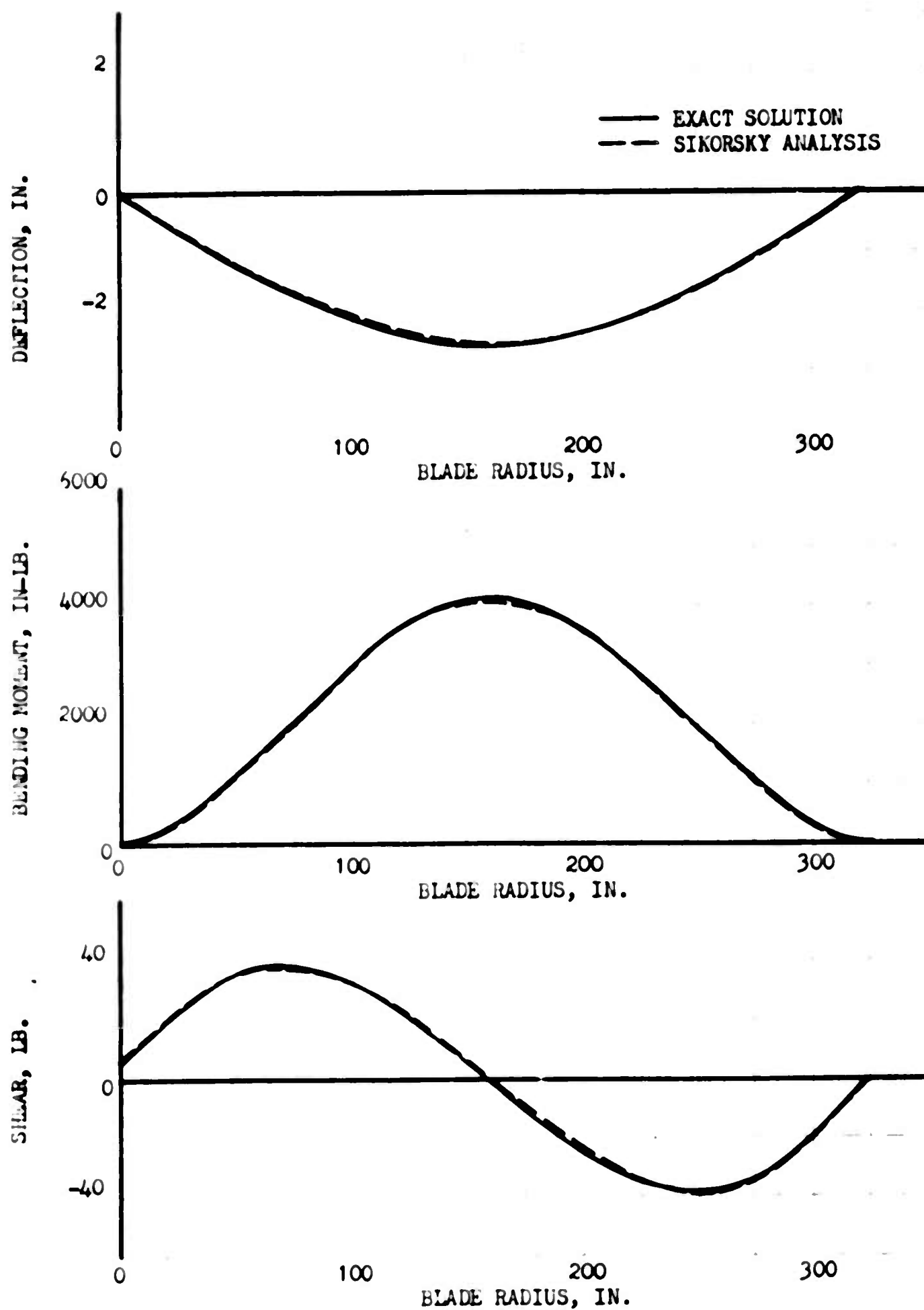
FIGURE 1. COMPARISON OF SIKORSKY BLADE ANALYSIS
WITH EXACT SOLUTION FOR A NONROTATING BEAM.
203 CYCLES PER MINUTE EXCITATION FREQUENCY.

6
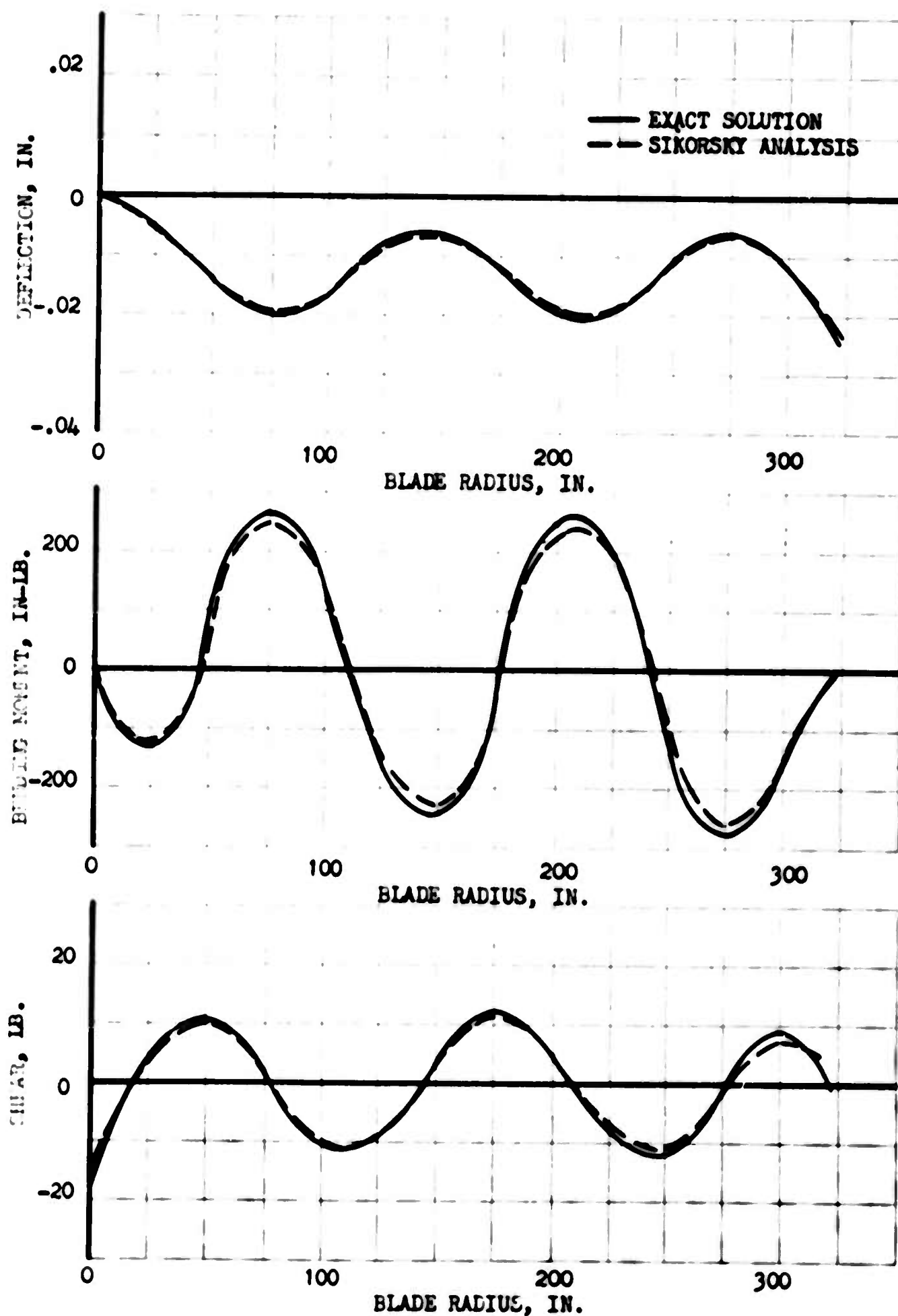
FIGURE 2. COMPARISON OF SIKORSKY BLADE ANALYSIS
WITH EXACT SOLUTION FOR A NONROTATING BEAM.
1233 CYCLES PER MINUTE EXCITATION FREQUENCY.

7

giving an accurate definition of blade dynamic behavior.

ESTABLISHMENT OF ROTOR PARAMETERS AND

FUSELAGE TRIM CONDITIONS

A study was made of the available data to determine what parameters affected the dynamic response most significantly, how the program should be modified to incorporate these parameters, and exactly what flight conditions should be evaluated to determine the validity of the assumptions made. Results from extensive use of the Sikorsky aeroelastic analysis as well as flight test data were used to determine what parameters and modifications should be considered.

The flight test data available for the H-34 and HU-1A aircraft (References 1, 6, 9, and 10) were an important source of information for the study. These data served to establish the importance of a number of parameters, and also as the standard with which analytical results could be compared. Perhaps in this regard, too much may be expected of the data. The general signature of the variation of the air load, moment, and other measurements with azimuth are probably given accurately by the test data. However, the test data used were not corrected for dynamic effects. The resolution and accuracy of the in strumentation and the data recording, reading, and reduction methods used may introduce some error. Therefore, exact correlation with test data is not necessarily the desired goal. However, any substantial deviation between analysis and test would indicate inadequacies in the analytical procedure.

There were several areas in which significant modifications to the Sikorsky analysis (References 5 and 12) were required. These modifications include a more realistic method for obtaining the hub forces and moment required for trim and more accurate damping coefficients to reflect nonlinear damping rates. These are described elsewhere in this report.

The original method used for trimming the rotor to give the proper hub moments and force involved the use of thrust

moments which are the moments of the blade thrust about the flapping axis. The steady and first harmonic components must balance the steady hub force and steady hub moment. This procedure locates the center of pressure on the rotor system correctly, but does not ensure that the values of shear at the root are those required to balance the hub forces and moments. In the dynamic system, it is these shear forces which must balance the hub forces. For this reason, the program was modified to provide for trimming the rotor system for the proper shear values.

Improvement in the method of determining lag-damper coefficients in the analysis was also required. Examination of test data for lag motion at the hub and the corresponding moments imposed by the lag damper revealed that the damping rate was a nonlinear function of rate of change of lag angle. The exact manner in which appropriate linearized coefficients were introduced for each response harmonic is described in PROVISIONS FOR LAG DAMPER on page 26

Similarly, the lift, drag, and pitching moment curves lead to aerodynamic damping terms which are also nonlinear. Suitable values for these coefficients were calculated as described in AERODYNAMIC DAMPING on page 21. Accuracy in the choice of aerodynamic damping coefficients is most important in this analysis. They serve the purpose of correcting the air loads on the blade for the effect of blade response. The damping coefficients are defined by the rate of change of air load with velocity. These damping coefficients must be generated for use in the forced response portion of the analysis since the aerodynamic section does not account for blade flapping or flexibility, but calculates air loads based on a rigid blade at the steady coning angle.

The data for the H-34 aircraft showed that there were large edgewise moments at the outer end of the blade. Preliminary analyses gave no indication that such moments existed. This difference was reconciled by consideration of the effect of the counterweights in the H-34 blade spar. The counterweights are mounted in rubber. Counterweight centrifugal forces are reacted in part by the spar through the rubber, and in part by a moment reaction at the tip cap. In the H-34 test blade, most of the force apparently was reacted by the tip cap, for inclusion of this moment reaction would account for the difference

9

between measured and computed moments. Figures 3 and 4 show the effects of inclusion of corrected lag-damper coefficients and counterweight moment on the edgewise bending moments. Good correlation is obtained outboard. While inclusion of these effects inboard does improve the correlation, further improvement would be desirable.

The above were the important changes made to the analysis. Certain additional changes in introducing flexibility effects in the air load calculations were made for the modified cases. These are reported in MODIFICATIONS TO ANALYSIS on page 63 . Examination of the H-34 test data and other knowledge of the behavior of the rotor system led to the choice of the following conditions for evaluation of the analytical techniques. For the H-34, flight conditions consisted of trim level flight with neutral C.G. at 41, 70 and 112 knots. An aft C.G. condition was evaluated at 73 knots, while the Bell HU-1A rotor was evaluated at 113 knots. A speed of 41 knots was chosen because the bending stresses on the rotor blades appear to reach a maximum point near that speed; and this case should further reveal the characteristics of the analysis at low speeds. One hundred and twelve knots, on the other hand, represent a high speed case where variable inflow might not be expected to yield substantial improvement over a constant inflow approach. Seventy knots represents an intermediate airspeed for which variable inflow is important. At this speed the effects of variation in C.G. should be evident, if they are in fact substantial. The H-34 test data indicate that C.G. effects on air loads and moments are not large. As the results will indicate, the analysis shows the same lack of sensitivity to C.G.

DEVELOPMENT OF AEROELASTIC MODEL

The mathematical model was developed for the study by extending the Sikorsky Aircraft blade aeroelastic program (References 5 and 12). The basic analysis is fully described in these references and only the significant extensions to the analysis will be covered in detail here. These extensions include: (1) incorporation of the variable induced velocity method of Reference 3, (2) inclusion of rotor trim criteria which provide for hub pitching and rolling moments as rotor head boundary conditions.(3) a more accurate treatment of aerodynamic damping due to blade flapping, (4) provision for
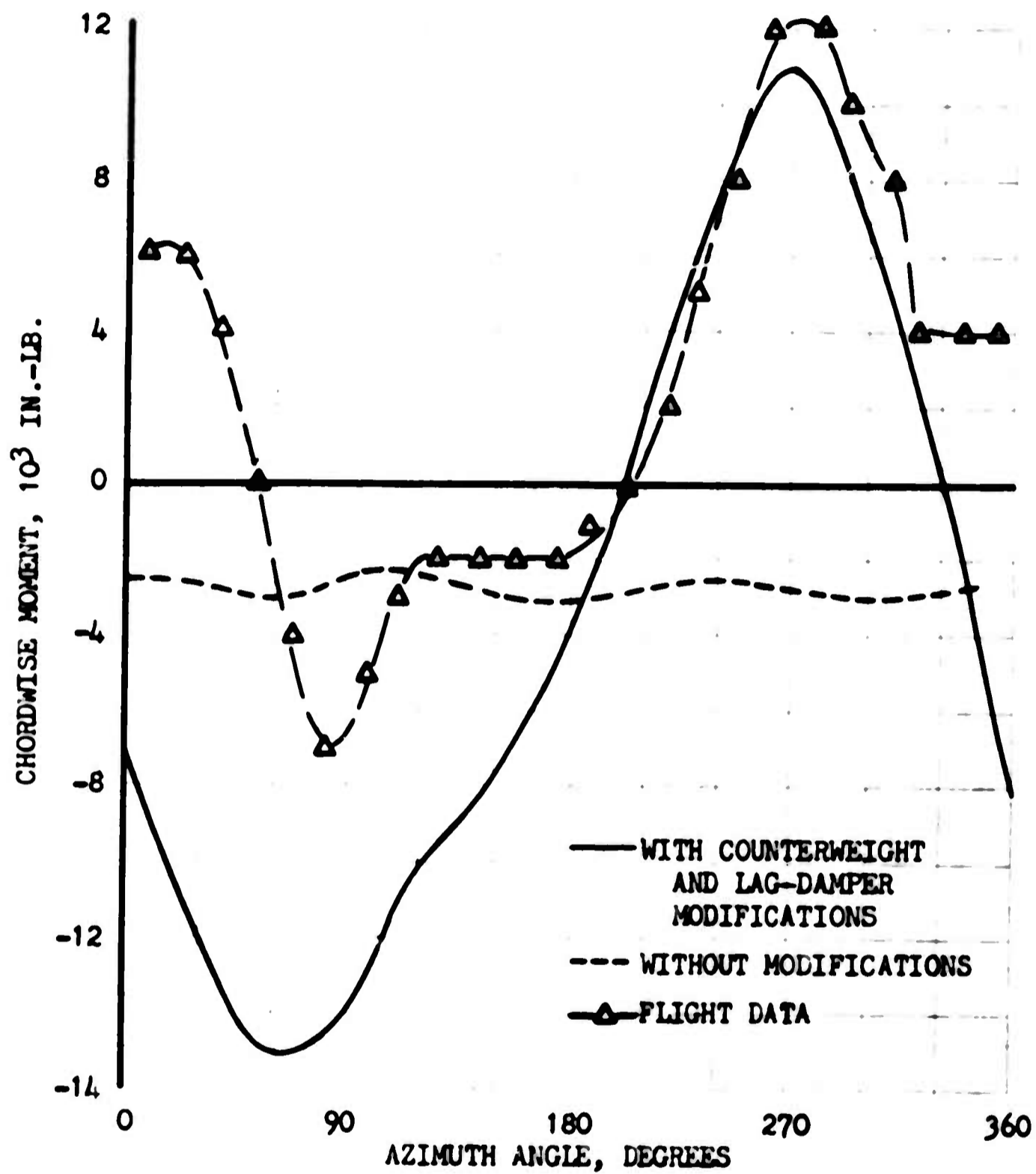
FIGURE 3. EFFECT OF COUNTERWEIGHT MOMENT AND
LAG DAMPER COEFFICIENT MODIFICATIONS ON H-34 EDGEWISE MOMENTS
AT 112 KNOTS AT 15 PERCENT RADIAL STATION.

11
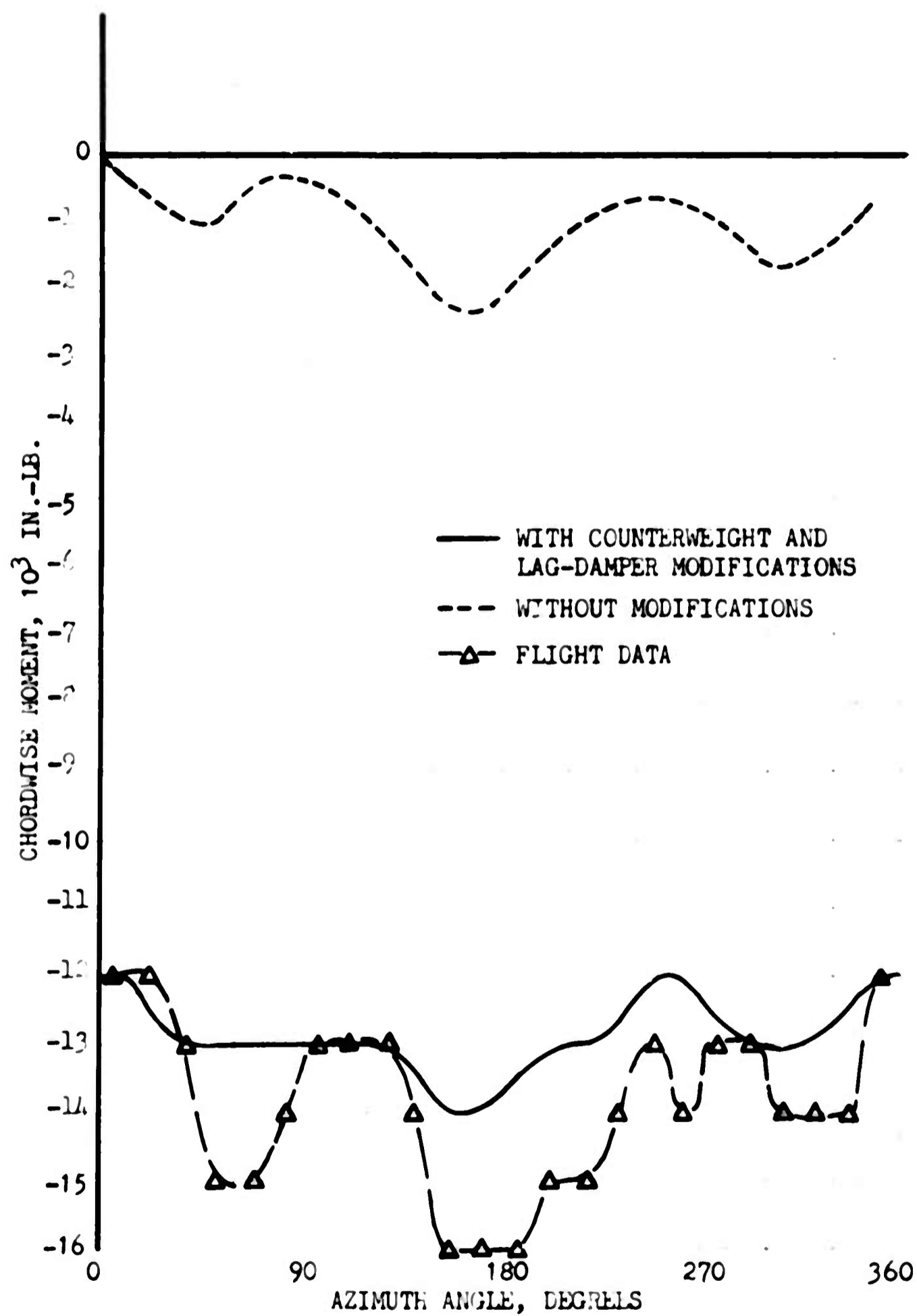
FIGURE 4. EFFECT OF COUNTERWEIGHT MOMENT AND
LAG-DAMPER COEFFICIENT MODIFICATIONS ON H-34 EDGEWISE MOMENTS
AT 112 KNOTS AT 80 PERCENT RADIAL STATION.

nonlinear lag-damper characteristics, (5) consideration of effects of flexible blade motions on aerodynamic load calculations.

Before proceeding to describe the various elements of the analysis in detail, a general description of the steps required to obtain a solution will be given. The procedure is outlined in Figure 5. Block numbers used in this section refer to that figure.

For the helicopter rotor to be analyzed, blade geometry, mass, and structural properties are required. In addition, fuselage drag, rotor angular speed, aircraft velocity, gross weight, fuselage lift, and auxiliary propulsion must be supplied, indicated by Block 1, as well as blade steady-state two-dimensional airfoil data.

Following the solid lines in Figure 5, initial rotor trim conditions are computed, (Block 2). Correct inclination and collective pitch of the rotor disk must be determined to provide enough propulsive force to overcome the net drag of the aircraft and to support the aircraft. There must also be sufficient cyclic pitch to keep the rotor in equilibrium.

These initial trim conditions, which may be obtained by applying a constant inflow condition to the aeroelastic analysis, are used in the variable inflow analysis (Block 3) to determine the variable induced velocity distribution on the rotor. A discussion of the variable inflow analysis is given in the CORNELL VARIABLE INFLOW PROGRAM on page 27.

For determination of aerodynamic loads (Block 4), two dimensional airfoil data are used. Compressibility effects are taken into account by using C_L versus α, C_D versus α, and C_M versus α curves for angles of attack from zero to thirty degrees, to define a family of C_L, C_D, and C_M curves for Mach numbers up to .95. To define stall regions above angles of attack of thirty degrees, single C_L versus α, C_D versus α, and C_M versus α curves are taken from Reference 4. The blade to be considered is subdivided into 21 segments. For each of 24 fifteen-degree azimuth intervals, the blade is analyzed at two blade pitch angles. These angles bracket the anticipated blade pitch angles. Blade segment aerodynamic lifts are then computed, from which the moment of the thrust about the flapping hinge is calculated as a function of blade pitch angle and azimuth. The rotor blade pitch necessary to maintain the rotor

13
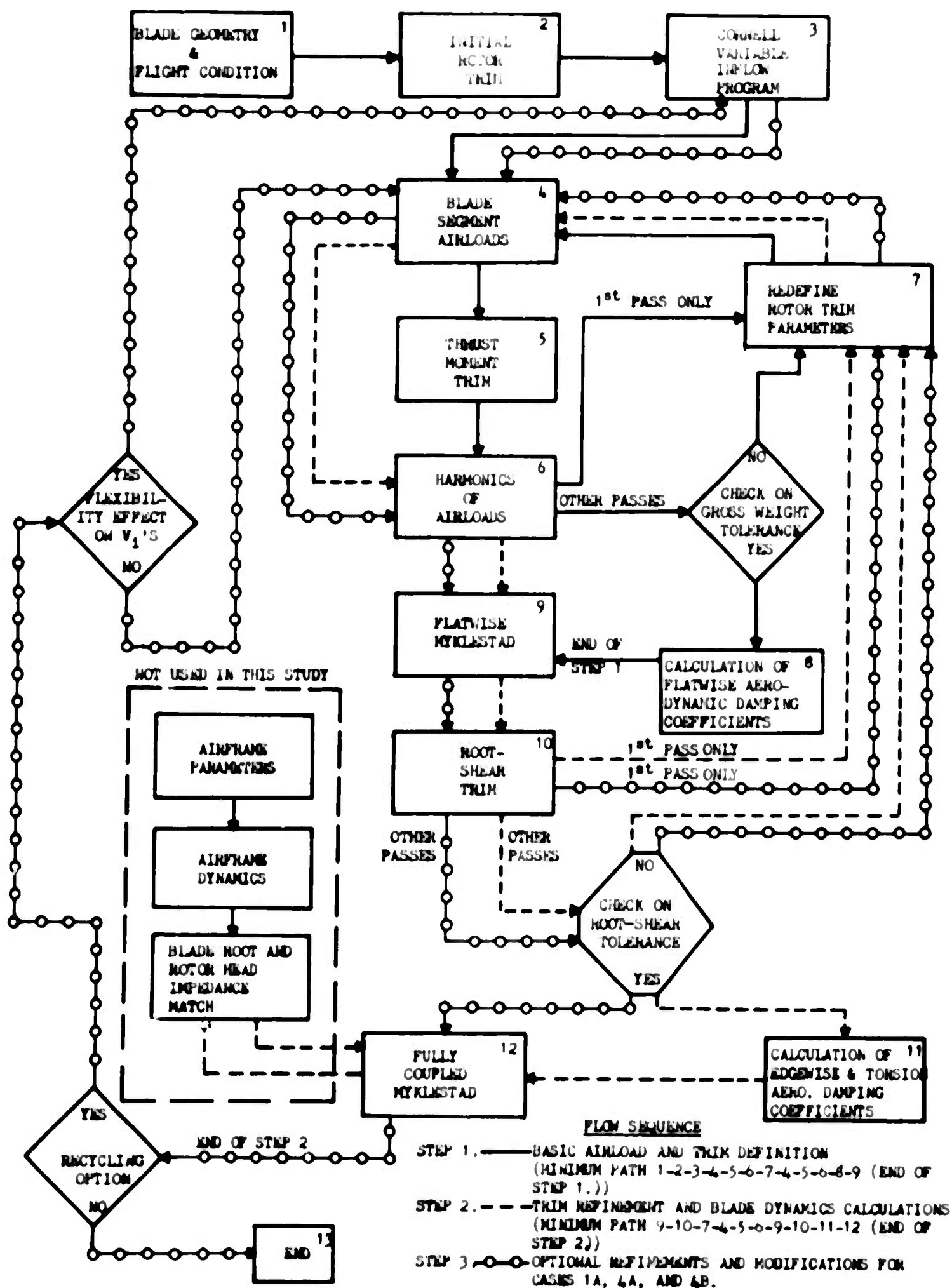
FIGURE 5. FLOW DIAGRAM OF AEROELASTIC ANALYSIS

system in equilibrium is calculated by a thrust moment iteration technique, described in PROVISION FOR ROTOR TRIM on page 17, which forces the first harmonic thrust moment about the flapping hinge to converge to the required value (Block 5). These values for blade pitch angles are obtained by a linear interpolation procedure. Blade segment aerodynamic lift, drag, and pitching moments are recalculated, using the previously trimmed values for pitch, at each of the 21 radial blade locations as harmonic functions of azimuth angle (Block 6). The magnitude of calculated helicopter gross weight is compared with the required gross weight, where calculated helicopter gross weight is based upon the mean value of thrust moment, rotor lift, rotor drag, and the blade radial location of the resultant thrust vector. If the two differ by more than the gross weight tolerance (normally 1%), refinements to rotor lift and rotor drag and other pertinent rotor attitude parameters are made (Block 7). Previously determined blade pitch angles are incremented and resubstituted to initiate new rotor equilibrium calculations. The iteration procedure is continued until the specified tolerance on gross weight is satisfied. Flatwise aerodynamic damping coefficients are then calculated (Block 8).

An additional refinement to rotor trim has been incorporated which employs steady hub rolling and pitching moments as boundary conditions. An analytical discussion of this trim procedure is given in PROVISION FOR ROTOR TRIM on page 17. The dashed lines in Figure 5 trace the procedure. Expressions for the hub rolling and pitching moments can be written in terms of blade root shears and moments; thus flexible dynamics as well as aerodynamic effects are accounted for in the trim procedure. For an articulated rotor, steady and first harmonic flatwise root shear and steady edgewise root shear are employed.

The steady edgewise shear can be determined from rotor torque requirements. To determine the flatwise root shears an uncoupled flatwise Myklestad analysis is used (Block 9). This gives the approximate shear values for the given aerodynamic loading. This analysis is used instead of a fully coupled analysis to decrease the running time of the program for the shear trim. A 3 by 3 matrix is formulated which relates increments of collective and cyclic blade pitch to increments of steady and first harmonic blade root shear. The increments of collective and cyclic pitch obtained from

15

the solution of the matrix equation are the values needed to satisfy the specified trim conditions (Block 10).

Calculation of the aerodynamic damping coefficients used in the Myklestad equations to account for blade flapping is discussed in full in AERODYNAMIC DAMPING on page 21 . Sine and cosine N per revolution flatwise perturbation velocities are superimposed upon the rotor equilibrium condition determined by the thrust moment iteration scheme. Changes in the harmonics of radial distribution of blade segment lift, drag, and pitching moment form three N by N complex aerodynamic damping matrices, where N indicates the number of harmonics of rotor speed considered. At present, the main diagonal elements of the three N by N matrices are introduced into the fully coupled Myklestad aeroelastic blade program. Interharmonic coupled damping coefficients are not considered. Complex aerodynamic damping coefficients are then multiplied by the appropriate blade segment velocities within the Myklestad analysis. This procedure thus defines the harmonics of complex aerodynamic damping force. Provisions are made in the Myklestad analysis to include aerodynamic damping forces because blade flapping velocities are not included in defining an inflow angle for air-load calculations. The pitch angle refinement calculation from the flatwise root-shear matrix method does include the effect of the damping forces and thus ensures that further air-load calculations do include the influence of blade segment flapping velocities.

Convergence of the shear iteration technique is obtained when a prescribed root-shear tolerance condition is met. After calculation of the edgewise and torsional damping coefficients (Block 11), the harmonics of air loads associated with the trim condition are applied to the fully coupled Myklestad relations. This analysis is described in detail in Reference 12. The lag-damper coefficients used in this analysis are supplied as input data and are obtained by the method described in PROVISIONS FOR LAG DAMPER on page 26.

In the present study, steady boundary conditions were used in the Myklestad analysis. However, it is possible to incorporate the airframe dynamic response in the analysis and use matched rotor and airframe impedance at the hub as boundary relations. The dynamic interaction of rotor system and airframe then would be considered directly in the analysis. The basis for this approach has

been developed by Sikorsky Aircraft (Reference 5).

The procedure to this point is that used for the basic calculation for the five flight conditions evaluated. Modifications were made to this procedure in an attempt to improve air-load definition. The changes involve a repetition of the entire procedure, as indicated by the circled solid lines, recalculating the air loads to account for the effects of blade bending from the previous solution. Blade segment torsional rotation and flatwise slopes are introduced into the air-load calculations.

The variable induced velocity distribution used in the aerodynamic analysis can be refined by introducing flexible motions from the fully coupled Myklestad analysis into the Cornell analysis. These modifications are described in MODIFICATIONS TO ANALYSIS on page 63.

The procedure followed after computation of the new air loads is exactly the same. The rotor system is retrimmed using the new air-load distribution. The fully coupled Myklestad analysis is then used to determine new values for blade response. Additional iterations may be made if desired for further refinement.

A.   PROVISION FOR ROTOR TRIM

A thrust moment iteration scheme has been used in the Sikorsky aeroelastic analysis for trimming a rotor system to obtain collective and cyclic blade pitch for a given steady-state level flight condition. This approach equates the steady thrust and moments produced by the air-load distribution over the rotor with the required thrust and moment on the rotor hub. Since the forces and moments transmitted to the rotor hub depend directly upon the shear and moments at the inboard end of the rotor blades, a new shear trim iteration scheme was developed to refine the pitch values given by the thrust moment iteration scheme. The shear iteration increments blade pitch to produce the required shear at the inboard end of the blade.

Initial rotor trim conditions are established by means of the thrust moment iteration procedure, in which rotor equilibrium is determined by enforcing sufficient blade pitch to give required first

17

harmonic thrust moment about the flapping hinge, and setting the steady thrust moment equal to the following value.

$$TM_0 = \frac{\bar{x}(gw - L_{fus} - L_{rotor})}{b\cos \alpha_t \cos \beta_0}$$ (Steady thrust moment)   (1)

where

$\bar{x}$ is the radial location of thrust vector

gw is the gross weight of ship

L_{fus} is the lift of fuselage

L_{rotor} is the vertical component of rotor drag

b is the number of blades

α_t is the angle of tip path plane

β_0 is the blade rigid body coning angle

As a result a 3 by 3 symmetric thrust moment-blade pitch matrix is established which allows direct solution of the blade pitch angle. Development of the matrix is based upon defining the Fourier coefficients of thrust moments as functions of linearized relations between thrust moment and blade pitch. Final converged values of blade pitch are obtained by specifying a tolerance on the calculated aircraft gross weight. Azimuthal thrust moment calculations using blade segment theory are made for an assumed upper and lower blade pitch setting. A linear variation of thrust moment and blade pitch for various azimuth positions is assumed.

$$TM(\psi) = m(\psi) \left[A_0 + B_1 \sin \psi + A_1 \cos \psi\right] + b(\psi)$$ (2)

where

$TM(\psi)$ is the azimuthal thrust moment

$m(\psi)$ is the slope of azimuth thrust moment blade pitch lines

$A_o + B_1 \sin \psi + A_1 \cos \psi$ is the blade pitch angle

$b(\psi)$ is the intercept of the thrust moment blade pitch zero line

The azimuthal distribution of thrust moment may be written in the following harmonic form.

$$TM(\psi) = TM_0 + TM_1 \cos\psi + \overline{TM}_1 \sin\psi + \ldots \qquad (3)$$

where

TM_0 is the steady thrust moment

TM_1 is the first harmonic cosine component of thrust moment

$\overline{TM}_1$ is the first harmonic sine component of thrust moment.

Upon comparing the coefficients of a Fourier series expression of Equation (2) with Equation (3) the following 3 by 3 matrix results.

$$
\begin{bmatrix}
2TM_0 - \frac{1}{\pi} \int_0^{2\pi} b(\psi) d\psi \\
TM_1 - \frac{1}{\pi} \int_0^{2\pi} b(\psi)\cos\psi \, d\psi \\
\overline{TM}_1 - \frac{1}{\pi} \int_0^{2\pi} b(\psi)\sin\psi \, d\psi
\end{bmatrix}
=
\begin{bmatrix}
a_{11} & a_{12} & a_{13} \\
a_{21} & a_{22} & a_{23} \\
a_{31} & a_{32} & a_{33}
\end{bmatrix}
\begin{bmatrix}
A_o \\
A_1 \\
B_1
\end{bmatrix}
\qquad (4)
$$

where the matrix coefficients are defined as:

$$a_{11} = \frac{1}{\pi} \int_0^{2\pi} m(\psi) \, d\psi \qquad a_{12} = a_{21} = \frac{1}{\pi} \int_0^{2\pi} m(\psi)\cos\psi \, d\psi$$

$$a_{22} = \frac{1}{\pi} \int_0^{2\pi} m(\psi) \cos^2\psi \, d\psi \qquad a_{13} = a_{31} = \frac{1}{\pi} \int_0^{2\pi} m(\psi)\sin\psi \, d\psi \qquad (5)$$

$$a_{33} = \frac{1}{\pi} \int_0^{2\pi} m(\psi) \sin^2\psi \, d\psi \qquad a_{23} = a_{32} = \frac{1}{\pi} \int_0^{2\pi} m(\psi)\sin\psi \cos\psi \, d\psi$$

Inversion of the matrix will yield the collective (A_o) and cyclic pitch (A_1, B_1) for rotor trim. Due to the nonlinear characteristics of thrust moment variation with blade pitch, several iterations on blade pitch must be made to meet gross weight and flapping

19

requirements.

Once convergence is obtained, the shear trim criteria are applied to obtain refined values for blade pitch. A set of boundary relations associating fixed hub rolling and pitching moments and vertical force as functions of blade root steady and first harmonic flatwise and edgewise shears, moments, and torques is used to determine the shear required at the blade root. Boundary relations may be chosen to allow the use of any type of blade root construction, whether fully articulated, semi-articulated, or rigid, and also allow a rotor system to be trimmed for off neutral center of gravity condition. For a fully articulated rotor, the following trim identities are used to define the shears required at the blade root.

$$F_z = S_0{}^F b \cos \alpha_t \qquad \text{(steady vertical hub force) (6)}$$

$$M_{xx} = -e \sin \alpha_t \, S_0{}^E b + e \cos \alpha_t \frac{\overline{S_1}{}^F b}{2} \qquad \text{(steady hub rolling moment) (7)}$$

$$\therefore \quad M_{yy} = \frac{-e S_1{}^F b}{2} \qquad \text{(steady hub pitching moment) (8)}$$

Vertical hub force is given by the rotor lift required. Steady hub rolling and pitching moments may be obtained from an aerodynamic equilibrium analysis. With an estimated value for shaft angle, α_t, the required steady edgewise shear, $S_0{}^E$, and steady and first harmonic flatwise shear, $S_0{}^F$, $S_1{}^F$, and $\overline{S_1}{}^F$, are determined. Actual $S_0{}^E$ on the blade is determined from rotor torque requirements and actual flatwise shears S_0, S_1, and $\overline{S_1}$, are found from applications of given air loads to an uncoupled flatwise Myklestad blade analysis. Changes in blade pitch required to satisfy the shear trim conditions can then be determined with an iterative procedure using the following equation.

$$
\begin{bmatrix} S_0{}^F - S_0 \\ \hline S_1{}^F - S_1 \\ \hline \overline{S}_1{}^F - \overline{S}_1 \end{bmatrix}
=
\begin{bmatrix}
\dfrac{\Delta S_0}{\Delta A_0} & \dfrac{\Delta S_0}{\Delta A_1} & \dfrac{\Delta S_0}{\Delta B_1} \\
\dfrac{\Delta S_1}{\Delta A_0} & \dfrac{\Delta S_1}{\Delta A_1} & \dfrac{\Delta S_1}{\Delta B_1} \\
\dfrac{\Delta \overline{S}_1}{\Delta A_0} & \dfrac{\Delta \overline{S}_1}{\Delta A_1} & \dfrac{\Delta \overline{S}_1}{\Delta B_1}
\end{bmatrix}
\begin{bmatrix} A_0 \\ \hline A_1 \\ \hline B_1 \end{bmatrix}
$$

20

The difference elements of the matrix are obtained by separately incrementing collective pitch and sine and cosine values of cyclic pitch, and determining the corresponding flatwise root shears from the flatwise blade analysis.

The incremental values of collective and cosine and sine components of blade pitch are ΔA_0, ΔA_1, and ΔB_1.

Upon inverting the matrix new values of blade pitch are obtained from

$$\theta (\psi) = (A_0 + \Delta A_0) + (A_1 + \Delta A_1) \cos \psi + (B_1 + \Delta B_1) \sin \psi$$

(10)

where A_0, A_1, B_1, are blade pitch angles established by the thrust moment iteration scheme or from earlier passes of the shear iteration.

B.   AERODYNAMIC DAMPING

A method of analysis was developed for determining aerodynamic damping coefficients associated with rotor blade flapping motions. The method makes use of a perturbation technique wherein increments are made to the blade segment flapping velocities associated with a particular rotor trim condition. From this procedure, corresponding changes in air loads are obtained. The aerodynamic damping coefficients acting on an element of the blade can then be defined by terms of the form

$$\left(\frac{\Delta L}{\Delta U_p}\right)_i \quad , \quad \left(\frac{\Delta D}{\Delta U_p}\right)_i \quad , \quad \left(\frac{\Delta PM}{\Delta U_p}\right)_i$$

These coefficients represent the respective change in blade lift, drag, and pitching moment for unit change in blade flapping velocity.

The total perturbation velocity is introduced in the aeroelastic model by incrementing the normal component of the total blade segment velocity by the following n/rev harmonic series:

21

$$\left(\Delta U_p \right)_i = \Delta(r\,\dot{\beta})_i = \sum (r\,\dot{\beta})_{ni}^{s} + (r\,\dot{\beta})_{ni}^{c} \tag{11}$$

where

$\left(\Delta U_p \right)_i = \Delta(r\,\dot{\beta})_i$ is the increment of normal component of total blade segment velocity

i is the blade segment location

$\dot{\beta}$ is the flapping angular velocity

r is the blade segment radial location

n is the number of harmonics

$(r\,\dot{\beta})_{ni}^{s}$ is the harmonic of sine perturbation velocity

$(r\,\dot{\beta})_{ni}^{c}$ is the harmonic of cosine perturbation velocity

Damping coefficients for each harmonic of the fully coupled Myklestad blade response analysis must be obtained. Incrementing $(U_p)_i$ by each harmonic of flapping velocity as expressed in Equation (11) yields the following complex matrix of aerodynamic damping coefficients:

$$\left[\frac{\Delta A}{\Delta r \dot{\beta}} \right]_i = \left[\frac{\Delta A}{\Delta r \dot{\beta}} \right]_i^{R} + j \left[\frac{\Delta A}{\Delta r \dot{\beta}} \right]_i^{I} \tag{12}$$

where A is a general notation indicating air load (lift, drag, or pitching moment)

$\left[\dfrac{\Delta A}{\Delta r \dot{\beta}} \right]_i$ is the complex aerodynamic damping coefficient matrix

$\left[\dfrac{\Delta A}{\Delta r \dot{\beta}} \right]_i^{R}$ is the real part of complex aerodynamic damping coefficient matrix

$\left[\dfrac{\Delta A}{\Delta r \dot{\beta}} \right]_i^{I}$ is the imaginary part of complex aerodynamic damping coefficient matrix

22

Real and imaginary parts of the complex aerodynamic damping coefficient matrix are expressed as:

$$
\left[\frac{\Delta A}{\Delta r\beta}\right]_i^R = \frac{1}{2}
\begin{bmatrix}
\left(\dfrac{\Delta A_{1i}^c}{\Delta(r\,\dot\beta)_{1i}^c} + \dfrac{\Delta A_{1i}^s}{\Delta(r\,\dot\beta)_{1i}^s}\right) & \cdots & \left(\dfrac{\Delta A_{ni}^c}{\Delta(r\,\dot\beta)_{1i}^c} + \dfrac{\Delta A_{ni}^s}{\Delta(r\,\dot\beta)_{1i}^s}\right) \\
\vdots & \ddots & \vdots \\
\left(\dfrac{\Delta A_{1i}^c}{\Delta(r\,\dot\beta)_{ni}^c} + \dfrac{\Delta A_{1i}^s}{\Delta(r\,\dot\beta)_{ni}^s}\right) & \cdots & \left(\dfrac{\Delta A_{ni}^c}{\Delta(r\,\dot\beta)_{ni}^c} + \dfrac{\Delta A_{ni}^s}{\Delta(r\,\dot\beta)_{ni}^s}\right)
\end{bmatrix}
$$

(13)

$$
\left[\frac{\Delta A}{\Delta r\beta}\right]_i^I = \frac{1}{2}
\begin{bmatrix}
\left(\dfrac{\Delta A_{1i}^s}{\Delta(r\,\dot\beta)_{1i}^c} - \dfrac{\Delta A_{1i}^c}{\Delta(r\,\dot\beta)_{1i}^s}\right) & \cdots & \left(\dfrac{\Delta A_{ni}^s}{\Delta(r\,\dot\beta)_{1i}^c} - \dfrac{\Delta A_{ni}^c}{\Delta(r\,\dot\beta)_{1i}^s}\right) \\
\vdots & \ddots & \vdots \\
\left(\dfrac{\Delta A_{1i}^s}{\Delta(r\,\dot\beta)_{ni}^c} - \dfrac{\Delta A_{1i}^c}{\Delta(r\,\dot\beta)_{ni}^s}\right) & \cdots & \left(\dfrac{\Delta A_{ni}^s}{\Delta(r\,\dot\beta)_{ni}^c} - \dfrac{\Delta A_{ni}^c}{\Delta(r\,\dot\beta)_{ni}^s}\right)
\end{bmatrix}
$$

where

(14)

$\dfrac{\Delta A_{ni}^c}{\Delta(r\,\dot\beta)_{ni}^c}$ is the incremental change in the nth/rev cosine component of total air load due to a nth/rev cosine component of flapping velocity

$\dfrac{\Delta A_{ni}^s}{\Delta(r\,\dot\beta)_{ni}^c}$ is the incremental change in the nth/rev sine component of total blade segment air load due to the nth/rev cosine component of segment flapping velocity.

$\dfrac{\Delta A_{ni}^c}{\Delta(r\,\dot\beta)_{ni}^s}$ is the incremental change in the nth/rev cosine component of total blade segment air load due to nth/rev sine component of segment flapping velocity

$\dfrac{\Delta A_{ni}^s}{\Delta(r\,\dot\beta)_{ni}^s}$ is the incremental change in the nth/rev sine component of total blade segment air load due to nth/rev sine component of segment flapping velocity

In the fully coupled Myklestad analysis. only the diagonal

23

elements in the coefficient matrix have been included. Interharmonic damping coefficients, which are defined by the off diagonal elements have been neglected. These coefficients were neglected on the basis that their effects would be small. However, examination of later results indicated that the effect of interharmonic damping becomes important when large harmonic blade flapping occurs. A further discussion is given in CORRELATION OF PREDICTED AND FLIGHT TEST LOADS on page 33.

It was noted that the coefficients on the main diagonal were almost identical in magnitude. Thus the first harmonic damping coefficient was substituted for the remaining main diagonal coefficients. Similar identities were also noted for the off diagonal coefficients.

The elements in the complex aerodynamic damping matrix obey the law of complex differentiation of an analytic function. If it is assumed that the Cauchy-Riemann relationships apply, the following must hold:

$$\left(\frac{\Delta A}{\Delta r \dot{\beta}}\right)_{ni} = \frac{\Delta A_{ni}^{c}}{\Delta (r \dot{\beta})_{ni}^{c}} + j \frac{\Delta A_{ni}^{s}}{\Delta (r \dot{\beta})_{ni}^{c}} = \frac{\Delta A_{ni}^{s}}{\Delta (r \dot{\beta})_{ni}^{s}} - j \frac{\Delta A_{ni}^{c}}{\Delta (r \dot{\beta})_{ni}^{s}}$$

or

$$\left(\frac{\Delta A}{\Delta r \dot{\beta}}\right)_{ni} = \frac{1}{2}\left(\frac{\Delta A_{ni}^{c}}{\Delta (r \dot{\beta})_{ni}^{c}} + \frac{\Delta A_{ni}^{s}}{\Delta (r \dot{\beta})_{ni}^{s}}\right) + \frac{1}{2} j \left(\frac{\Delta A_{ni}^{s}}{\Delta (r \dot{\beta})_{ni}^{s}} - \frac{\Delta A_{ni}^{c}}{\Delta (r \dot{\beta})_{ni}^{s}}\right)$$

Calculation of each element did reveal that: (15)

$$\frac{\Delta A_{ni}^{c}}{\Delta (r \dot{\beta})_{ni}^{c}} \approx \frac{\Delta A_{ni}^{s}}{\Delta (r \dot{\beta})_{ni}^{s}} \quad \text{and} \quad \frac{\Delta A_{ni}^{s}}{\Delta (r \dot{\beta})_{ni}^{c}} \approx \frac{\Delta A_{ni}^{c}}{\Delta (r \dot{\beta})_{ni}^{s}}$$

(16)

Because the terms were not exactly equal, an average of the two values was used. For simplification, define the elements of the complex aerodynamic coefficient matrix by:

$$\frac{1}{2}\left(\frac{\Delta A_{ni}^{c}}{\Delta (r \dot{\beta})_{qi}^{c}} + \frac{\Delta A_{ni}^{s}}{\Delta (r \dot{\beta})_{qi}^{s}}\right) \equiv (C_{nq})_{i}^{R}$$

(17)

where

n, q   are indices indicating change in nth harmonic of airload

24

due to qth harmonic of flapping velocity.

i   is the blade radial station.

Likewise each element of the imaginary part of the coefficient matrix will be designated by:

$$\frac{1}{2}\left(\frac{\Delta A_{ni}}{\Delta(r\ \beta\ )_{qi}^{c}} - \frac{\Delta A_{ni}^{c}}{\Delta(r\ \beta\ )_{qi}^{s}}\right) = (C_{nq})_{i}^{I} \qquad (17a)$$

Equation (15) will then be expressed as:

$$(C_{nq})_i = (C_{nq})_i^R + j\ (C_{nq})_i^I \qquad (18)$$

The complex damping force F_n will include the influence of all interharmonic coefficients. Its magnitude is obtained by multiplying Equation (18) by the appropriate harmonic of blade segment velocity. To define the blade velocity, suppose the displacement of the blade is expressed by the following harmonic series:

$$(y_q)_i = (y_q)_i^R + j\ (y_q)_i^I \qquad (19)$$

The velocity is obtained by taking the time derivative of Equation (19).

$$\left(\frac{dy_q}{dt}\right)_i = (v_q)_i = (v_q)_i^R + j(v_q)_i^I \qquad (20)$$

The complex aerodynamic damping force is thus:

$$(F_n)_i = \sum_{q=1}^{n}(C_{nq})_i\ (v_q)_i$$

or

$$(F_n)_i = \sum_{q=1}^{n}\left\{\left[(C_{nq})_i^R(v_q)_i^R - (C_{nq})_i^I\ (v_q)_i^I\right] + j\left[(C_{nq})_i^I(v_q)_i^R + (C_{nq})_i^R(v_q)_i^I\right]\right\} \qquad (21)$$

As an example the real part of the first harmonic damping force is: (22)

$$(F_1)_i^R = \left[(C_{11})_i^R(v_1)_i^R - (C_{11})_i^I(v_1)_i^I\right] + \cdots \left[(C_{1n})_i^R(v_n)_i^R - (C_{1n})_i^I(v_n)_i^I\right]$$

25

where n is the number of harmonics used.

When interharmonic damping coefficients are neglected the equation for F_{ni} reduces to

$$(F_n)_i = (C_{nn})_i \, (v_n)_i \tag{23}$$

This simplification was used in the program. It was believed that inclusion of interharmonic terms would significantly increase the running time of the program without providing much of a change in the damping force. However, as was stated earlier, results given in CORRELATION OF PREDICTED AND FLIGHT TEST LOADS on page 33, indicate that the interharmonic terms may be important for some cases.

C.   PROVISIONS FOR LAG DAMPER

To incorporate the nonlinear characteristics of a lag-hinge damper with relief valve provision in the fully coupled analysis, the following procedure was developed. For a representative speed during trimmed level flight, measured edgewise bending moments at the blade root and lead-lag angles are used to define the magnitude of the damping coefficients. Moment and lag angle data are analyzed to obtain harmonics in terms of azimuth angle. The harmonics of angular blade lagging velocity are then calculated from the lag angle harmonics. These may be described by:

$$M^E(\psi) = \sum_{1}^{n} M_n^E \cos n\psi + \overline{M}_n^E \sin n\psi \qquad \text{measured blade root edgewise moment} \tag{24}$$

$$\zeta(\psi) = \sum_{1}^{n} E_n \cos n\psi + F_n \sin n\psi \qquad \text{measured blade lagging angle} \tag{25}$$

$$\dot{\zeta}(\psi) = \sum_{1}^{n} -n\Omega E_n \sin n\psi + n\Omega F_n \cos n\psi \qquad \text{computed lagging angular velocity} \tag{26}$$

From these relations, the lag damper coefficient is defined in general as:

$$C(\psi) = \frac{M^E(\psi)}{\dot{\zeta}(\psi)} \tag{27}$$

In view of the harmonic definition of the blade lagging angular

26

velocity and its root edgewise moment, a damping coefficient is constructed for each harmonic of rotor speed.

This coefficient is defined by the sine component of root edgewise moment divided by the cosine component of lagging blade velocity and the cosine component of root edgewise moment divided by the sine component of lagging blade velocity.

$$C_n = \frac{1}{2}\left(\frac{M_n^E}{n \Omega \; E_n} + \frac{\bar{M}_n^E}{n \Omega \; F_n} \right)\Big/ 2 \qquad (28)$$

The damping coefficient used to describe the nonlinear characteristic of a lag-hinge damper is expressed for each harmonic of rotor speed where n indicates the order of the harmonic.

The damping coefficient for each harmonic of rotor speed is then introduced in the fully coupled Sikorsky blade response program where it is coupled to the appropriate harmonic of lag motion.

D. THE VARIABLE INFLOW PROGRAM

Description of Analysis

The variable inflow distributions required for the Sikorsky Aeroelastic Program were calculated using the Cornell Aeronautical Laboratory Variable Inflow Computer Program developed under TRECOM (now USAAVLABS) Contract No. DA 44-177-TC-698 (References 3, 7, and 8). The mathematical model consists of the representation of each blade by a segmented lifting line, and the helical wake of the rotor by a mesh of discrete segmented vortex filaments consisting of both trailing and shed vorticity. The shed vortex elements result from the azimuthwise variation of bound circulation and the trailing vortex elements result from the spanwise variation of bound circulation. The circulation of the wake for each blade changes with azimuth position and is periodic for each rotor revolution. The blades are divided into a finite number of radial segments, and the induced velocity at the center of each selected blade segment is computed by summing the contributions of each bound trailing wake, and shed wake vortex filament. The contribution of each vortex filament is obtained through use of the Biot-Savart equation which expresses the induced velocity in terms of the circulation strength of the vortex filament

and its geometrical position relative to the blade segment at which the induced velocity is desired.

The program can be considered as having two basic parts: (1) the determination of the blade-wake geometry and (2) the determination of the circulation distribution and its associated induced velocity distribution. The wake geometry is determined by assuming that each element of wake vorticity travels with the speed and in the direction of the instantaneous velocity imparted to it at the time it was generated at the blade. The wake geometry is thus fixed by the choice of the input wake velocity distribution, rotor dimensions, and flight condition. In reality, the wake transport velocities and resultant wake geometry are greatly influenced by interaction effects between the various elements of vorticity in the wake. However, the inclusion of such wake vortex-vortex interaction effects was beyond the scope of the variable inflow program used for the results reported herein. The bound circulation distribution is determined by relating the wake circulations to the bound circulations, expressing the wake induced velocities in terms of the unknown bound vortex strengths by means of the Biot-Savart equation, and developing a set of simultaneous equations relating the bound circulation and local blade angle of attack at each blade segment. These equations thus involve the known flight condition, wake geometry, lift-curve slope, and blade motion and control parameters and the unknown bound circulation values. Solution of these equations yields the desired bound circulation values which, when combined with the appropriate geometrical relations in the Biot-Savart law, produce the required induced velocity distribution.

Assumptions of the Analysis

The state of the art concerning variable inflow theory is continuously advancing and many of the assumptions listed below are currently under investigation. In this research program, the Cornell variable inflow analysis of Reference 3 was used. There is a newer version of the Cornell program in which there are provisions for rolling up the trailing wake filaments and the elimination of the shed wake filaments in the far wake region (generally assumed to lie a quarter of a revolution downstream of the blade). This treatment of the vortex interaction and dissipation phenomenon was com-

28

pleted by the Cornell personnel during the period of this contract but was not included in the analysis reported herein. Since further study of the rotor wake geometry problem is currently in progress at Cornell Aeronautical Laboratory, and the inclusion of the above-mentioned initial wake modifications served principally to reduce computer time rather than to effect any major changes in the predicted induced velocity and air load distribution, the original variable inflow program described in Reference 3 was used in obtaining the results presented herein. This method incorporates a wake model for which the near wake geometrical distribution of trailing and shed wake elements is retained in the far wake. This original program had been previously evaluated by United Aircraft Corporation Research Laboratory and Sikorsky Aircraft, and much of the discussion and conclusions concerning the program are based on that evaluation.

The following is a list of the principal assumptions of the Cornell variable inflow program used to compute the induced velocity distributions employed in this report.

1. The flight condition is steady.

2. The blades and rotor wake are represented by vortex elements based on lifting line theory rather than finite vortex core and lifting surface theory. Thus, aerodynamic boundary conditions at the blade are satisfied at only one point on the chord.

3. Viscous dissipation effects on the wake circulation strengths are neglected inasmuch as the circulation strength of a given wake element is constant with time. However, the number of wake revolutions retained in the analysis can be limited.

4. Unsteady aerodynamic effects resulting from the variation of bound circulation strength with blade azimuth position are represented by the inclusion of shed wake elements and the provision for varying circulation strength between successive trailing wake elements. However, due to the rather coarse spacing of the shed vorticity and the representation of the blade by a lifting line, the ac-

29

curacy of the unsteady aerodynamic model is questionable.

5. Stall is included by limiting the maximum lift coefficient value and thus the maximum circulation. It is assumed that the stalled lift is circulatory.

6. Reversed flow effects are included by the correct directions of the velocity components. The location of the bound vortex does not change from the 1/4- to the 3/4-chord position.

7. Small angle assumptions are included in the analysis.

8. Mach number and Reynolds number effects are included by using as input to the program lift-curve slope values which may vary over the rotor disc but not with angle of attack.

9. In-plane components of induced velocity are neglected.

10. Interference effects of the rotor hub, fuselage, etc. are neglected.

11. The wake geometry is specified by wake transport velocities which are assumed to be equal to the velocities imparted to the various wake elements at the time they were generated at the blade. Wake vortex interaction and viscous dissipation effects are thus neglected.

12. Blade flapping harmonics above the first, lag, and bending effects, with the exception of steady bending, are not included in the establishment of the wake geometry, and therefore in the determination of the blade element to wake element distances.

E. COUPLING OF THE VARIABLE INFLOW PROGRAM WITH THE SIKORSKY AEROELASTIC ANALYSIS

The variable inflow program, in its present form, separates the air-load problem from the blade response problem. The circula-

tion and induced velocity distributions are determined from known blade motions and control parameters. If the circulation distribution thus computed is used directly to obtain air loads, it is generally found that the aircraft trim conditions (lift, drag, etc.) and the blade boundary conditions are not satisfied. Thus, in coupling the variable inflow program to the Sikorsky aeroelastic analysis, it was necessary to establish an approach which would satisfy these conditions.

The original approach considered involved an iteration procedure which used only that portion of the variable inflow program defining the wake geometric coefficients (σ's) by the Biot-Savart equation. An initial estimate of blade motions, control parameters, and lift distribution was obtained from the blade dynamic response program using constant momentum inflow, but satisfying the blade boundary conditions, and aircraft trim conditions. The circulation values were then obtained from the lift distribution and combined with the wake geometric coefficients determined by the variable inflow program to produce an initial estimate of the induced velocity distribution. This variable induced velocity distribution was then used as input to the blade response program and a new circulation distribution was obtained. This procedure was continued until the circulation values converged. Due to the change in inflow distribution, it was then necessary to include an iteration to adjust the collective pitch, etc. to satisfy aircraft trim requirements.

This approach was discontinued due to convergence problems associated with the circulation iteration method which were encountered whenever wake vortex elements were in close proximity to the blade stations at which the air loads were being evaluated. The nature of the difficulties can be illustrated by expressing the circulation iteration procedure in terms of a representative set of simultaneous equations which have the form indicated in Equation (6) of Reference 3.

$$\Gamma_k^j = \pm \left[I_k + a_k b_k \sum_{i=1}^{nN} \sigma_{ki} \Gamma_i^{j-1} \right] \tag{29}$$

This relation expresses the bound circulation values of the jth iteration, Γ_k^j, in terms of the local geometric angle-of-attack distribution and blade plunging motions, I_k, the wake geometric coefficients, σ_{ki}, the wake circulation values of the j-1 iteration, Γ_i^{j-1}, and the pro-

31

ducts of the lift-curve slope and blade semichord, $a_k b_k$. Nondimensionalizing the above equation by dividing by $a_k b_k V_k$, relating the wake circulation values to the bound circulation values, and writing it in matrix form:

$$\{\Gamma\}^j = \{\bar{I}\} + [\sigma] \{\bar{\Gamma}\}^{j-1} \qquad (30)$$

Bound   Blade   Wake   Wake Circulation
Circulation   Dynamics   Geometry   in Terms of
                                                     Bound Circulation

Induced Velocity

The convergence of the iteration method represented by the above set of simultaneous algebraic equations was investigated by examining the effect of the magnitude of the σ matrix coefficients on convergence characteristics. It was determined that, for a specific value of I, convergence difficulties should be expected whenever the magnitude of any of the matrix coefficients approaches approximately .5 to 1. These values correspond to critical σ coefficients of $.5/a_k b_k$ to $1/a_k b_k$. Examination of the elements of the variable inflow program σ matrices for several flight conditions of interest indicated potential convergence difficulties under the following circumstances:

1. Whenever blade segment lengths were less than approximately 5 per cent of the rotor radius.

2. At low speeds where blades pass in close proximity to vortex elements generated by previous blades.

3. At high speeds where reverse flow effects cause shed vortexes to approach and pass the blade generating the vortexes.

In view of these anticipated difficulties this iteration approach was abandoned.

The revised iteration method involves more extensive use of the existing variable inflow program in that the procedure given by the program for calculating the rotor circulation distribution is em-

ployed in addition to the procedure for calculation of the wake geometric coefficients. In effect, this replaces the portion of the original circulation iteration method by a closed-form solution, thereby eliminating the iteration difficulties previously mentioned. It is noted that the method for computing circulation includes the assumption of constant lift-curve slope values for each Mach number. However, as mentioned previously, the Cornell variable inflow solution does not satisfy blade boundary conditions, and hence an iteration between the variable inflow program and the blade analysis is necessary. It should also be noted that aircraft trim conditions (lift, drag, etc.) are satisfied by the blade analysis through adjustments in collective pitch, cyclic pitch, and rotor angle of attack.

Due to the dependence of the variable induced velocity distribution obtained from the variable inflow program on the blade motion and control parameter input, it was necessary to include a test of the convergence of this input after each pass through the blade aeroelastic analysis. However, it was generally found that inflow convergence was rapid, and one iteration pass was sufficient.

CORRELATION OF PREDICTED AND FLIGHT TEST LOADS

The analysis was applied to the main rotors of the H-34 and HU-1A helicopters. Four flight conditions were evaluated for the H-34, while one flight condition was considered for the HU-1A. These cases correspond to steady state level flight conditions for which flight test data are available. The cases considered are:

Case 1. H-34; steady-state level flight at 41 knots with neutral C.G.
Case 2. H-34; steady-state level flight at 73 knots with aft C.G.
Case 3. H-34; steady-state level flight at 70 knots with neutral C.G.
Case 4. H-34; steady-state level flight at 112 knots with neutral C.G.
Case 5. HU-1A; steady-state level flight at 113 knots with neutral C.G.

Test data for the cases were obtained from the following sources: Case 1 from Table V in Reference 9; Case 2 from Table

33

104 in Reference 10; Case 3 from Run 2 in Reference 6; Case 4 from Table 21 in Reference 10; and Case 5 from condition 31 in Reference 1.

The following sections present the input data used in the analysis, the significant results obtained, and the correlation with test data.

A.   BASIC BLADE DATA

The H-34 and HU-1A have significantly different rotor systems. The H-34 has a four-bladed fully articulated rotor system with lag dampers. This helicopter was evaluated at a gross weight of 11,800 pounds. The HU-1A has a two-bladed teetering rotor system. Since the blade is not free to hunt, lag dampers are not required. This helicopter was evaluated at a gross weight of 6027 pounds.

The basic blade data for the two aircraft are presented in Tables 1 and 2 (page 35 and 36). These tables give the radial station breakdown used in the aeroelastic analysis, and the blade properties at each station. The calculated natural frequencies of these blades are shown in Table 3 (page 37).

Presented in Table 4 (page 38) are the trim conditions used for each of the five cases.

Trim values of first harmonic flatwise root shear for the H-34 cases were obtained from calculations of required steady hub rolling and pitching moments. A preliminary aerodynamic analysis based on constant inflow was used to obtain the required rolling and pitching moments. Zero first harmonic shear was used for the HU-1A.

Analysis of the teetering rotor of the Bell HU-1A requires the choice of appropriate boundary conditions for each harmonic considered. The boundary conditions chosen correspond to those given in Reference 2. For response to steady loads, the rotor was considered cantilevered both flatwise and edgewise. For the 1, 3, 5, and 7 per rev. harmonics, the blade was pinned flatwise and cantilevered edgewise. For the 2, 4, and 6 per rev. harmonics the blade was cantilevered flatwise and pinned edgewise. A canti-

TABLE 1
BASIC BLADE DATA H-34 HELICOPTER
GROSS WEIGHT 11,800 POUNDS. TWIST -8 DEGREES

Radius (In.)	Chord (In.)	Segment Weight (Lb.)	Moments of Inertia		
			Flatwise (In.⁴)	Edgewise (In.⁴)	Torsion (In.⁴)
332.	16.4	3.35	1.47	15.94	4.65
324.	16.4	6.	1.47	15.94	4.65
316.	16.4	6.15	1.47	15.94	4.65
299.	16.4	9.35	1.47	15.94	4.65
282.	16.4	7.8	1.47	15.94	4.65
265.	16.4	8.1	1.47	15.94	4.65
248.	16.4	7.85	1.47	15.94	4.65
231.	16.4	7.8	1.47	15.94	4.65
214.	16.4	7.8	1.47	15.94	4.65
197.	16.4	7.8	1.47	15.94	4.65
180.	16.4	9.	1.47	15.94	4.65
163	16.4	7.8	1.47	15.94	4.65
146	16.4	7.8	1.47	15.94	4.65
129.	16.4	9.1	1.47	15.94	4.65
112.	16.4	7.8	1.47	15.94	4.65
95.	16.4	7.9	1.47	15.94	4.65
78.	16.4	8.	1.47	15.94	5.4
61.	16.4	6.4	1.71	17.18	5.6
44.	7.25	7.3	15.83	30.35	11.9
27.	7.25	60.	50.	46.2	11.9
12.	7.25	40.	50.	46.2	11.9

TABLE 2
BASIC BLADE DATA HU-1A HELICOPTER
GROSS WEIGHT 602 POUNDS. TWIST - 12 DEGREES

Radius (In.)	Chord (In.)	Segment Weight (Lb.)	Moments of Inertia		
			Flatwise (In.4)	Edgewise (In.4)	Torsion (In.4)
260	15.17	3.078	2.55	96.	3.75
255.25	15.17	3.668	2.55	96.	3.75
252.	15.17	1.63	2.55	96.	3.75
248.	15.17	4.89	2.55	96.	3.75
240.	15.17	8.15	2.55	96.	3.75
230.	15.17	8.15	2.55	96.	3.75
220.	15.17	7.341	2.55	96.	3.75
205.	15.17	12.	2.4	80.	3.75
185.	15.17	12.	2.4	80.	3.75
165.	15.17	11.505	2.4	80.	3.75
145.	15.17	9.251	2.36	75.	3.75
125.	15.17	9.45	2.35	76.5	3.75
105.	15.17	10.	2.31	87.	3.75
85.	15.17	10.05	2.3	115.	3.75
65.	15.17	10.86	2.6	114.	5.25
50.	15.17	7.35	4.9	140.	8.5
40.	15.17	9.75	7.55	175.	10.58
30.	15.17	12.8	11.6	225.	12.63
20.	15.17	15.85	581.	757.	14.75
10.	0.	18.5	581.	757.	16.88
0.	0.	10.175	581.	757.	19.

36

TABLE 3

CALCULATED BLADE NATURAL FREQUENCIES

| | Mode | Natural Frequencies, CPM | | | |
		Flatwise Pinned	Edgewise Pinned	Flatwise Cantilevered	Edgewise Cantilevered
HU-1A*	1	574.2	715.3	375.5	530.5
	2	1063.1	1886.6	1126.8	3198.8
	3	1718.5	3679.6	2237.9	
H-34**	1	872.3	1857.6		
	2	1607.1	5616.0		
	3	2819.7			

* Ω = 311.5 RPM
** Ω = 216 RPM

TABLE 4

BASIC FLIGHT PARAMETERS

Case	Airspeed (Kt)	RPM	Air Density (slugs/ft^3)	Flatwise Root Shear (Lb.)		Fuselage Drag (Lb.)
				Sine	Cosine	
1	41	213	.0025	+162.	+350.	-200
2	73	226	.00216	-497.	-1780.	-552.
3	70	226	.00216	-313.	+220.	-552.
4	112	216	.00209	-441.	+308.	-1315.
5	113.5	311.5	.00213	0	0	-891.

38

levered condition was assumed for torsion.

The H-34 was considered to be pinned both flatwise and edge-wise and cantilevered in torsion.

Data for the 0012 airfoil of the H-34 were available at Sikorsky Aircraft. C_L, C_D, and C_M versus α curves were used for the range of Mach numbers up to .95. Data for the HU-1A 0015 airfoil were supplied by Bell Helicopter Company. Only C_L and C_D data were available, so 0012 values were used for the C_M. The difference in C_M values between the 0012 and 0015 airfoil was believed to be relatively insignificant in this analysis.

B.   VARIABLE INFLOW ANALYSIS INPUT

The input parameters required for the variable inflow analysis consist of rotor geometry, flight conditions, choice of blade segments, wake geometry, airfoil data, and blade motion and control parameters.

The rotor dimensions and flight condition parameters, with the exception of the rotor angle of attack, were obtained from References 1, 6, 9, and 10.

The lift-curve slope values were obtained by averaging the slope values in the unstalled linear region of the Sikorsky 0012 airfoil data and the 0015 data supplied by the Bell Helicopter Company for the appropriate Mach numbers at each point in the rotor disc. An angle-of-attack value of 11.5 degrees was used to limit the wing lift coefficient in the stalled region for both configurations, the H-34 and the HU-1A. A check of the Mach number angle-of-attack combinations at each point in the rotor disc revealed that these assumptions had little effect on the results because the flight conditions chosen for this study were essentially unstalled; that is, all blade sections for the HU-1A, with the exception of those in the proximity of the reversed flow region boundary at the higher advance ratios, operated in the linear lift-curve slope region and below the assumed 11.5 degree stall angle, whereas the H-34 operated slightly into the stalled region above the 11.5 degree stall angle.

In Reference 7 the Cornell variable inflow analysis was used to calculate air loads for the HU-1A at 110 knots. Flight test data

for Condition 67 of Reference 1 were used for correlation (and not Condition 31 which was used in the present study.) The results indicated a stalled region for this condition. The absence of stall in the present study is due to the use of aircraft gross weight for rotor lift. Actual lift was somewhat higher as can be seen from Figure 37 which shows the steady air-load component for the HU-1A at 113 knots. Since rotor lift was underestimated, low values for pitch angle were calculated (see Table 5 on page 46) which indicated that the rotor did not stall. In the work of Reference 7, the problem of determining actual lift was avoided by using pitch angle and not lift as the input parameter. The effects of downwash on the fuselage and negative fuselage lift due to forward tilt of the aircraft are most likely the reason for rotor lift exceeding aircraft gross weight.

Nine blade radial segments were used to represent both the H-34 and the HU-1A blades in the variable inflow program. The segment midpoints were located at $r/R = .23, .375, .525, .65, .75, .85, .925, .965,$ and $.99$. The number and positioning of the segments determine not only the blade segment distribution but also the number of wake segments, their location and spacing. Results comparing the harmonics of blade loading for a five and nine segment representation of a model blade at an advance ration of .15 in Reference 3 indicate that the choice of the number of segments can affect the air loads. To evaluate this effect, the use of seven and nine segments was compared for the H-34 rotor at the 41-knot flight condition (Figure 6). A comparison of the harmonics of induced velocity and air-load distribution for the two segment distributions produced relatively small differences except at the tip segment, and all differences were less than the difference between the analytical results and the model data. However, nine segments were used to give a reasonable tip segment distribution and to allow for possible increased sensitivity at higher speeds.

An azimuth increment of 15 degrees was employed in defining the rotor and wake model in the variable inflow program and was the minimum value possible considering program limits. A comparison of the harmonics of inflow obtained from the variable inflow program using 15-degree, 22.5-degree, and 30-degree azimuth increments for a 39-knot flight condition indicated that the results for the 22.5-degree and 15-degree increments are essentially the same. It was not possible to investigate the effect of small increments. However, it is possible that the treatment of the shed wakes in the immediate
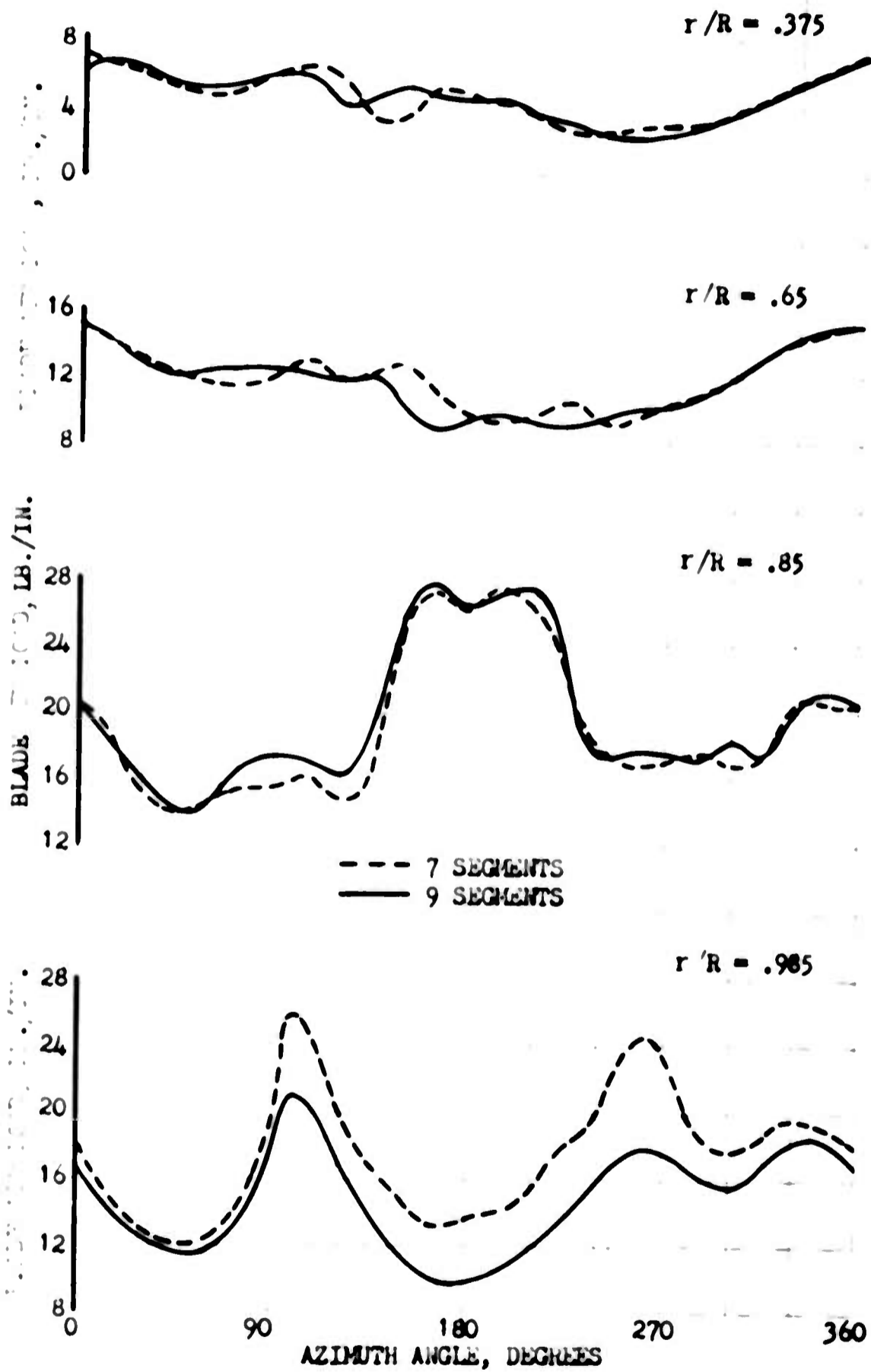
40

FIGURE 6. EFFECT OF NUMBER OF BLADE SEGMENTS IN THE
CORNELL VARIABLE INFLOW PROGRAM ON BLADE
AIR-LOAD DISTRIBUTION.

41

vicinity of the blade could produce difficulties if small azimuth increments are used.

The number of wake revolutions retained for the wake model for the H-34 helicopter 41-knot, 70-knot, and 112-knot conditions were three, two and one, respectively. Also, one wake revolution was retained for the HU-1A helicopter 113-knot condition. The choice of number of wake revolutions was based on the determination of the sensitivity of the resultant air loads to this parameter as indicated by the results of Reference 1. It is mentioned in Reference 3 that truncating the wake at three revolutions provided sufficient accuracy for model rotor at an advance ratio of .15. The use of three revolutions was also found to be adequate for the H-34 rotor at an advance ratio of .11. The insensitivity of the air loads to the effects of additional wake revolutions for these flight conditions is due to the increased average distance between this portion of the wake and the rotor. Inasmuch as the rotor is moving away from its wake even faster at higher speeds, it is to be expected that at the higher flight speeds the number of wake revolutions necessary to maintain the same accuracy will be decreased. This reasoning was used to determine the smaller number of wakes used for the H-34 at 70-knot and 112-knot conditions, and the HU-1A at 113-knot condition. The distance between corresponding points on the rotor and the farthest wake revolution for these conditions was maintained at approximately the same value as that of the 41-knot, three revolutions case. The H-34 at 112 knot condition was investigated for both one and two wake revolutions. Differences in calculated inflow were very small.

The wake transport velocity input to the variable inflow program was generally assumed to be the constant induced velocity determined from momentum considerations. It is realized that this assumption is not completely accurate inasmuch as significant distortions of the helical wake structure can be produced by wake vortex interaction effects. The use of this model is justified for the following reasons: (1) No provision is made in the existing variable inflow program for putting in realistic time varying wake transport velocities, (2) Questions still exist as to what displacement time history should be used for a particular rotor and operating condition (Reference 3), and (3) Initial results presented in Reference 3 also indicate that the use of a uniform inflow distribution, determined from momentum considerations, resulted in computed air loads which correlate reasonably well with measured air loads for a two-bladed rotor.

Calculated variable inflow distributions for the H-34 at 41 and 112 knots are shown in Figures 7 and 8. These plots show the inflow distribution over the rotor disc. There is a wide variation in inflow over the disc with steep velocity gradients near the outer edge.

C.   ROTOR TRIM ANGLES

For the calculation of the results presented here, it was necessary to choose estimated values for blade pitch and shaft inclination for the determination of rotor inflow in the variable inflow analysis. Application of this inflow to the Sikorsky aeroelastic analysis results leads to a redefinition of these parameters for proper rotor trim. Close correlation between the values used to determine inflow and the resulting values given by the aeroelastic analysis was obtained.

Listed in Table 5 (page 46) is a comparison between the analytical and flight test values for collective and cyclic pitch, rotor shaft angle, and steady coning. The pitch values are given with reference to the root for the H-34 and to station 23 for the HU-1A. Positive signs indicate pitch leading edge up, shaft angle rearward, and coning up.

D.   PRESENTATION OF RESULTS

Results of the analysis have been plotted with comparable flight test data. Plots representing the azimuthal variation of airloads, flatwise bending moments, edgewise bending moments, torsional moments, and control loads have been made and are available, but are not presented in this report. Plots are presented for the radial variation of air loads, flatwise bending moments, and edgewise bending moments. These plots show the harmonic content of the loads. These were obtained from a 24-point harmonic analysis of the data. The harmonic coefficients are defined by the following relations.

$$Y(\psi) = \frac{1}{2} A_{co} + \sum_{n=1}^{7} \left[A_{cn} \cos n\psi + A_{sn} \sin n\psi \right] \tag{31}$$

where

$$A_{cn} = \frac{1}{12} \sum_{k=0}^{23} Y(\psi_k) \cos \left(\frac{\pi kn}{12} \right)$$

43

DIRECTION OF FLIGHT
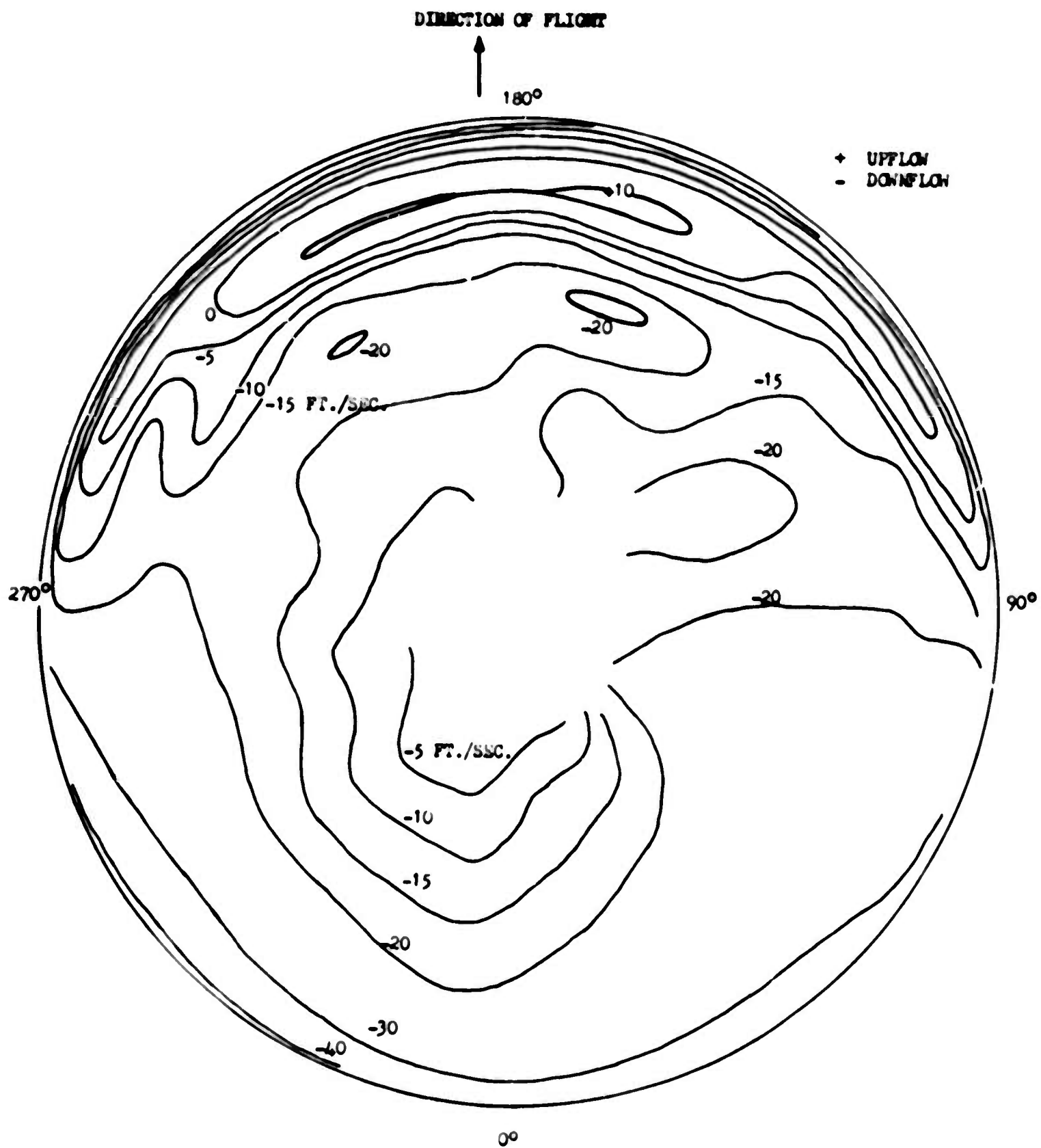
180°

+ UPFLOW
- DOWNFLOW

FIGURE 7. CALCULATED INDUCED VELOCITY DISTRIBUTION
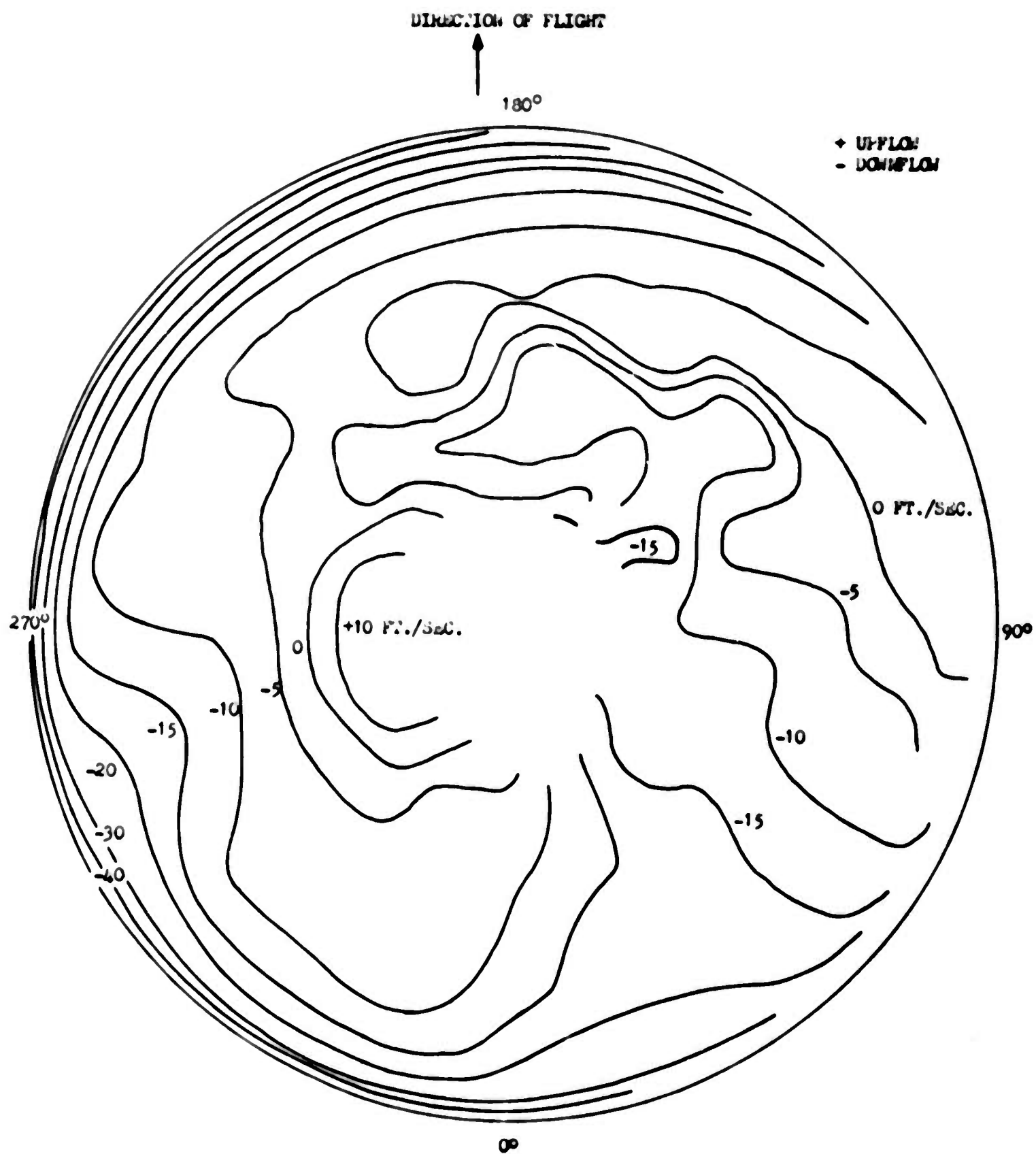CASE 1: H-34 AT 41 KNOTS

44

FIGURE 8. CALCULATED INDUCED VELOCITY DISTRIBUTION
CASE 5: H-34 AT 112 KNOTS

45

TABLE 5

COMPARISON OF ROTOR TRIM ANGLES FROM ANALYSIS AND TEST

	CASE 1		CASE 2		CASE 3		CASE 4		CASE 5	
	Anal.	Test	Anal.	Test	Anal.	Test	Anal.	Test	Anal.	Test
A_0	11.48	10.67	10.86	11.57	11.71	13.72	14.85	17.34	23.15	27.76
B_1	-2.03	-1.57	-.31	-6.06	-3.3	-4.82	-7.23	-8.04	-6.12	-7.6
A_1	1.85	1.49	.68	2.68	1.08	.70	.96	1.78	.80	3.18
α_s	-1.1	-.6	-2.85	-.9	-2.85	-2.15	-6.0	-7.2	-8.9	-6.5
β_0	4.6	3.18	3.91	2.88	4.05	4.08	4.45	3.71	3.	3.

46

$$A_{sn} = \frac{1}{12} \sum_{K=0}^{23} Y(\psi_K) \sin \left(\frac{\pi Kn}{12} \right)$$

The value of the plotted variable at azimuth angle ψ is $Y(\psi)$, and the angle ψ_K is defined by $\psi_K = (15K)°$. To aid in comparing the harmonic content of measured and analytical results, the harmonics are tabulated in terms of amplitude A_n, and phase angle θ_n, defined by

or

$$A_n \cos (n\psi - \theta_n) \equiv A_{cn} \cos n\psi + A_{sn} \sin n\psi \qquad (32)$$

$$A_n = \sqrt{A_{cn}^2 + A_{sn}^2}$$

$$\theta_n = \tan^{-1} \left(\frac{A_{sn}}{A_{cn}} \right)$$

The following sign convention was used in the presentation of results. A positive value of section aerodynamic loading indicates a force in the lift direction. Positive signs indicate compression in the upper surface of the blade for flatwise bending moment, compression in the leading edge of the blade for edgewise bending moment, a couple tending to rotate blade trailing edge upward for torsional moment, and an upload on the end of the pitch horn for pitch horn load.

E.   DATA CORRELATION

Examination of the results shown in Figures 19 through 45 reveals that fairly good correlation between test and analysis was obtained. However, significant differences do exist, which indicate that further work is required to produce an analysis capable of reliably predicting blade behavior. In general, there appear to be no significant differences between the correlation found for air loads and moments. Computed moment distributions correspond to those which would be expected from the applied air-load distributions, which shows the dynamic system is responding properly. The following evaluation summarizes the significant points concerning data correlation.

Case 1.   H-34 at 41 Knots

This is a low speed case where substantial discrepancies had

47

been found between analytical results based on constant inflow and test data. Use of variable inflow does improve correlation. Examination of the azimuthal variation in air loads shows that the analytical results do follow the general signature of the test data. However, particularly near the blade tip, the rapid changes in air loads are not matched by analysis. This indicates that the higher harmonic content of the analytical air loads is not sufficiently defined. Examination of the radial distribution of the harmonics (Figures 19 through 21) reveals that the steady and first harmonic amplitude and phase match H-34 test data quite well. Somewhat larger differences occur in the second harmonic amplitude outboard of $r/R = .7$. The third, fourth, and fifth harmonics show differences in amplitude and in phase near the tip. The present analysis does not produce an adequate definition of the air loads near the tip.

The radial flatwise moment plots of Figures 22 through 24 bear this out. Low values of air loads on the outboard half of the blade were calculated for the second, third, and fourth harmonics. It is these harmonics of flatwise moment which were found to be low. Better correlation was found for the first and third harmonics where air loads correlate well also. The reason for the difference between steady moments cannot be determined. Reference 10 indicates that the steady flatwise moments which are tabulated are not reliable, since consistent values of steady moment could not be obtained for the same flight condition on different days. This was due to difficulties in obtaining a true zero reference. The azimuthal plots of flatwise moments confirm the above.

Chordwise moment radial distribution, shown in Figures 25 through 27, follow the same pattern. Torsional moments and control loads calculations yielded higher values for the lower harmonics than was found in test.

Cases 2 and 3. H-34 at 73 Knots with Aft C.G. and at 70 Knots with Neutral C.G.

These two cases should be considered together. They differ mainly in the C.G. location which produces a difference in steady moment acting on the rotor head, and consequently different amounts of first harmonic flapping. Flapping should produce only small changes in airloads, as shown by the test data. However, sig-

48

nificant differences in air loads were found in the analytical results. Investigation revealed that these differences were largely due to the absence of interharmonic damping in the analysis. This investigation is discussed more fully later in this section. The main point is that the presence of first harmonic flapping produces a substantial difference in the second harmonic content of the air loads. For the aft C.G. case the magnitude of the second harmonic is approximately half the magnitude for the neutral C.G. case. The difference is almost equal to the correction which inclusion of interharmonic damping would make.

Examination of the results shows that, in general, correlation was better for the 70-knot neutral C.G. case than for the aft C.G. case. There is a trend throughout the results of poor correlation near an azimuth angle of 0 degrees. This difference will, of course, affect all harmonics. With the exception of the second harmonic difference, air loads for the two cases correlated with test equally well. Flatwise moments showed somewhat better correlation for the neutral C.G. case than for the aft C.G. case. There is a substantial difference in chordwise moments. For the neutral C.G. case, chordwise moments correlate well outboard and differ mainly by a shift in the steady moment at inboard stations. The aft C.G. case shows a large shift in first harmonic phase as well as a difference in steady moments inboard, with comparable correlation outboard. Calculated torsional moments and control loads correlated fairly well with test data for the advancing blade, but not very closely for the retreating blade.

Case 4. H-34 at 112 Knots

The results for this case are presented as radial distributions of harmonics as shown in Figures 28 through 36. Air loads for this case show fairly good correlation with test data in terms of amplitudes. However, there is a significant shift in phase between test and analytical results. This shift in phase is also evident in the flatwise bending moment curves. These moments otherwise show good correlation except at azimuth angles in the neighborhood of zero degrees. Comparison of the harmonics of air-load and flatwise bending moment, both in magnitude and phase angle, shows that the correlation of flatwise moments follows quite consistently the correlation of air loads. The harmonics for which air loads correlate closely with H-34 data also show close correlation of flatwise moments. If

49

calculated air loads are small, moments are small also. This indicates that lack of correlation is largely due to inaccurate definition of air loads. This topic is discussed in EVALUATION OF ANALYSIS on page 68. Chordwise moments show a significant difference in steady moment inboard. Calculated higher harmonics, especially the third and fourth, are much lower than H-34 data. The general signature of the chordwise moments, however is quite good. Torsional moments and control load correlation showed large differences for the retreating blade.

Case 5. HU-1A at 113 Knots

Results for this case are presented in Figures 37 through 45 which show radial distribution of the air-load and bending moment harmonics. Air-load correlation is fairly good. There is a phase shift between test and calculated data. This is most evident near zero azimuth and, as in other cases, leads to poor correlation of air loads in that region. Unfortunately, rotor thrust was underestimated by about 15% (see page 39) which yielded low calculated steady air loads, and low values for the second and third harmonics. The radial plots show good correlation for the first and fourth harmonics. Flatwise moment calculated values were high for the first and fourth harmonics but other harmonics correlated very well. Chordwise moment correlation was more erratic. In general, calculated moment values were less than test values. This is most evident in the steady, second, and fourth harmonics. The differences in the second and fourth harmonics are most likely due to the boundary conditions used for these harmonics. The rotor was considered to be pinned for these modes to reflect the flexibility of the rotor support and the antisymmetric character of the response. The results show that higher moments should exist on the inboard section of the blade. This indicates that a cantilevered boundary condition would have been more realistic. Torsional moments and control load have approximately the correct magnitude but poor phase correlation.

F.   COMPARISON WITH CONSTANT INFLOW

The use of the variable inflow analysis has produced significant improvements in correlation with test data. Typical results for the H-34 at 41 knots and at 112 knots are shown in Figures 9

50

through 12. At 41-knots, constant inflow (without a tip loss factor) correlates poorly with H-34 data, while the variable inflow results show good correlation. On the other hand, at 112 knots, there is much less difference between correlation obtained with variable inflow and with constant inflow. The reason for this is that at 41 knots the induced velocities vary widely across the rotor disc, and constant inflow is a poor approximation. However, for speeds in the range of 112 knots, the variation of inflow have much less effect on air loads and the constant inflow approximation is more valid. Therefore, better correlation would be expected. There is a difference in phase between calculated air loads and flight test data as shown in Figure 11. Similar phase differences were found in the work of Reference 7. It appears, therefore, that the phase difference results from the inflow distribution used in the analysis.

G.   ROOT-SHEAR FORCES

The use of variable inflow has produced more realistic values for root-shear forces. These are the forces which are transmitted to the rotor hub to produce airframe excitation. Earlier studies (Reference 5) showed that root shear forces predicted by constant inflow were less than those required for airframe excitation. Calculated airframe response using these shear forces was much below measured response.

Plots of the harmonics of root-shear forces for both variable and constant inflow show more than a 100 per cent increase in the important third, fourth, and fifth harmonics for the H-34 at both 41 and 112 knots (Figures 13 and 14). These harmonics are the main contributors to airframe excitation due to the filtering action of the rotor hub. Other harmonic shears are increased as well. While these increases in root shear forces are substantial, it is estimated that still larger forces are needed for correlation.

H.   CORRELATION OF ONE-HALF PEAK-TO-PEAK BENDING MOMENTS

For the determination of blade fatigue life, knowledge of one-half peak-to-peak vibratory stresses is essential. The incorporation of variable inflow in the analysis produced little change in the ability

51
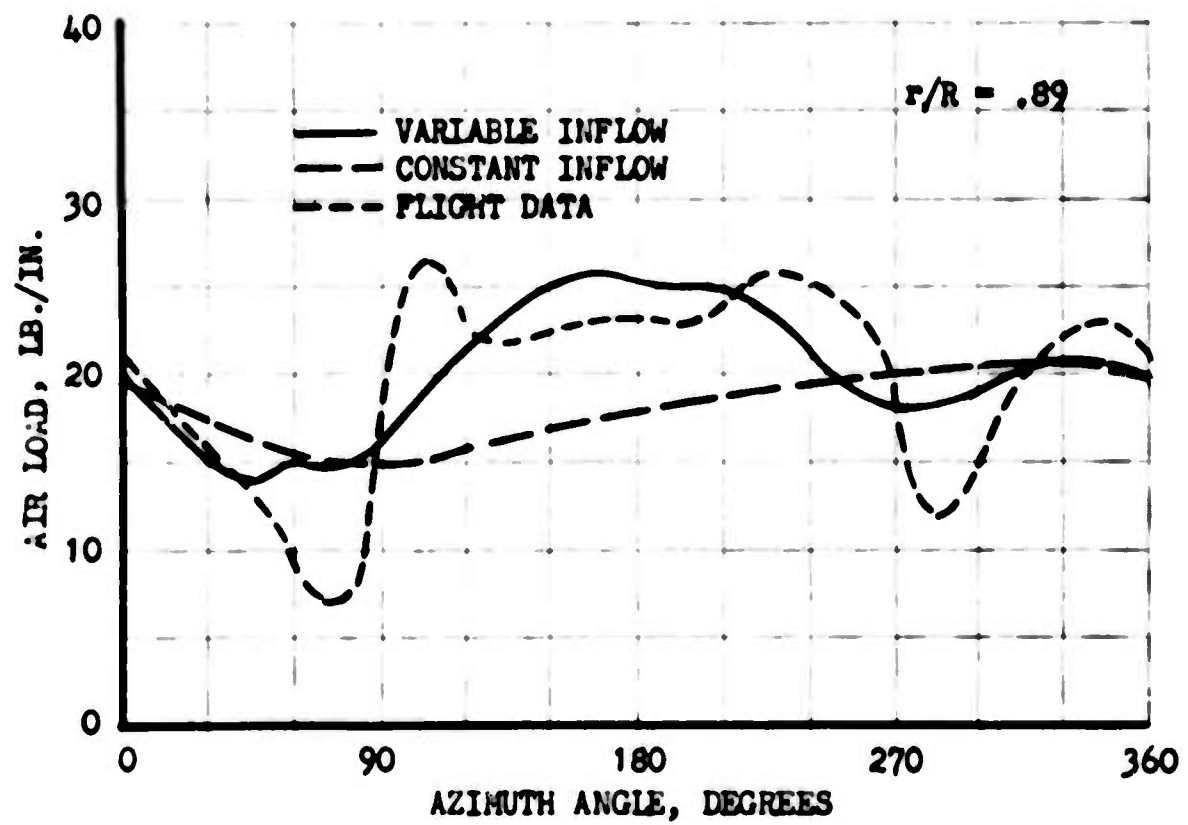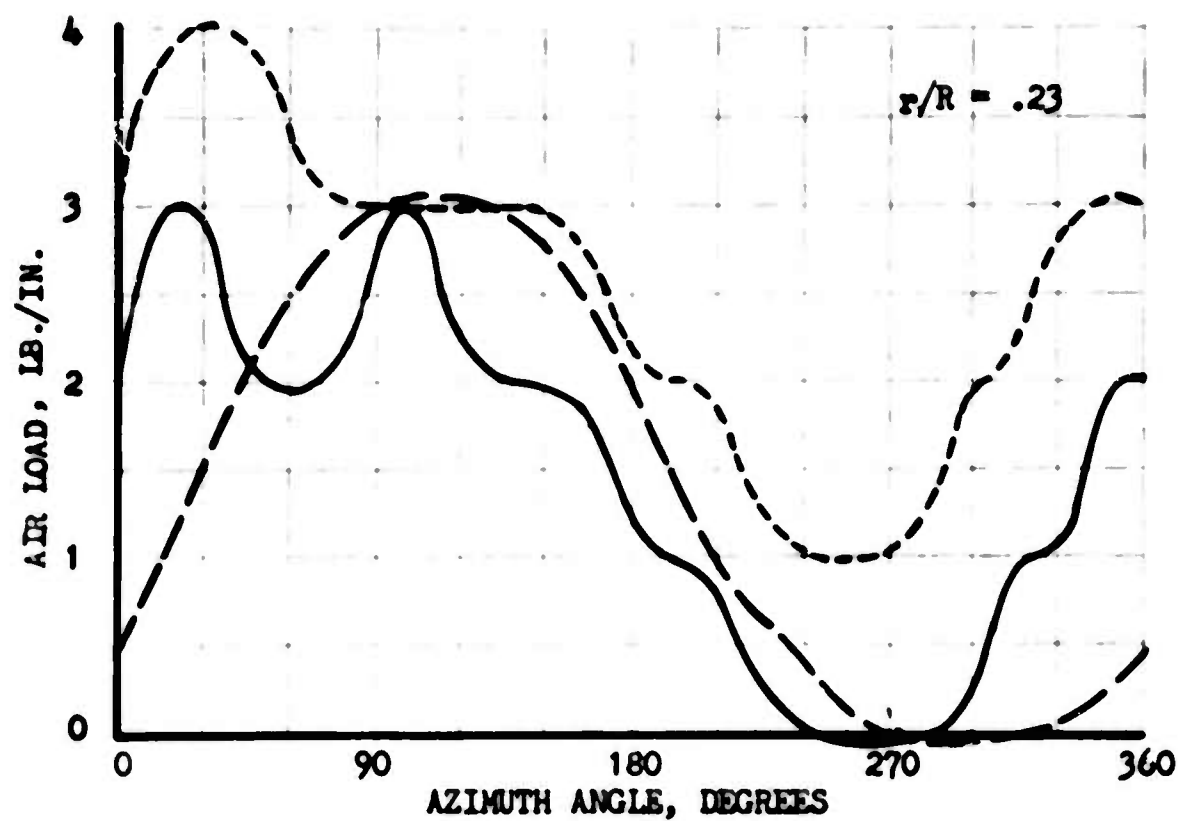
FIGURE 9. H-34 AIR LOADS AT 41 KNOTS
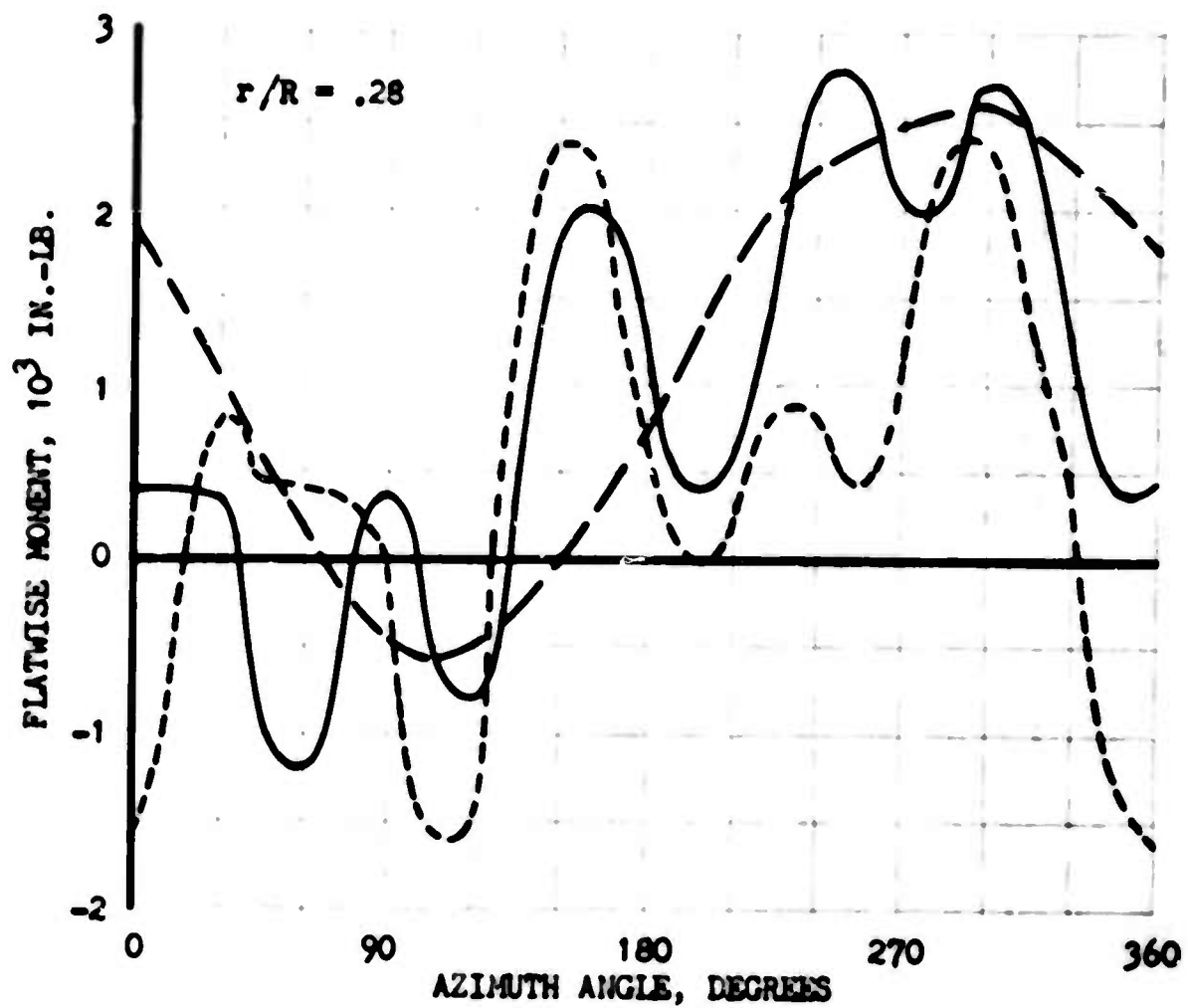COMPARISON OF CONSTANT AND VARIABLE INFLOW.

52
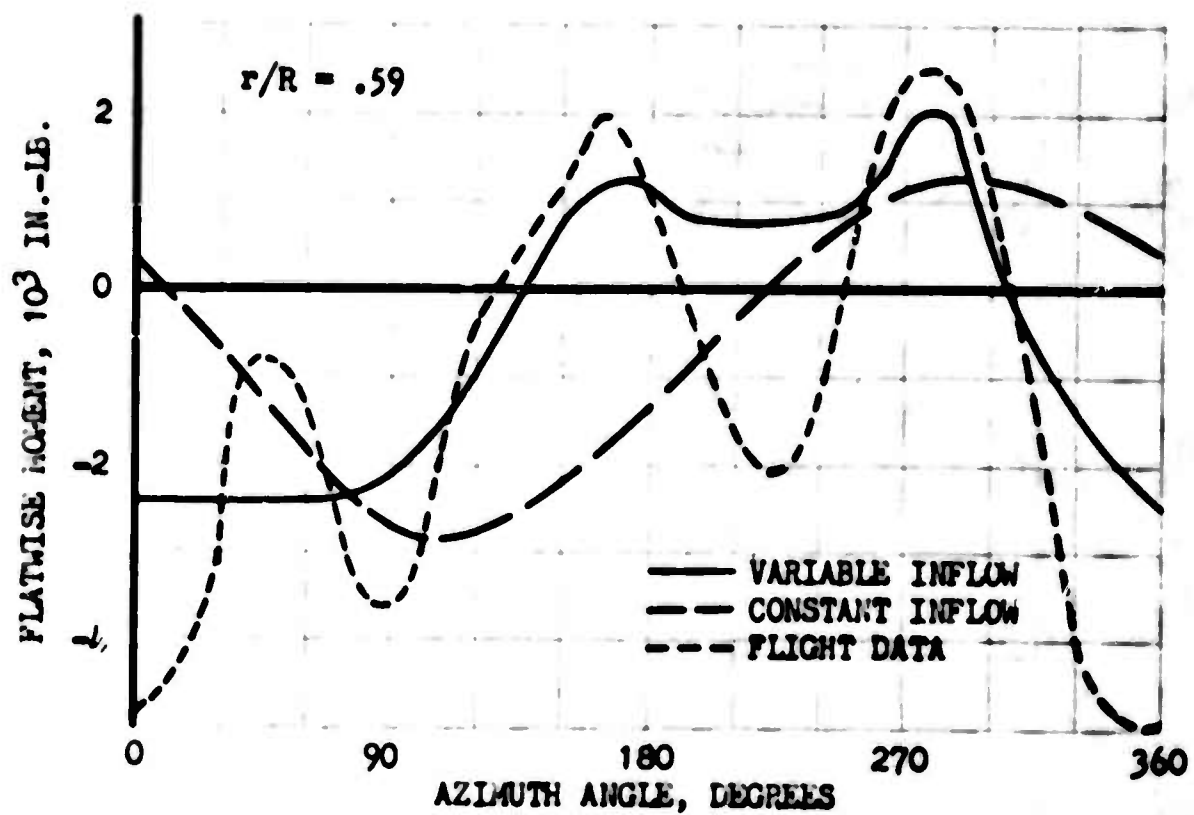
FIGURE 10.   H-34 FLATWISE MOMENTS AT 41 KNOTS
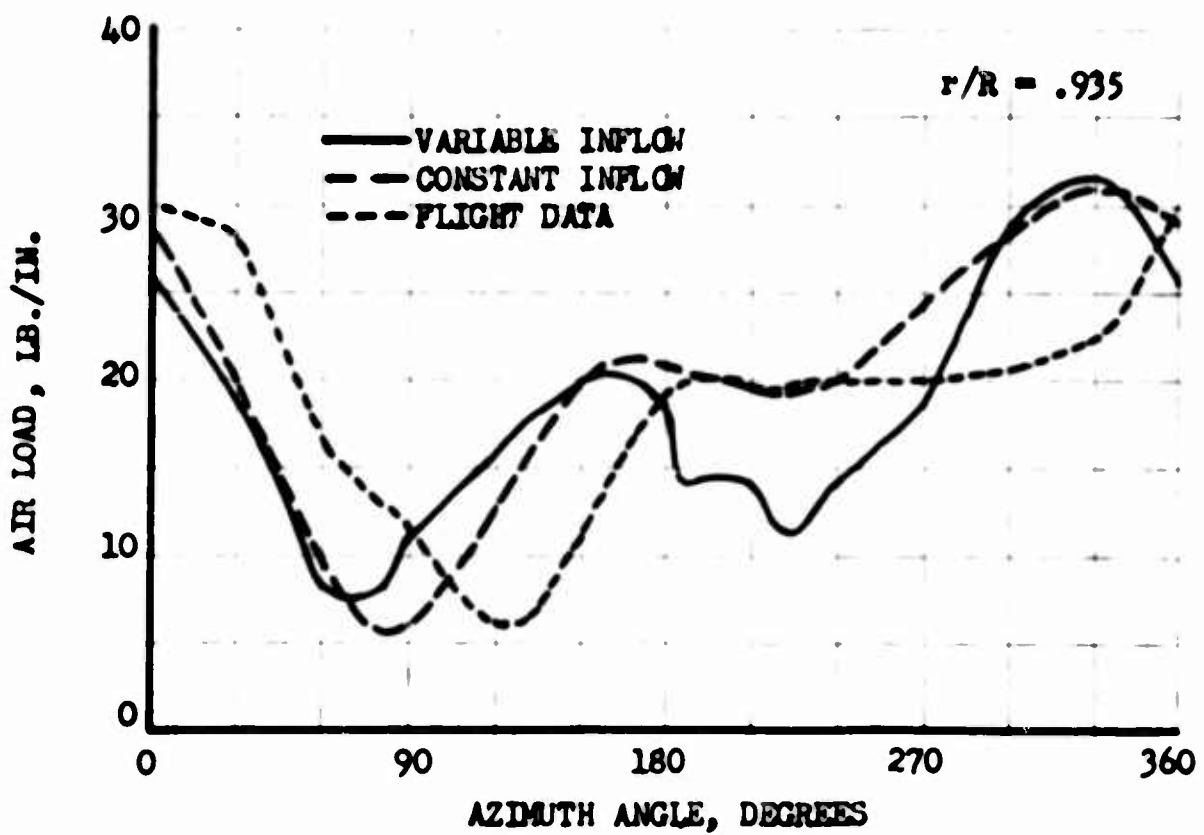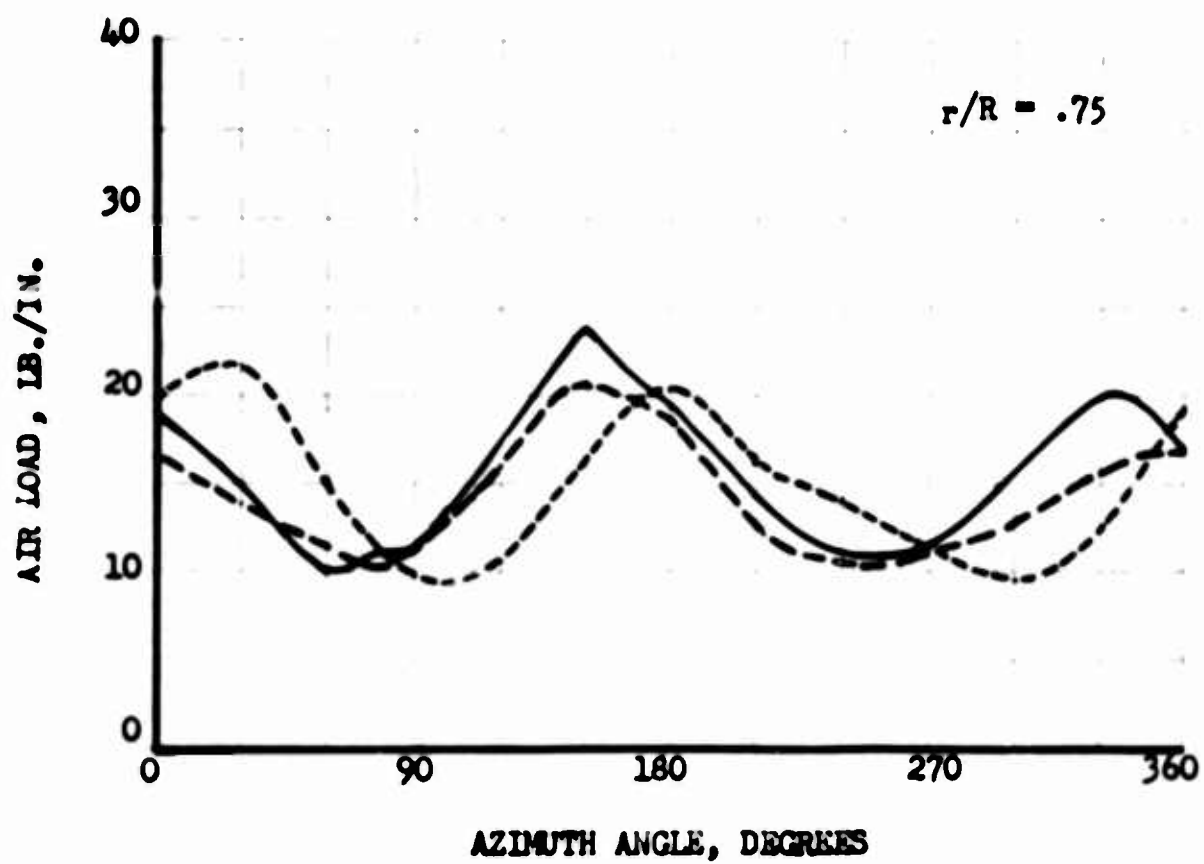COMPARISON OF CONSTANT AND VARIABLE INFLOW.

53

FIGURE 11. H-34 AIR LOADS AT 112 KNOTS
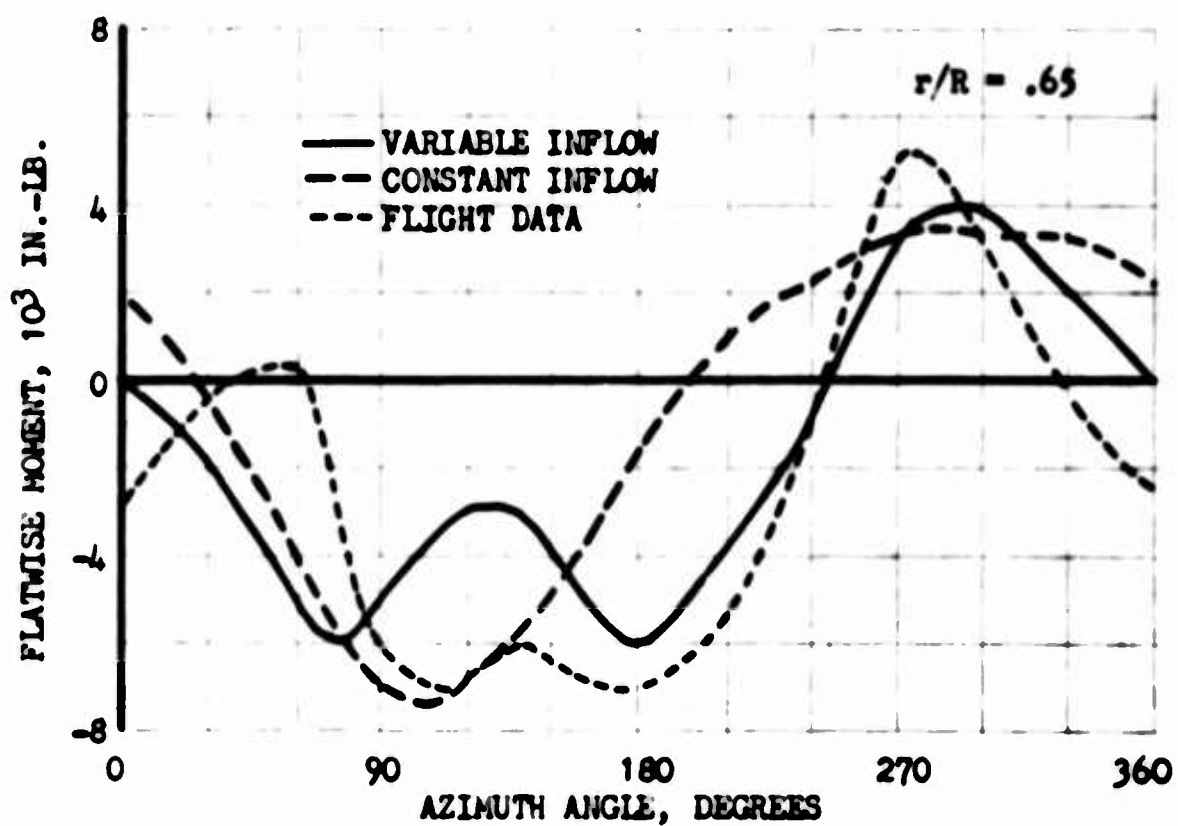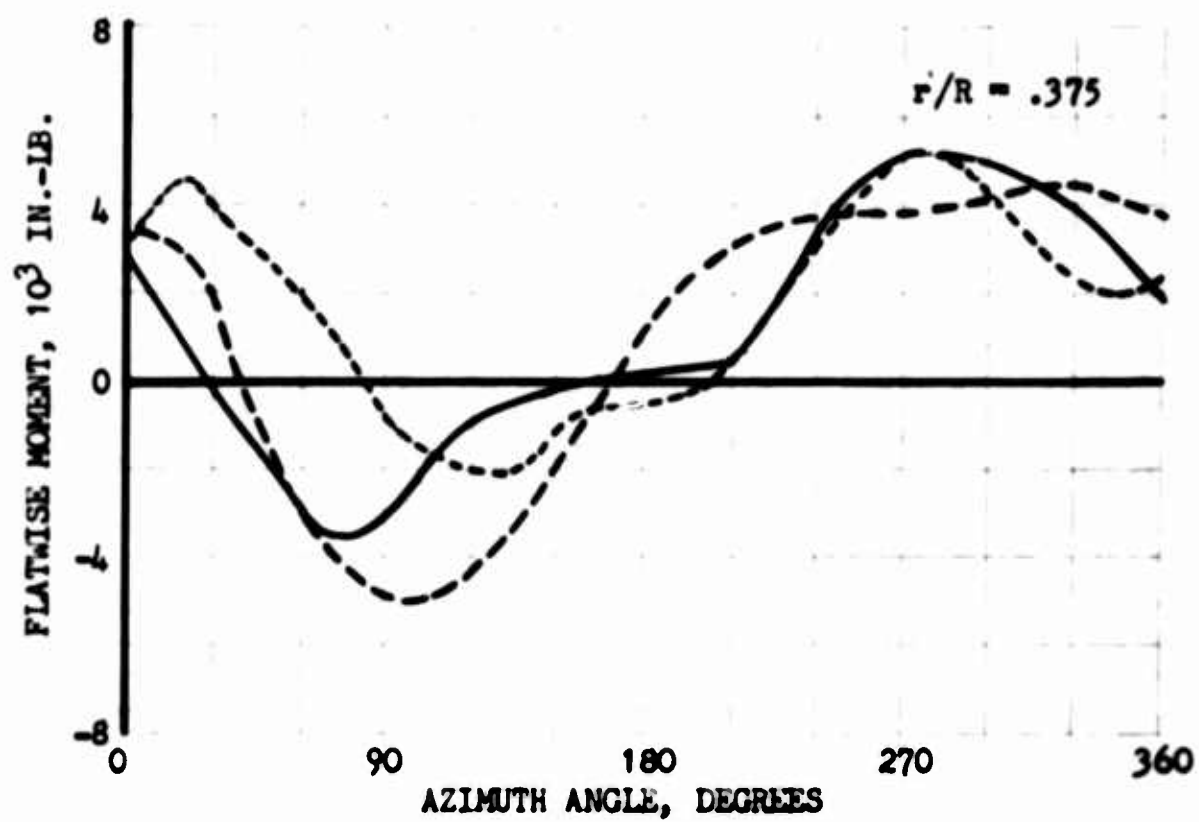COMPARISON OF CONSTANT AND VARIABLE INFLOW.

FIGURE 12. H-34 FLATWISE MOMENTS AT 112 KNOTS
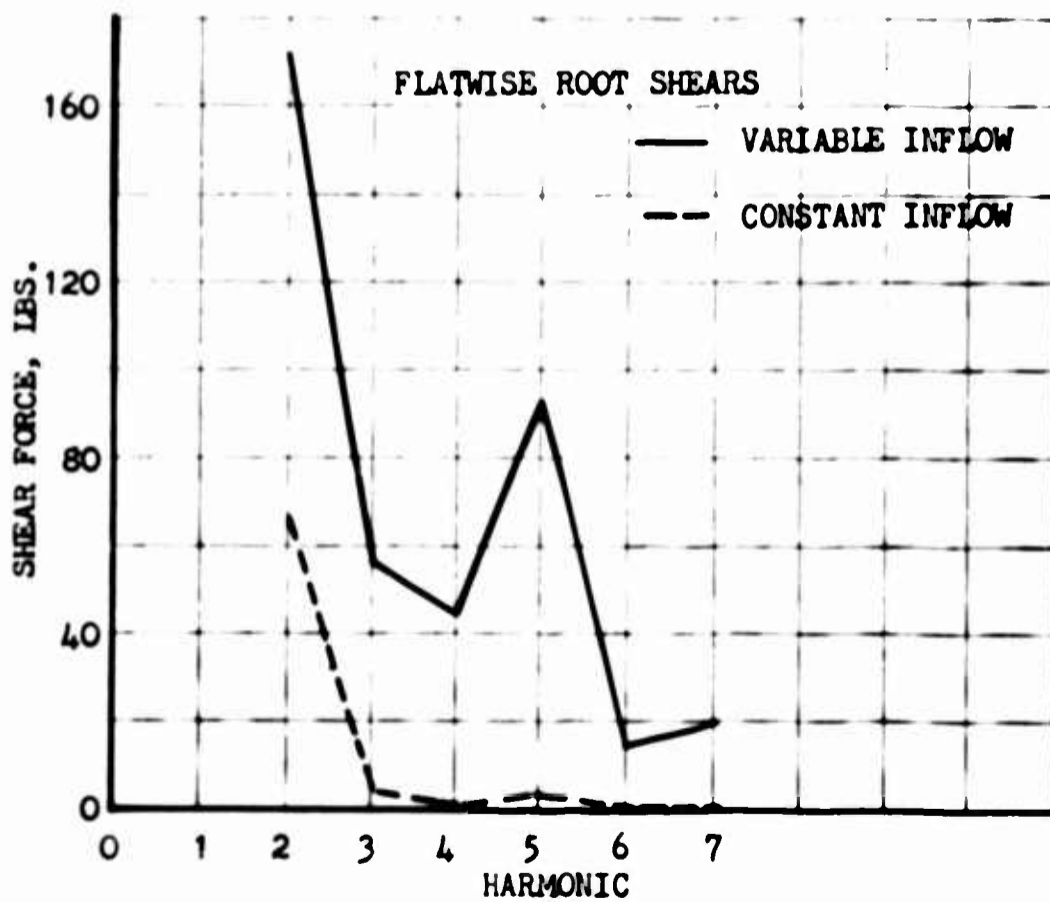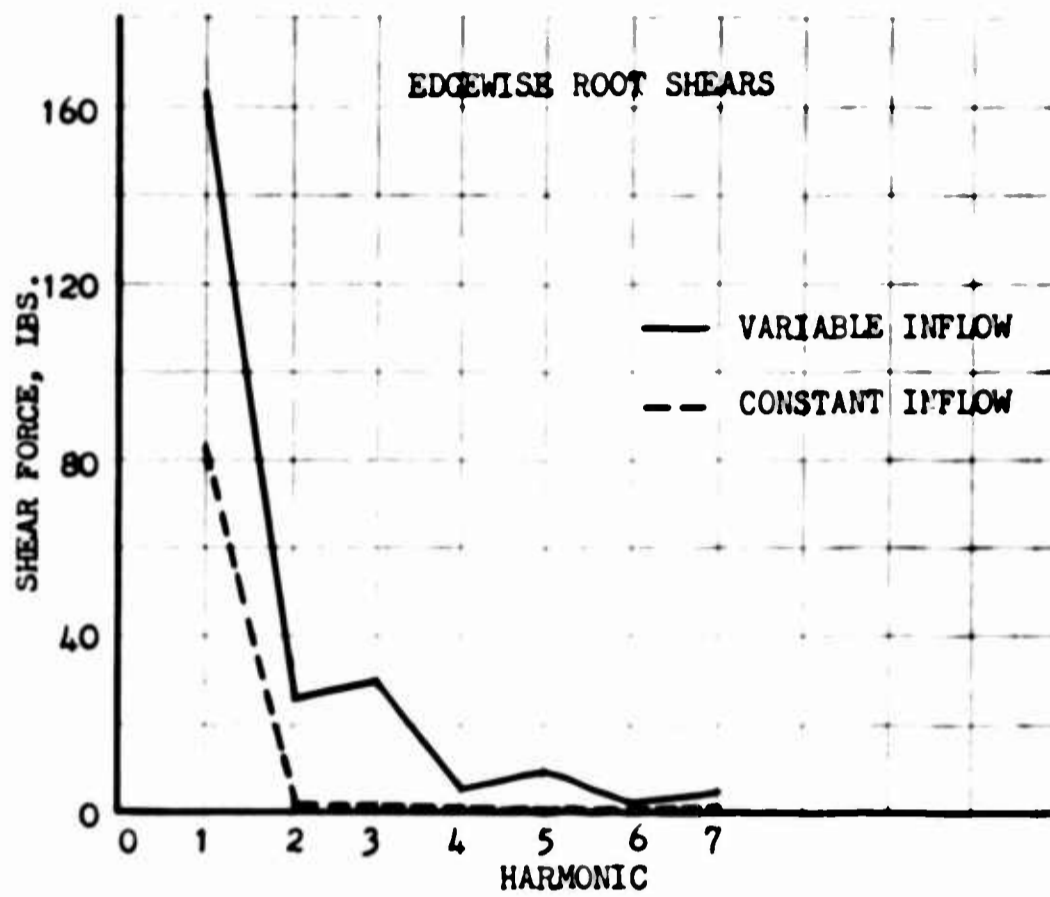COMPARISON OF CONSTANT AND VARIABLE INFLOW.

55

FIGURE 13. CALCULATED HARMONICS OF
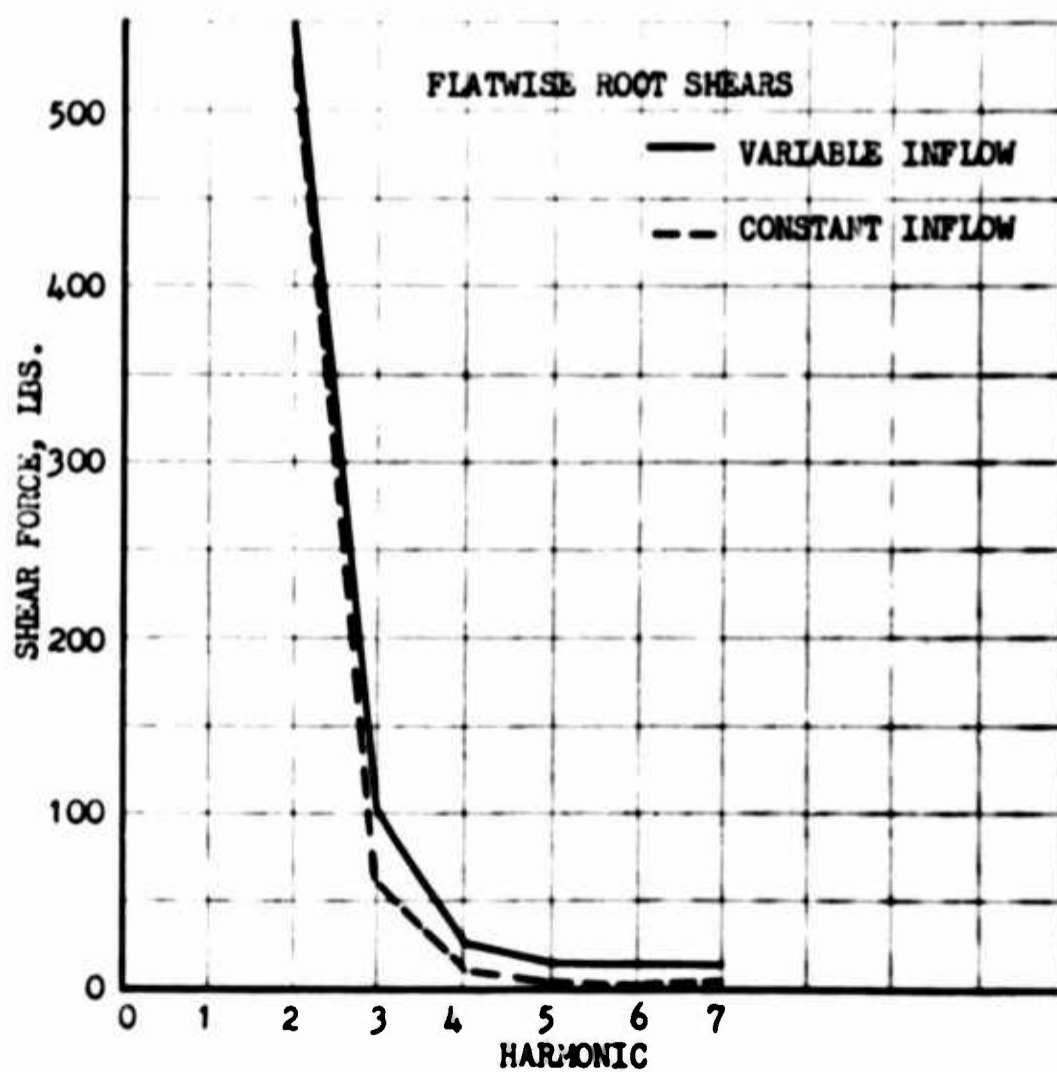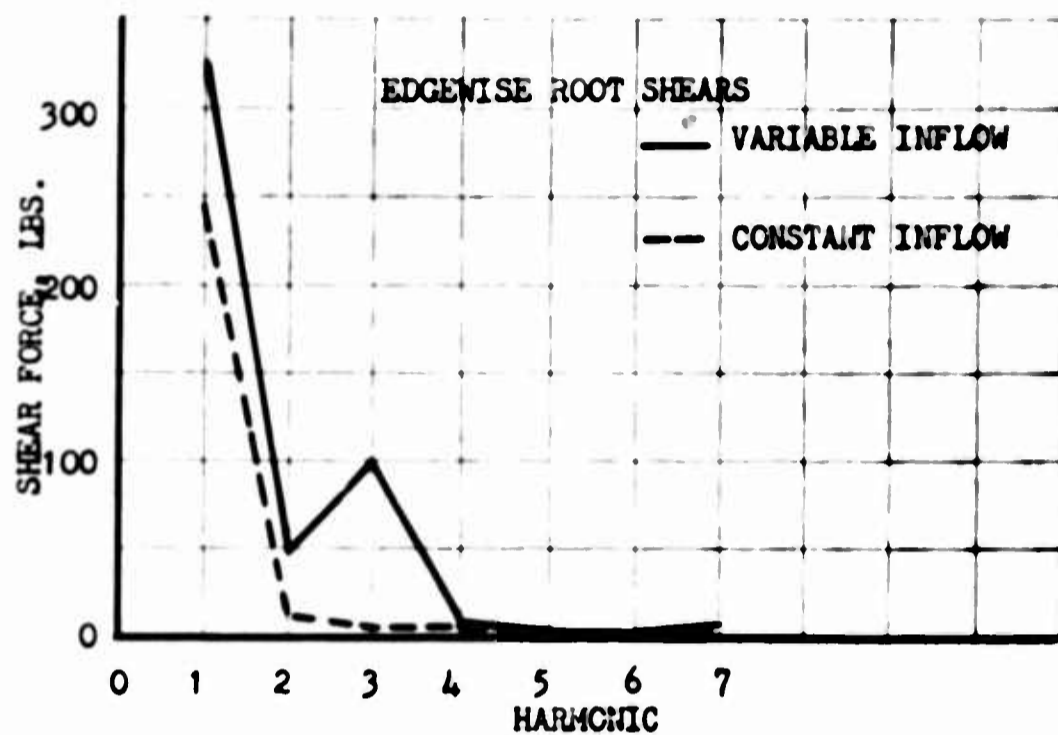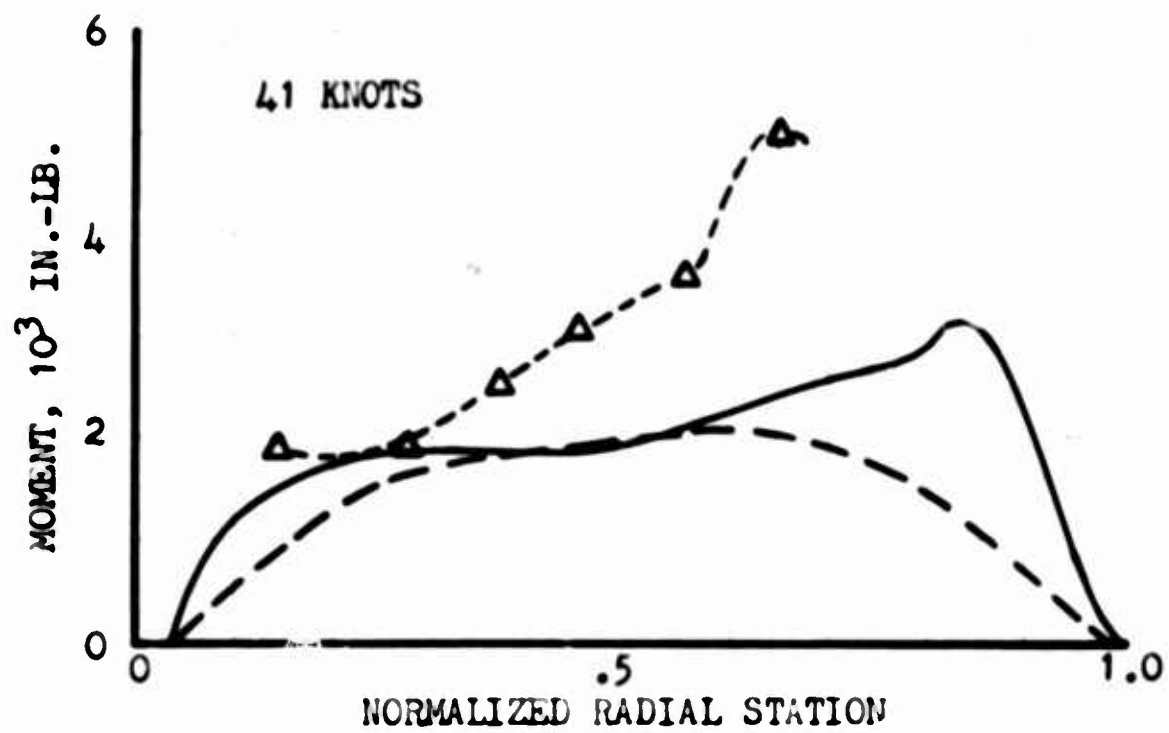ROOT SHEAR FORCES FOR H-34 AT 41 KNOTS (CASE 1)

FIGURE 14.   CALCULATED HARMONICS OF
ROOT SHEAR FORCES FOR H-34 AT 112 KNOTS (CASE 4)
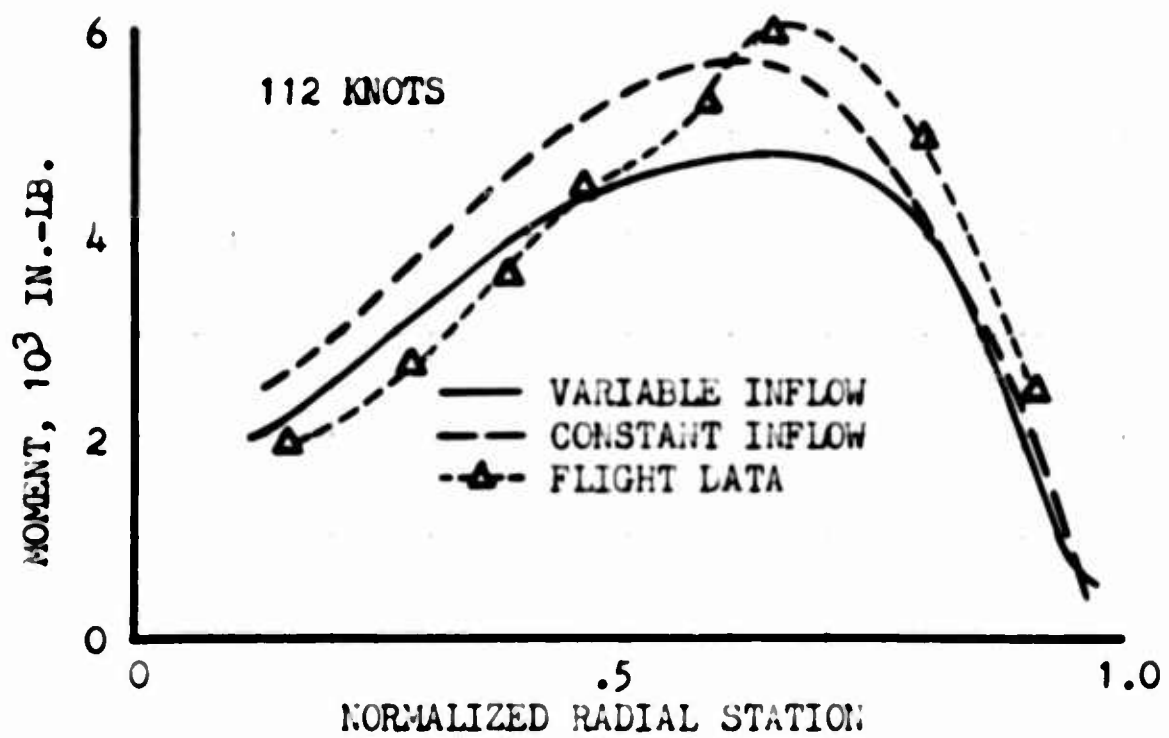
FIGURE 15. ONE-HALF PEAK-TO-PEAK
FLATWISE BENDING MOMENTS FOR THE H-34.

to predict these stresses. Typical results are shown in the form of one-half peak-to-peak bending moment for the H-34 at 41 and 112 knots (Figure 15). At 112 knots fairly good correlation with H-34 data was obtained, but constant inflow gave somewhat better correlation than variable inflow, at least in predicting maximum values. At 41 knots, the use of variable inflow did improve correlation. However, the H-34 data indicated higher values for the moments than did the analysis. It is the high speed flight conditions which produce the high vibratory stresses for which blades are designed for fatigue life. Constant inflow has produced good correlation of the one-half peak-to-peak vibratory stresses at high speeds, and its continued use for blade design can be justified. At high speeds the effects of variable inflow are not as significant. The main contribution to the vibratory stresses at high speeds is made up of the lower harmonics. Constant inflow does not provide the full contribution of the higher harmonics, but does lead to good definition of the lower harmonics. The addition of the higher harmonic terms introduced by the use of variable inflow may lead to less accurate one-half peak-to-peak vibratory stress correlation through phasing errors in the summation of those harmonics.

The main contribution of variable inflow is in its ability to provide better definition of the magnitudes of the higher harmonic blade root shears which are the forces producing airframe vibration. These forces are large at low speeds as well as high speed. The differences in the shear forces given by constant and variable inflow are substantial as was discussed in the previous section.

I.   EFFECT OF INTERHARMONIC DAMPING

The differences between air loads calculated for the H-34 at 70 knots with neutral C.G. and at 73 knots with aft C.G. were larger than were expected. Since azimuthal plots of the difference between calculated air loads for the two cases showed the difference to be primarily in the second harmonic, it was believed that exclusion of interharmonic damping might be the cause of the differences. The reason is that the main difference between the neutral C.G. case and the aft C.G. case is the presence of first harmonic blade flapping about the rotor shaft axis. This flapping coupled with the cyclic pitch effects would cause an indicated difference in the steady and second harmonic air loads. No real difference should exist. It is the role

59

of the damping terms to compensate for effects of flatwise blade motions, either due to flapping or bending, on air loads. Inclusion of only the harmonic damping terms gives satisfactory results for neutral C. G. cases where periodic flatwise blade motions are relatively small. However, the aft C. G. case gives large first harmonic flapping motions relative to the shaft axis. This creates substantial first harmonic damping forces and would create large second harmonic damping forces if the interharmonic damping coefficients were included. The important point here is that the aerodynamic damping forces serve two purposes. First they are corrective forces which modify the undamped air loads calculated for a rigid non-flapping blade to give the true air loads acting on the flapping and bending blade at its actual location in space. These corrective forces do have the characteristics of damping forces and, therefore, serve to damp the motions which a blade would have if excited only by the undamped rigid-blade air loads. The two effects cannot be separated for they are in reality merely two different ways of looking at the same effect. Therefore, exclusion of interharmonic damping forces can be considered to give either insufficiently corrected air loads or inaccurate damping. This can best be seen by considering an example.

At a radial station of $r/R = .89$, the undamped air loads calculated for the neutral and aft C. G. cases show a difference (Figure 16) which is made up primarily of a first and second harmonic. It can be seen that the first harmonic difference is virtually eliminated and only a second harmonic difference remains. The damping force due to first harmonic flapping has cancelled the effect on undamped air loads caused by differences primarily in blade pitch between the two cases. Also shown in Figure 16 is the additional damping force which inclusion of interharmonic damping coefficients for the first three harmonics would produce. This force would greatly diminish the second harmonic content of the different plots and make the air loads for the two C. G. cases match more closely, as they should. On this basis it does appear that the interharmonic damping effects are important when aft C. G. cases are to be considered. Note that if the aeroelastic analysis had been written in terms of a tip path plane axis system and not a shaft axis system, the interharmonic damping effects due to first harmonic flapping would not enter in. The tip path plane would be by definition the plane in which no first harmonic flapping occurred. However, since the tip path plane is defined by blade response, it becomes an unwieldy axis system in which to write the equations of motion.
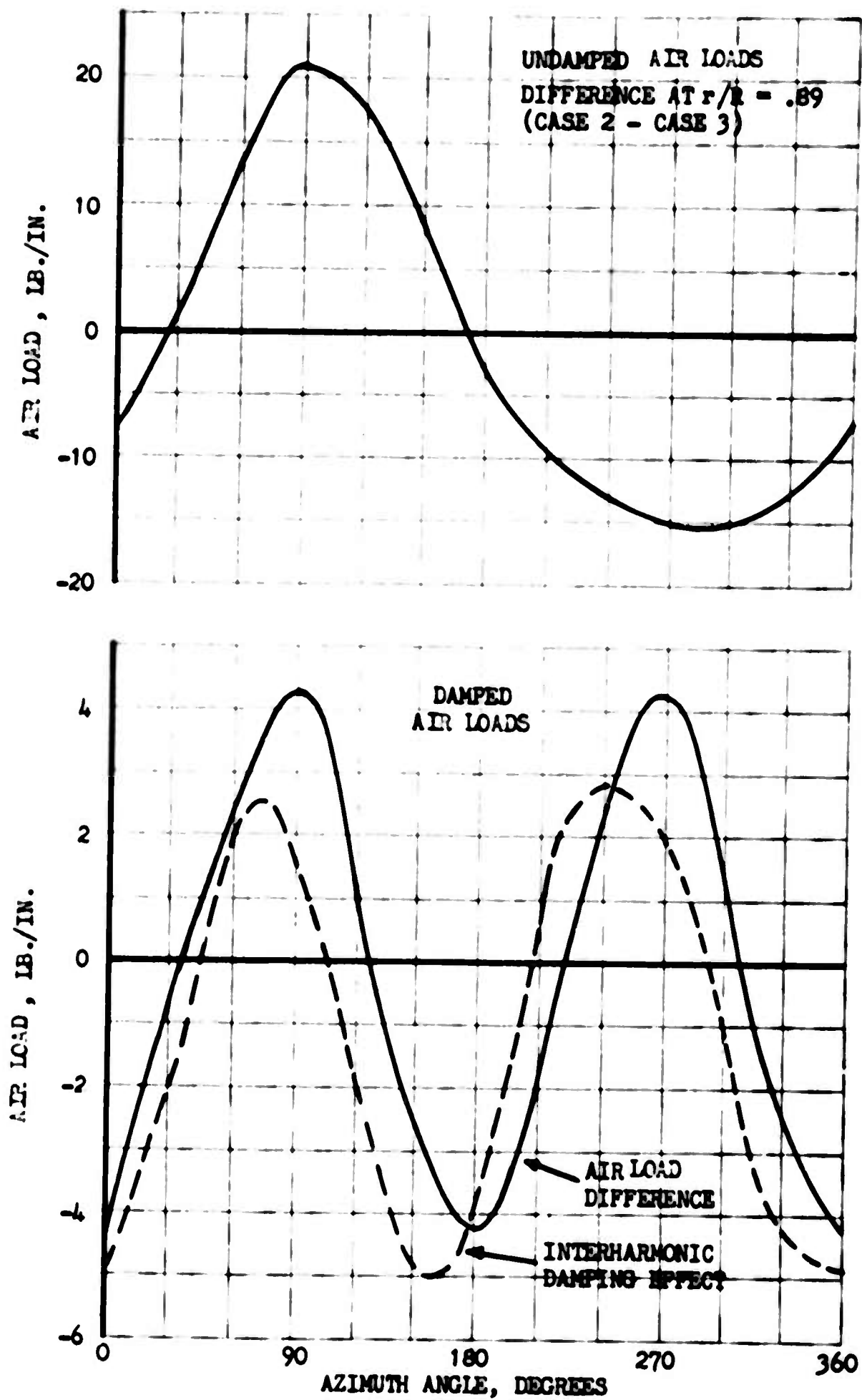
60

FIGURE 16. DIFFERENCES BETWEEN CALCULATED AIR LOADS
FOR H-34 AT 70 KNOTS, NEUTRAL CENTER OF GRAVITY AND 70
KNOTS AFT CENTER OF GRAVITY

Interharmonic damping effects can be important whenever there is a large difference in relative magnitude between adjacent harmonics of blade motion. The first harmonic flapping occuring for the aft C.G. case considered here provides the most obvious example of such a difference, as the second harmonic displacement for this case is relatively small. Other instances of such differences may occur even for neutral C.G. cases, for which there is no flapping. Calculations of interharmonic damping magnitudes for the first three harmonics of the 70-knot and 73-knot cases showed that in the absence of flapping the interharmonic damping terms were not of sufficient magnitude to affect the airload signature. Therefore, no significant improvement in overall correlation of air-load signature can be expected for neutral C.G. cases as a result of the inclusion of interharmonic damping; however better definition of some harmonics may result.

J.   SUMMARY OF DATA CORRELATION

The results of this analytical study have shown equally good correlation for all air speeds considered. Some important differences were noticed between neutral C.G. and aft C.G. cases. This apparently is due largely to the effect of interharmonic damping. Otherwise certain generalities can be made about the results. Harmonics of both air loads and moments showed better amplitude than phase correlation. In fact, the azimuthal plots show a general trend towards a phase shift between test and analytical data. This phase shift is apparent in the air-load data and is carried through to the moments. The similarity in correlation between test and analytical air-load harmonics and corresponding test and analytical bending moment harmonics points toward the conclusion that better definition of air loads is necessary, for bending moment correlation cannot be expected to be better than air-load correlation.

Another interesting result is that a comparison between air loads for the H-34 and the HU-1A at 112 knots indicated better air-load correlation for the HU-1A. One important difference between the two aircraft is in the number of rotor blades. The two-bladed HU-1A could be expected to show better air-load correlation as the basis of greater simplicity of wake geometry. The four-bladed H-34 rotor may produce a wake pattern in which interaction between rotor blades becomes more important. This could lead to actual wake be-

havior which deviates further from the wake model used in the analysis than does the wake of a two-bladed rotor. This observation is merely a speculation at the present time. However, it is certainly obvious that the wake geometry considered in the variable inflow program is an idealization of true wake behavior. It is an idealization which makes possible a significant advance in the ability to predict air loads. Nevertheless, it is not unreasonable to speculate that the approach may be more valid for a simpler two-bladed rotor than for a rotor with a greater number of blades.

MODIFICATIONS TO ANALYSIS

As discussed in the previous section, further modifications to the analysis are necessary to improve correlation with H-34 test data. Results indicated that better definition of the air loads was needed. Therefore, three cases were run to determine the effects of refinements to the basic calculation of air loads. These are as follows:

Case 1A   H-34; steady-state level flight at 41 knots using inflow velocities generated from a radial distribution of assumed downwash.

Case 4A   H-34; steady-state level flight at 112 knots with air loads recalculated to include effect of blade bending.

Case 4B   Extension of case 4A to include effects of blade bending on inflow distribution used to define air loads.

Cases 4A and 4B were run to ascertain the effect flexible motions had on the calculation of induced velocities and air loads. In the aerodynamic analysis, the relation for the vertical component of air velocity on a blade element, U_p, as given below, was modified to accept a radial and azimuthal distribution of flatwise bending slope, β, which was obtained from the fully coupled Myklestad response analysis for Case 4.

$$U_p = \cos\beta \, (V_i + V\sin\alpha_t) + V\cos\alpha_t \sin\beta \cos\psi \qquad (33)$$

The equation used in the standard program is the above equation with

β equal to the steady coning angle.

At the same time, the angle of attack of the blade at each radial station and azimuth position was modified by the addition of torsional deformation of the blade as obtained from the fully coupled analysis for Case 4.

Air loads were then recomputed and the trim conditions once more satisfied. This entire procedure can be repeated until desired convergence is obtained.

The second modification at 112 knots (in Case 4B) was the inclusion of blade deflection on variable inflow calculations. The blade displacements from Case 4 were supplied as input to the variable inflow analysis of Reference 3. The analysis considers the effect of these motions only as local effects along the blade. No change in wake behavior results from the inclusion of flexible motions. The new values for induced velocity which the program calculates are then used in a second pass through the Sikorsky aeroelastic analysis.

A third change was made for the 41-knot case (Case 1A) to determine the importance of wake variations. The wake transport velocity input to the variable inflow program in the other cases was assumed to be equal to the constant induced velocity determined from momentum considerations. It is realized that this assumption is not correct, for it is known that the rotor wake is definitely not comprised of undistorted helical vortices traveling at equal velocities from the rotor. However, as is stated in Reference 3, the question as to what displacement time history should be used for a particular rotor and operating condition remains unsolved. Initial results presented in Reference 3 also indicate that the use of a uniform inflow distribution, determined from momentum considerations, has previously resulted in computed air loads which correlate well with measured air loads for a two-bladed rotor. In addition, no provision is made in the existing variable inflow program for putting in realistic time varying wake transport velocities which take into account wake interaction effects.

The effect of the assumed wake geometry on the resultant induced velocity and air-load distributions is of greatest significance at low flight speed conditions because the wake velocity with respect to the rotor, and thus the distance between a specific wake revolution

64

and the rotor, decreases with decreasing flight speed and rotor angle of attack. It was therefore reasoned that the results for the H-34 helicopter 41-knot flight condition are the most sensitive to the wake geometry assumption.

An attempt had been made to use the variable induced velocity distribution from the variable inflow program for the 41-knot condition as the wake transport velocity input in a second pass through the program. This resulted in a divergent situation with extreme fluctuations in loading due to the passage of blades close to or actually through vortices generated by previous blades.

In order to obtain additional information on the effect of the assumed wake geometry for the results included herein, a radially varying velocity distribution was used to define the wake geometry (Figure 17). This radial velocity distribution consists of the steady component of the velocity distribution used in the divergent case described in the previous paragraph. The azimuthal variation of velocity was neglected. With this radially varying distribution convergence was obtained. It is noted that the average inflow value from the variable inflow results did not equal the momentum value. This is due to the fact that the induced velocities from the variable inflow program used to define the wake are the velocities that the blades encounter and are in the rotating coordinate system, and thus are not the true wake transport velocities which should be defined in the non-rotating coordinate system. To correct the inflow distribution, the inflow values at each radial station were decreased by three feet per second so that the average value of inflow across the rotor disc matched the momentum value.

The results of the three refined cases show that the modifications produced little change in either air loads or bending moments.

Case 4A and 4B show only small changes in results versus azimuth and in magnitude and phase of harmonic content.

Shown in Figure 18 is a comparison of air load at r/R equal to .96 for the standard Case 4 versus Cases 4A and 4B. Also shown is the result of applying the variable inflow distribution of Case 4B without introducing other flexibility effects on the air-load calculations. As can be seen, small differences in phase occur and the largest change in magnitude occurs at around ψ = 225 degrees for the com-
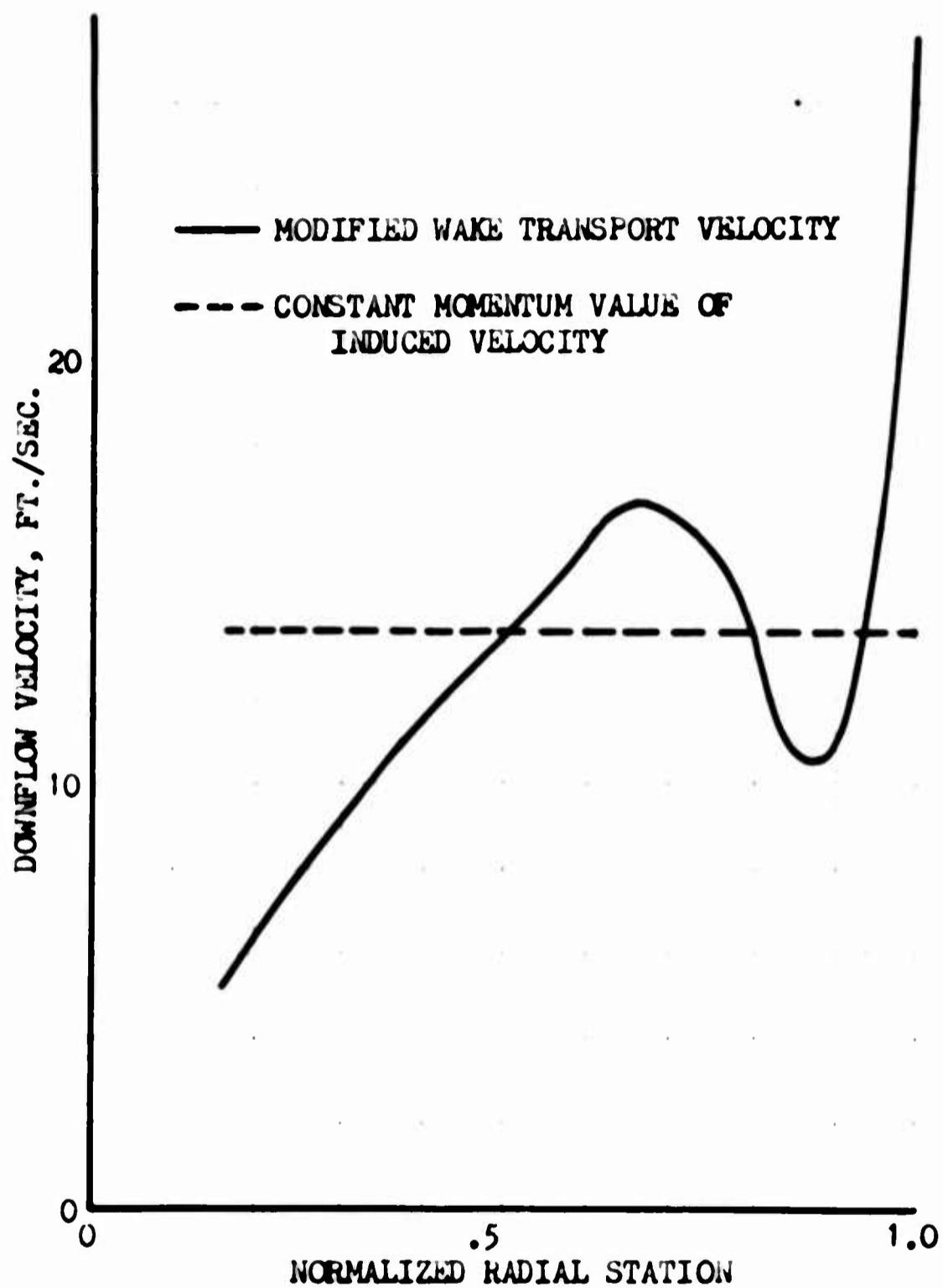
65

FIGURE 17.   RADIAL DISTRIBUTION OF INDUCED VELOCITY
USED AS WAKE TRANSPORT VELOCITY INPUT
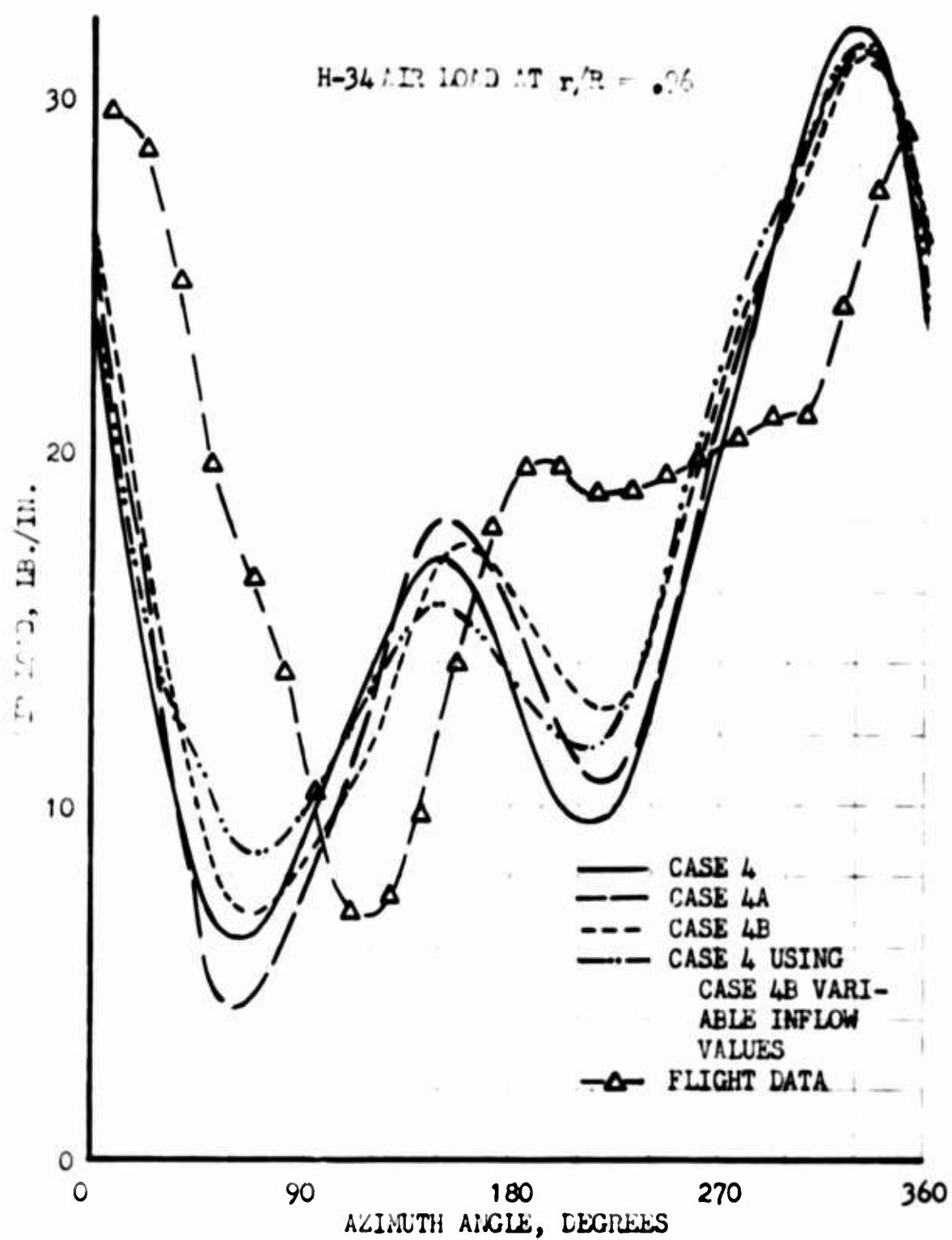TO THE VARIABLE INFLOW PROGRAM. H-34
AT 41 KNOTS.

FIGURE 18. EFFECT OF MODIFICATIONS
ON H-34 AIRLOAD COMPUTATIONAL
MODEL AT 112 KNOTS

67

bined flexibility case. The fact that blade deflection has as little effect on air loads as is shown is of interest. This indicates that the effects of higher harmonic flapping on U_p and the effect of torsion on blade angle of attack are only of second order.

For Case 1A, a significant change in air loads occurs in the 180-degree azimuth, .85 blade station region. This is due to the passage of the tip wake of the previous blade directly beneath this region. By assuming a greater wake velocity generated at the blade tip the tip wake is moved farther away from the rotor in a given period of time and thus induces a lower velocity at the blade. Relatively small changes are noted elsewhere in the rotor disc, due to the fact that the radial distribution assumption introduces small differences of induced velocity input in comparison to the momentum value except at the tip as is shown in Figure 17. It is emphasized that this simplified assumption for the wake transport velocities represents only an initial effort to obtain some indication of the influence of the assumed wake geometry on the induced velocity distribution and associated air loads and bending moments.

In general, the little improvement in correlation resulting from these modifications indicates that more fundamental changes are needed, such as the inclusion of wake contraction effects in the variable inflow analysis.

EVALUATION OF ANALYSIS

The results of this program have shown that fairly good correlation can be obtained from the combination of variable inflow with the fully coupled aeroelastic analysis. It is also quite obvious that further improvement in correlation should be possible. The process of developing improvements for the aeroelastic analysis and the incorporation of the variable inflow analysis have served to demonstrate the complexity of the problem. A great number of variables is involved in a rotor analysis. The success achieved with the analytical methods chosen was in many ways encouraging and in other ways disappointing. In either case much valuable information concerning the importance of various parameters was obtained.

The basic question that arises is what improvements should be made to improve correlation. There are three distinct areas to

be considered: the basic blade dynamic analysis, the trim conditions used, and the air-load analysis. The air-load analysis is the most complex of these areas, for it depends not only on the inflow analysis, but also on the way in which the inflow is combined with trim conditions and blade dynamics.

The basic Myklestad blade analysis used was shown in SUBSTANTIATION OF METHODS on page 3 to give valid results for a nonrotating beam. It was found that the number of mass points chosen is adequate to define accurately the blade response. There are certain improvements which can be made to this analysis. When using an analysis based on harmonics, it must be appreciated that the harmonics are not independent, but that the use of fully coupled motions introduces some interharmonic coupling terms. The analysis, as presently formulated, neglects these terms on the basis that deflections are small, and interharmonic effects due to such deflections can be neglected. It is true that the 73-knot aft C.G. case pointed out the importance of the interharmonic damping effect of first harmonic flapping when using the shaft-axis system. In that case, the flapping motion, which is a rigid-body rotation of the blade and not a small deflection, proved to have an important effect. Consideration should be given to extending the analysis to incorporate this and any other significant interharmonic effects. Effects to be considered would include such items as the changes that blade dynamic rotation produces on flatwise and edgewise bending through corresponding rotation of the principal axes of stiffness of the blade.

The basic trim procedure used is considered to give a good definition of trim conditions. Agreement is obtained both for gross weight, and for the root-shear requirements by the double iteration technique used for thrust moment and root shears. The pitch angles obtained through use of this procedure differed somewhat from the measured values as shown in Table V on page 46. Collective pitch angle correlation showed the analytical values to be generally low. However, except for the HU-1A analysis (see page 39), the radial distribution of steady air loads correlated well, showing that the analytical thrust values matched test data. Cyclic pitch values correlate closely, in general. The differences which do exist in cyclic pitch values and in phasing between test and analytical blade response are related. The inflow distribution as well as rotor trim conditions affects pitch values and the resulting air loads. The differences are believed to be more dependent on the inflow values than on the trim

conditions which were used.

Another item which might be considered as a trim condition is the determination of lag-damper coefficients. This is most important for good edgewise moment correlation. While correlation of edgewise moments could be improved, correlation was found to be about the same for the H-34, with lag dampers, and the HU-1A, which has no lag dampers. While this does not verify the validity of the present lag-damper coefficient analysis, it does indicate that the lag damper analysis is not one of the prime reasons for lack of correlation.

The problem of improving correlation appears to center on the determination of air loads, which is the most complex part of the program. Inaccuracies in air-load calculation can occur from two sources. First, the inflow velocities can be inaccurate. Secondly, the way in which rotor dynamics is incorporated in the air load calculations can introduce errors. The differences which definition of induced velocities can make is quite obvious from comparison of the results obtained using constant inflow with those using variable inflow. Therefore, the degree to which the variable inflow analysis of Reference 3 simulates the variable inflow distribution through a rotor is most important. This will be discussed in subsequent paragraphs. Consider first the calculation of air loads using a given inflow distribution.

Initially, undamped air loads are calculated for the rotor system using the variable inflow distribution as well as rotor plane inclinations and blade pitch determined from the iteration procedure. Airloads are corrected for blade flapping and bending motion effects by the introduction of aerodynamic damping terms. The importance of including interharmonic damping coefficients when using the shaft-axis system has already been discussed. It was shown that inclusion of interharmonic damping for the H-34 73-knot aft C.G. case would make those air loads compare with the 70-knot neutral C.G. air loads. However, calculated air loads for 70 knots did not correlate with test data as well as would be desired. Thus while it would appear that inclusion of interharmonic damping would improve air-load definition, this improvement would not be sufficient to achieve precise correlation.

The effect of blade bending and torsion on blade angle of attack

70

was also introduced into the air-load calculation in the modified H-34 112-knot case. However, the small changes in results which this made would strongly indicate that this flexibility correction is not the key to better correlation.

There remains the complex area of the variable inflow analysis. Further improvement in the definition of the variable inflow distribution over the rotor is necessary for substantial improvement in correlation. The variable inflow analysis of Reference 3 is an excellent step towards accurate air-load definition. However, the model used still represents a substantial simplification of rotor wake behavior. It is recognized that improvements in the analysis are presently being investigated. Such improvements should further enhance the potential of this analysis.

It is believed that full use has been made of the capabilities of the present variable inflow analysis in this program. Further manipulations of input values cannot be expected to yield much improvement in correlation. One of the modified cases, Case 1A, used a radial wake velocity variation with little resulting improvement. The inability to obtain convergence with azimuthal wake velocity variation in earlier work was unfortunate, for it seems probable that azimuthal wake velocity variation would improve the wake description and increase the higher harmonic content of the air loads. This area bears further investigation.

There are certainly numerous areas in the variable inflow analysis which should be studied to determine their importance. The list of assumptions used in the analysis given in THE CORNELL VARIABLE INFLOW PROGRAM on page 27 is useful in this regard, for each of these assumptions should be evaluated. Probably the area of greatest concern is the definition of wake geometry. The assumption that wake vortex elements retain the strength and velocity imparted to them as they leave the blade is not realistic. Wake vortex interaction could be important. Wind tunnel tests have shown the importance of hub and fuselage interference effects both on wake geometry and on flow through the rotor. The true wake geometry is more complex than that which can be derived with the assumptions used in the present analysis. Further refinements do appear to be necessary to obtain a more realistic wake definition.

The use of vortex elements based on lifting line theory rather

71

than finite vortex and lifting surface theory may also prove to be important, especially in two areas. First, the treatment of shed vortices in Reference 3 may not influence inflow correctly during the important first azimuthal increment due to the finite chord of the blade. The use of vortex elements may not give adequate definition of the airflow behavior near the blade tip. The tip area is most important for defining the response of the entire blade. The sharp discontinuity at the tip resulting from the lifting line theory may lead to significant errors. The data show that air-load correlation near the tip does need further improvement.

To sum up, it would appear that as presently formulated the variable inflow analysis and the Sikorsky aeroelastic analysis can give fairly good definition of rotor blade dynamics. The improvements in correlation which were obtained make this combined analysis a more useful design tool than has been available. Both analyses have room for improvement. However, significant improvements in correlation can be made by combining the present Sikorsky aeroelastic analysis with a refined variable inflow analysis. The development of the present variable inflow analysis by Cornell Aeronautical Laboratory has been an important contribution to rotor system analysis. Their continued interest and the interest of others in this field should lead to even better definition of inflow in the near future.

CONCLUSIONS

The purpose of this program was to develop a blade rotor dynamic analysis combining the Sikorsky blade analysis with the CAL variable inflow analysis of Reference 3. Results of this analysis were correlated with flight test data. This procedure has demonstrated the accuracy which can be obtained by this analysis.

It has also provided an opportunity to gain a better understanding of the significance of the various parameters and methods considered. As a result a number of conclusions can be drawn from this study. These are summarized below.

A. CORRELATION WITH TEST DATA

1. The combined Sikorsky-CAL analysis provides an improved design tool for the prediction of rotor dynamic response for steady-state level flight. Better correlation with flight test data was obtained using variable inflow than has been obtained previously with constant inflow. The improvement is most significant at low airspeeds.

2. General correlation between analysis and test was fairly good. Amplitudes of harmonics of air loads, bending moments, and torsional moments correlated better than do azimuthal phase angles. There is a trend throughout the correlation study toward a consistent shift in phase angle between test data and analysis.

3. Larger and more realistic values for root-shear forces were obtained using variable inflow.

4. The variable inflow analysis does not match the good correlation of peak-to-peak stress values obtained using a constant inflow analysis at the high speed conditions used for blade design.

5. Correlation was limited by the accuracy of air-load calculations. Flatwise moment correlation corresponded closely to correlation of air loads, indicating that improved air-load definition would improve moment correlation.

6.   Air-load definition can be most significantly improved by refinement in methods for determining variable inflow.

B.   EFFECT OF IMPORTANT PARAMETERS

1.   The inclusion of blade bending deflections in the variable inflow analysis produces only minor changes in inflow velocities. These changes have little effect on air loads. Blade bending deflections do have an important effect on air loads through the aerodynamic damping expressions in the dynamic analysis. The inclusions of blade torsional deformations and the higher harmonics of radial slope of the blade due to bending had little effect on air loads.

2.   Changes in first harmonic flapping resulting from shifts in C.G. location have little effect on air loads for an articulated rotor with moderate offset. At present the analysis does indicate a change in air loads with flapping. This is due to the use of a shaft-axis reference system. The addition of interharmonic damping terms in the analysis would compensate for this change.

3.   Careful definition of the physical and aerodynamic representation of the blade tip area is essential. Closely spaced blade stations were required near the tip for adequate definition of vortex effects and centrifugal force effects. A moment boundary condition at the blade tip was required to account for the centrifugal forces of the rubber- mounted blade counterweights reacting against the blade tip cap of the H-34. Such reactions are not normally encountered at the blade tip.

RECOMMENDATIONS

While the results of this program show that improved correlation has been obtained, there obviously is still room for improvement. The following are some of the areas which should be considered for further research.

1. Continued development of the variable inflow analysis to provide refinements in inflow predictions. Better definition of wake geometry is an important aspect of such work.

2. Further development of the aeroelastic analysis to consider inclusion of significant interharmonic effects such as interharmonic damping.

3. Incorporation of the combined analysis used in this program into a fully integrated rotor system and airframe analysis using the basic procedure developed by Sikorsky Aircraft (Reference 5). Rotor and airframe dynamic response, and the interaction between the two subsystems would then be solved for simultaneously by matching the impedances of the fuselage hub and the blade root. This would provide a more useful design tool but would not be expected to provide improved air-load correlation. The shears at the blade root however, should be noticeably improved.

REFERENCES

- 1. Bell Helicopter Company, Measurement of Dynamic Air Loads on a Full Scale Semi-rigid Rotor, TCREC Technical Report 62-42, Bell Helicopter Company Report 525-099-001, U. S. Army Aviation Laboratories*, Fort Eustis, Virginia, December, 1962.

2. Blankenship, B. L., and Harvey, K. W., A Digital Analysis for Helicopter Performance and Rotor Blade Bending Moments, Journal of the American Helicopter Society, Volume 7, Number 4, October, 1962.

3. Cornell Aeronautical Laboratory, A Method for Computing Rotary Wing Airload Distributions in Forward Flight, TCREC Technical Report 62-44, U. S. Army Aviation Laboratories Fort Eustis, Virginia, CAL Report BB-1495-S-1, July, 1962.

4. Critzos, C., Heyson, H., and Boswinkle, R., Jr.: Aerodynamic Characteristics in High Speed Flight, I. A. S. Paper Number 63-72, January, 1963.

5. Gerstenberger, W. and Wood, E. R., Analysis of Helicopter Aeroelastic Characteristics in High Speed Flight, I. A. S. Paper Number 63-72, January 1963.

6. Information and Preliminary Data on Helicopter Rotor Blade Dynamic Airloads and Moments as Measured in Flight, Letter to U. S. Army TRECOM from NASA, Langley Research Center, May 24, 1961.

7. Piziali, R., Daughaday, H., and DuWaldt, F.: Rotor Airloads Proceedings CAL/TRECOM Symposium, Volume 1, Buffalo, New York, June 26-28, 1963.

8. Piziali, R. and DuWaldt, F.: Computed Induced Velocity, Induced Drag, and Angle of Attack Distributions for a Two-Bladed Rotor, Proceedings of the 19th Annual Forum of the American Helicopter Society, Washington D. C., May, 1963.

* Formerly Transportation Research Command

9. Scheiman, J. and Ludi, L. H.: Qualitative Evaluation of Effect of Helicopter Rotor-Blade Tip Vortex on Blade Airloads. NASA TN D-1637, May, 1963.

10. Scheiman, J.: A Tabulation of Helicopter Rotor Blade Differential Pressures, Stresses, and Motions as Measured in Flight. NASA TM X-952, March, 1964.

11. Sikorsky Aircraft, Parametric Investigation of the Aerodynamic and Aeroelastic Characteristics of Articulated and Rigid (Hingeless) Helicopter Rotor Systems, TCREC Technical Report 64-15 Sikorsky Engineering Report 50359, U. S. Army Aviation Materiel Laboratories, Fort Eustis, Virginia, April 1964.

12. Wood, E. R. and Hilzinger, K. D., A Method for Determining the Fully Coupled Aeroelastic Response of Helicopter Rotor Blades, Proceedings of the American Helicopter Society, May, 1963.

77

APPENDIX I

DEVELOPMENT OF CLOSED-FORM ANALYTICAL SOLUTION
FOR A UNIFORM BEAM

The general problem of a uniform pinned-free nonrotating beam of mass μ per unit length excited by a uniformly distributed p'/rev harmonic force, F_O Sin $p'\omega$ t, is expressed by the following nonhomogeneous partial differential equation.

$$a^2 y_{rrrr} + y_{tt} = k' \sin p'\omega t \qquad (34)$$

where $a^2 = E I/\mu$, $k' = F_O/\mu$, $p' = 1, 2, \ldots n$ and ω is the exciting frequency. The letter "y" denotes the displacement of the centroid of any section at right angles to the unstrained central line. Subscripts r and t indicate the respective differentiation.

The equation of flexural vibration was derived on the basis of the following assumptions:

1. Plane sections remain plane.

2. Stress is proportional to strain.

3. Bending occurs in the principal plane.

4. Slope of deflection curves are small.

5. Deflection due to shear is negligible.

6. Rotary inertia effect is negligible.

The above equation is readily reduced to a homogeneous ordinary differential equation of amplitude by the steady-state solution in the form.

$$y(r, t) = X(r) \sin p'\omega t \qquad (35)$$

where $X(r)$ is the spatial variation of the amplitude.

Sin $p'\omega$ t is the steady-state time variation of the deflection. Substituting (35) in (34), we obtain the deflection equation

79

$$X_{rrrr} = -\frac{p^2}{a^2} X = k$$

where $\qquad\qquad k = F_0/\mu a^2 \quad$ and $\quad p = p'\omega$

Considering only the homogeneous portion of Equation (36). The complementary solution of the amplitude becomes a function of trigonometric and hyperbolic functions.

$$X(r)_c = A\sin\sqrt{p/a}\ r + B\cos\sqrt{p/a}\ r + C\cosh\sqrt{p/a}\ r + D\sinh\sqrt{p/a}\ r \tag{37}$$

where A, B, C and D are constants, whose
value depends upon the end constraints.

The particular solution of Equation (36) can be written in the form:

$$X(r)_p = \frac{-a^2}{p^2}\ k \tag{38}$$

Thus the general solution of the amplitudes is defined as the sum of its complementary and particular form.

$$X(r) = X(r)_c + X(r)_p$$

$$X(r) = A\sin\sqrt{p/a}\ r + B\cos\sqrt{p/a}\ r + C\cosh\sqrt{p/a}\ r +$$

$$D\sinh\sqrt{p/a}\ r - \frac{a^2}{p^2}\ k \tag{39}$$

The boundary conditions of a pinned-free nonrotating beam are:

1. Deflection $\quad y(o, t) = X(o) \sin p'\omega\ t \tag{40}$

2. Moment $\quad -EI\ y_{rr}(o, t) = -EI\ X_{rr}(o) \sin p'\omega\ t$

3. Moment $\quad -EI\ y_{rr}(L, t) = -EI\ X_{rr}(L) \sin p'\omega\ t$

4. Shear $\quad -EI\ y_{rr}(L, t) = -EI\ X_{rrr}(L) \sin p'\omega\ t$

Introducing these relations into (39), the constants are evaluated

$$A = \frac{(a^2/p^2)\frac{k}{2}\left\{1-\sin\sqrt{p/a}\,L\,\sinh\sqrt{p/a}\,L-\cos\sqrt{p/a}\,L\,\cosh\sqrt{p/a}\,L\right\}}{\left\{-\cos\sqrt{p/a}\,L\,\sinh\sqrt{p/a}\,L+\sin\sqrt{p/a}\,L\,\cosh\sqrt{p/a}\,L\right\}} \tag{41}$$

$$B = \frac{1}{2}(a^2/p^2)k \tag{42}$$

$$C = \frac{1}{2}(a^2/p^2)k \tag{43}$$

$$D = \frac{(a^2/p^2)\frac{k}{2}\left\{\cosh\sqrt{p/a}\,L\,\cos\sqrt{p/a}\,L-\sinh\sqrt{p/a}L\,\sin\sqrt{p/a}\,L-1\right\}}{\left\{\cosh\sqrt{p/a}\,L\,\sin\sqrt{p/a}\,L-\sinh\sqrt{p/a}\,L\,\cos\sqrt{p/a}\,L\right\}} \tag{44}$$

The coefficients being known, we are able to calculate steady-state deflections, and likewise by successive differentiation the steady-state slopes, moments and shears produced by a uniformly distributed p'/rev. harmonic force.

By virtue of equation (35) the steady-state deflection along the nonrotating beam is given by:

$$y(r,t) = \frac{a^2 k}{2p^2}\left\{\Phi_1\sin\sqrt{p/a}\,r + \Phi_2\sinh\sqrt{p/a}\,r + \cos\sqrt{p/a}\,r - \cosh\sqrt{p/a}\,r - 2\right\}\sin p'\omega t \tag{45}$$

Differentiating Equation (45), the slope becomes:

$$y_x(r,t) = \frac{k}{2}\left(\frac{a}{p}\right)^{3/2}\left\{\Phi_1\cos\sqrt{p/a}\,r + \Phi_2\cosh\sqrt{p/a}\,r - \sin\sqrt{p/a}\,r + \sinh\sqrt{p/a}\,r\right\}\sin p'\omega t \tag{46}$$

The spanwise moment distribution is defined as:

$$M = E I y_{rr}$$

81

$$M = \frac{EIak}{2p} \left\{ -\Phi_1 \sin\sqrt{p/a}\,r + \Phi_2 \sinh\sqrt{p/a}\,r - \right.$$

$$\left. \cos\sqrt{p/a}\,r + \cosh\sqrt{p/a}\,r \right\} \sin p'\omega t \qquad (47)$$

Finally the shear distribution becomes:

$$Q = E I y_{rrr}$$

$$Q = \frac{E I \sqrt{a/p}\,k}{2} \left\{ -\Phi_1 \cos\sqrt{p/a}\,r + \Phi_2 \cosh\sqrt{p/a}\,r + \right.$$

$$\left. \sin\sqrt{p/a}\,r + \sinh\sqrt{p/a}\,r \right\} \sin p'\omega t \qquad (48)$$

Quantities Φ_1 and Φ_2 appearing in Equations (45), (46), (47), and (48) are defined by the following expressions.

$$\Phi_1 = \left\{ \frac{1 - \sin\sqrt{p/a}\,L \sinh\sqrt{p/a}\,L - \cos\sqrt{p/a}\,L \cosh\sqrt{p/a}\,L}{-\cos\sqrt{p/a}\,L \sinh\sqrt{p/a}\,L + \sin\sqrt{p/a}\,L \cosh\sqrt{p/a}\,L} \right\} \qquad (49)$$

$$\Phi_2 = \left\{ \frac{\cosh\sqrt{p/a}\,L \cos\sqrt{p/a}\,L - \sinh\sqrt{p/a}\,L \sin\sqrt{p/a}\,L - 1}{\cosh\sqrt{p/a}\,L \sin\sqrt{p/a}\,L - \sinh\sqrt{p/a}\,L \cos\sqrt{p/a}\,L} \right\} \qquad (50)$$
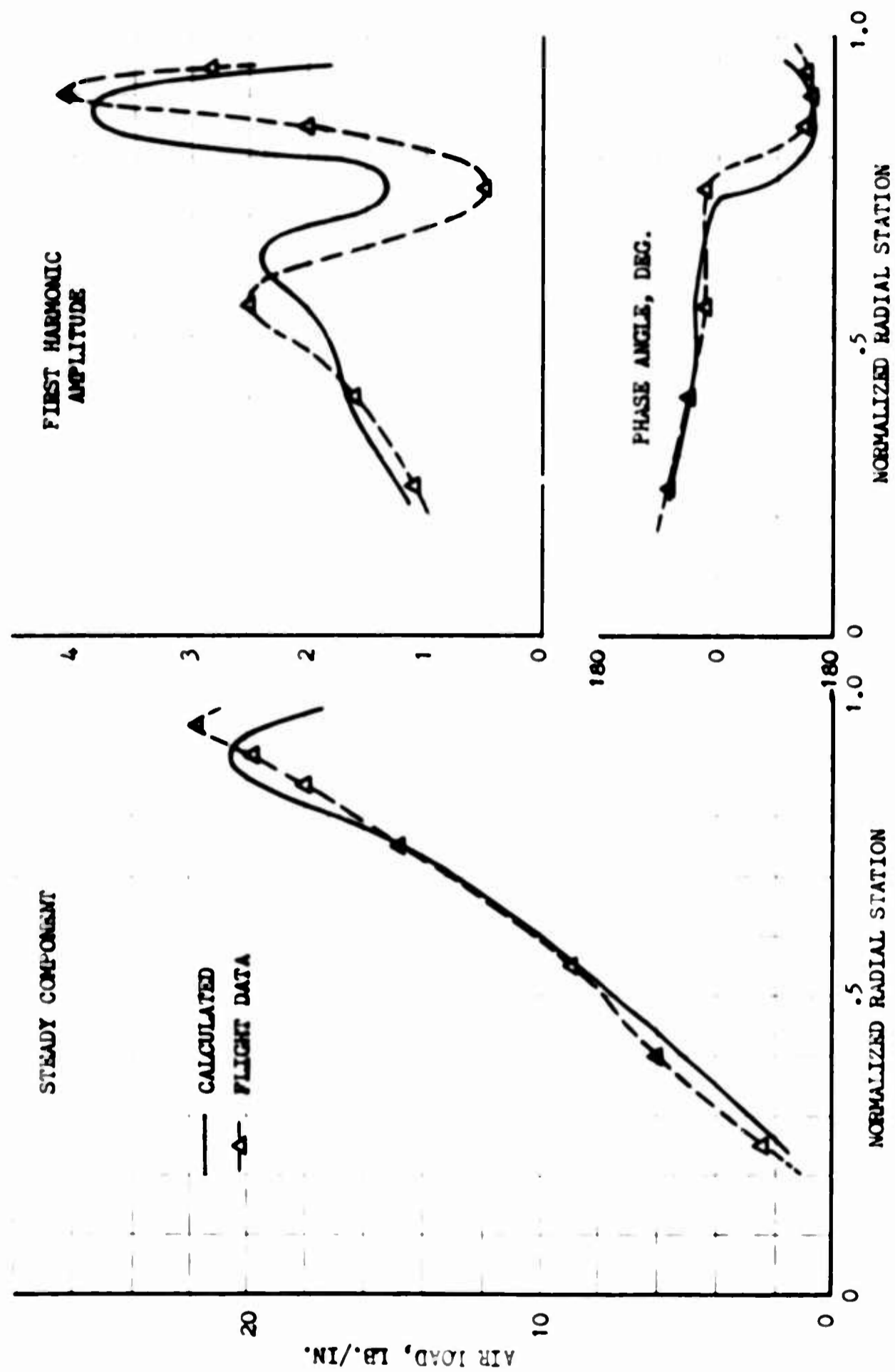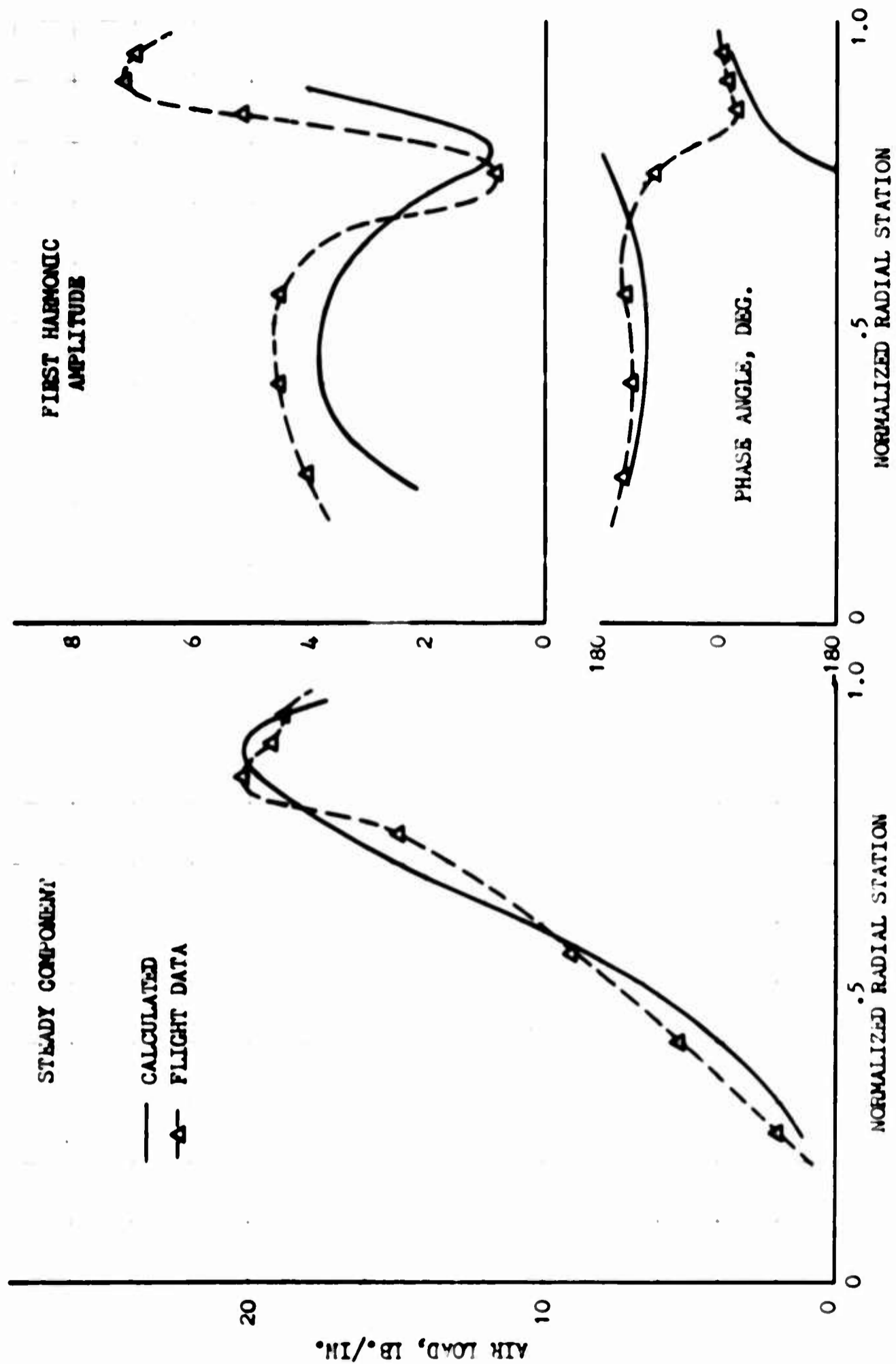
FIGURE 19. CASE 1: H-34 AIR LOADS AT 41 KNOTS

83
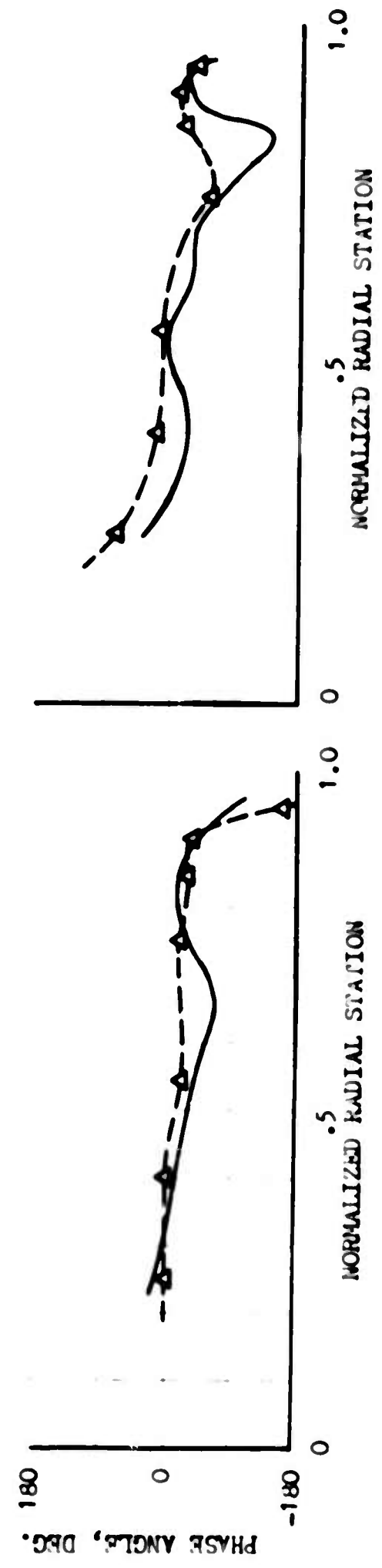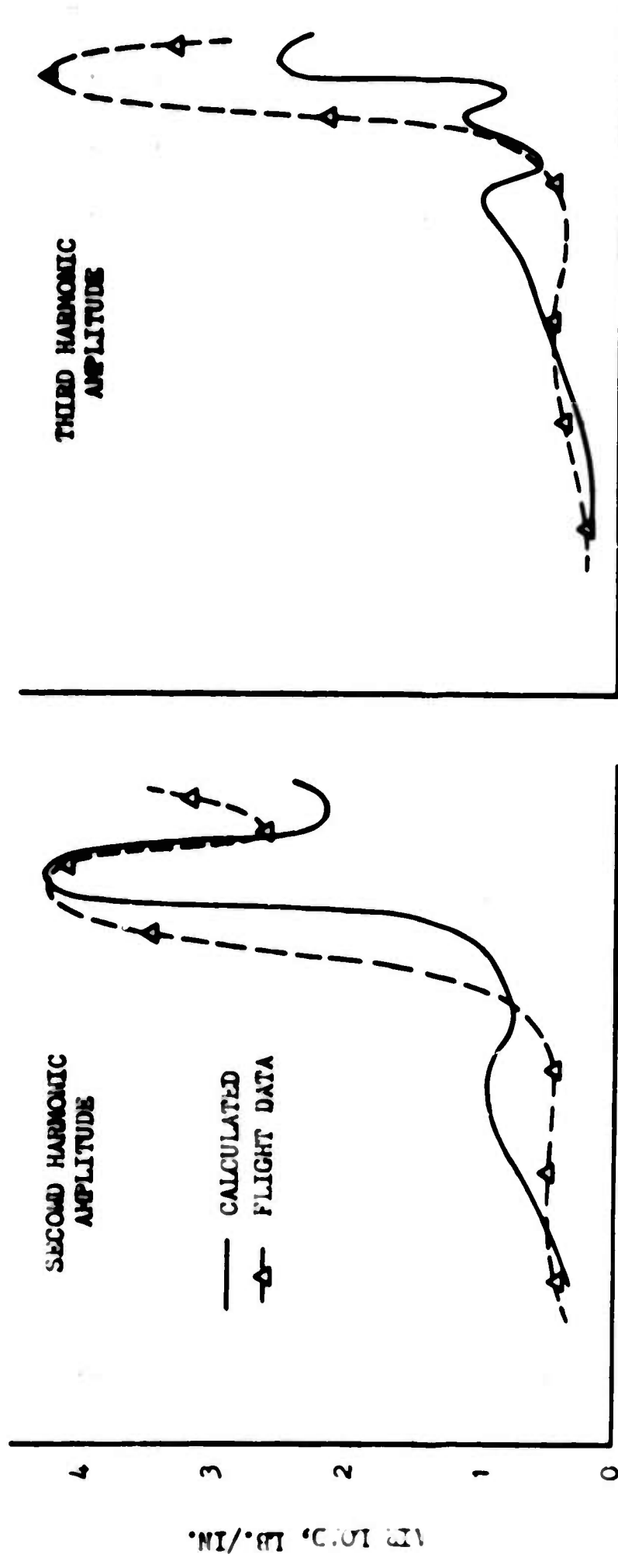
FIGURE 20. CASE 1: H-34 AIR LOADS AT 40 KNOTS
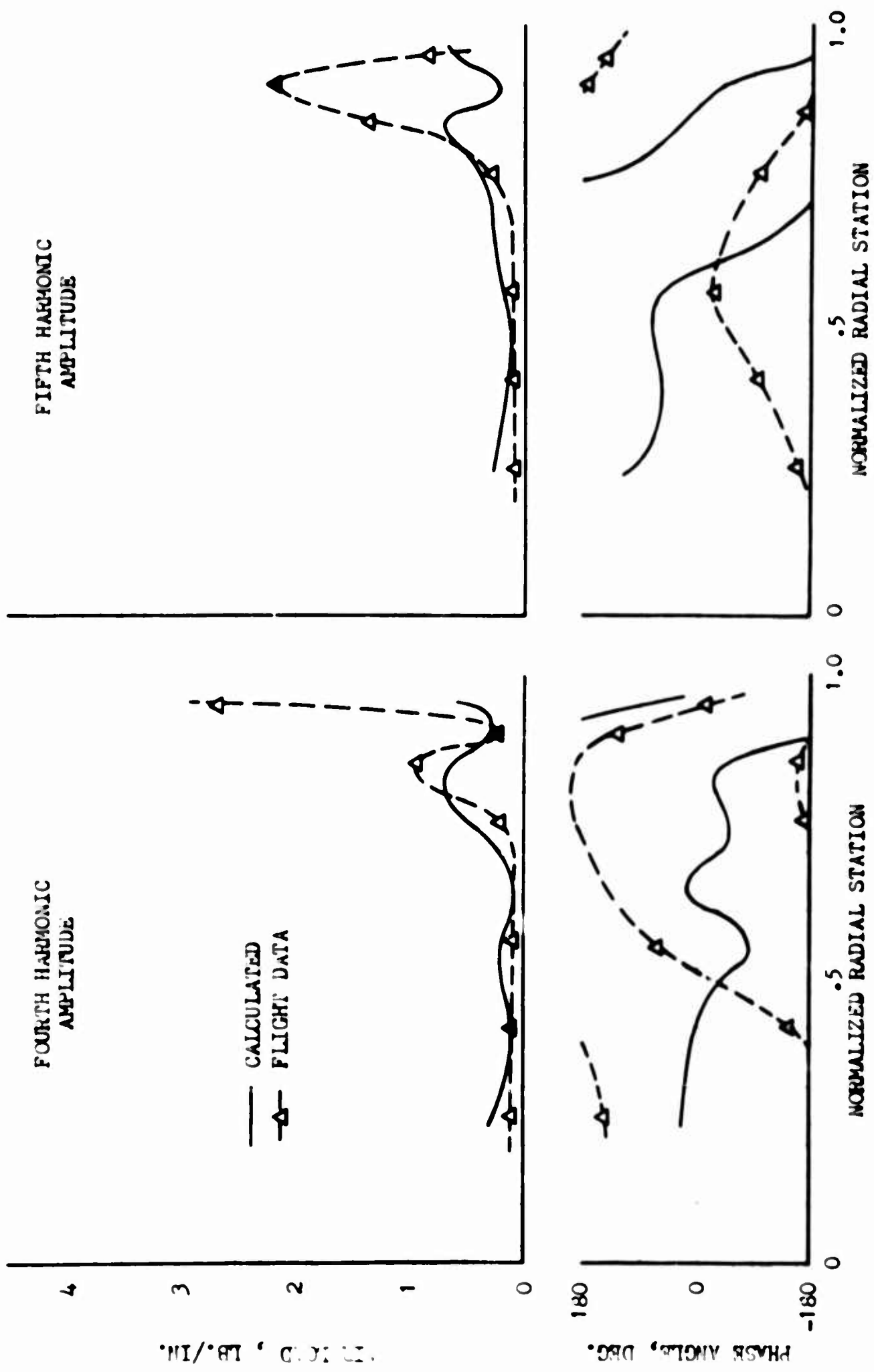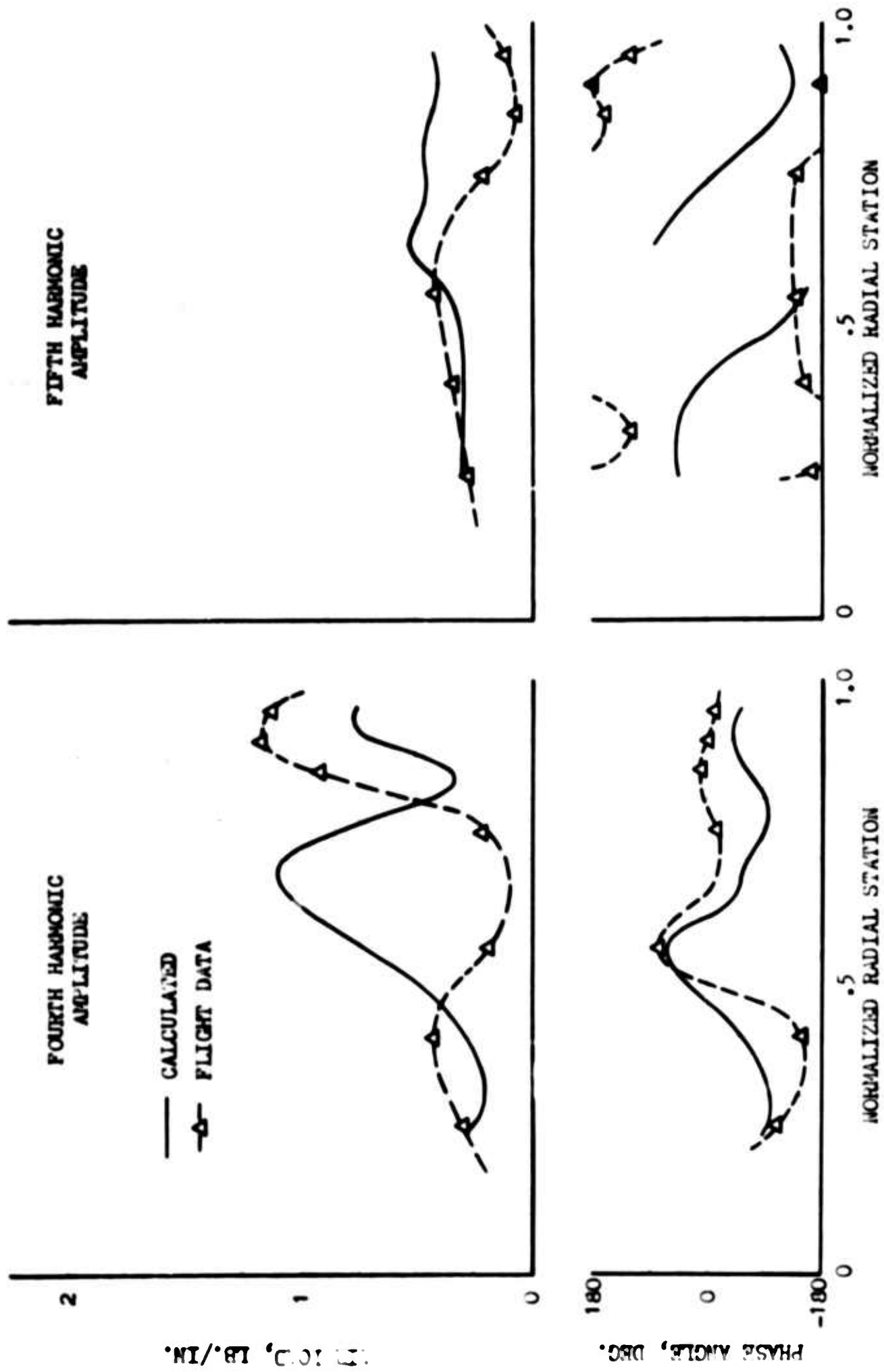
FIGURE 21. CASE 1: H-34 AIR LOADS AT 41 KNOTS

85

FIRST HARMONIC
AMPLITUDE

PHASE ANGLE, DEG.

NORMALIZED RADIAL STATION

STEADY COMPONENT

CALCULATED

FLIGHT DATA

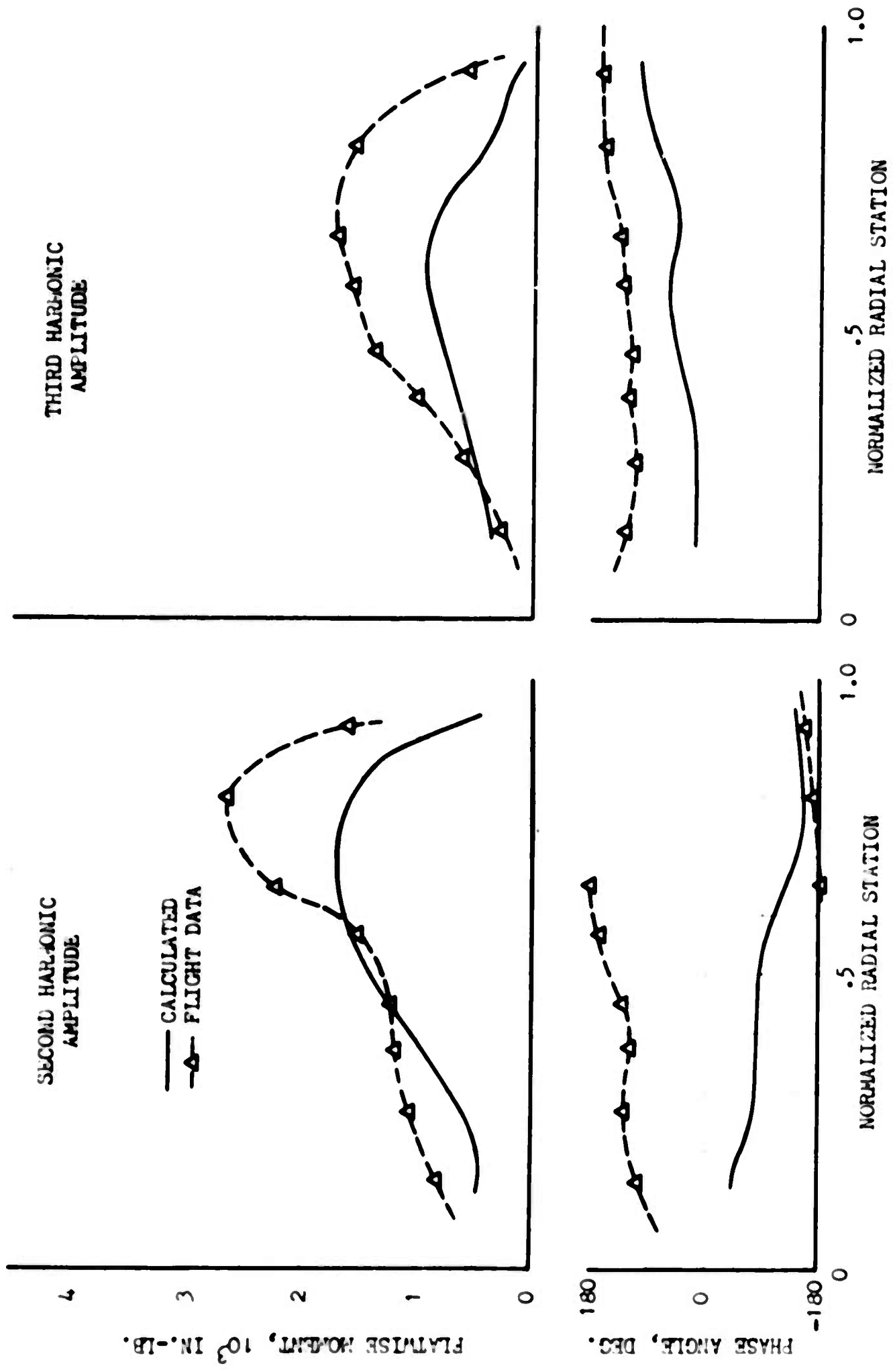NORMALIZED RADIAL STATION

FLATWISE MOMENT, 10^3 IN.-LB.
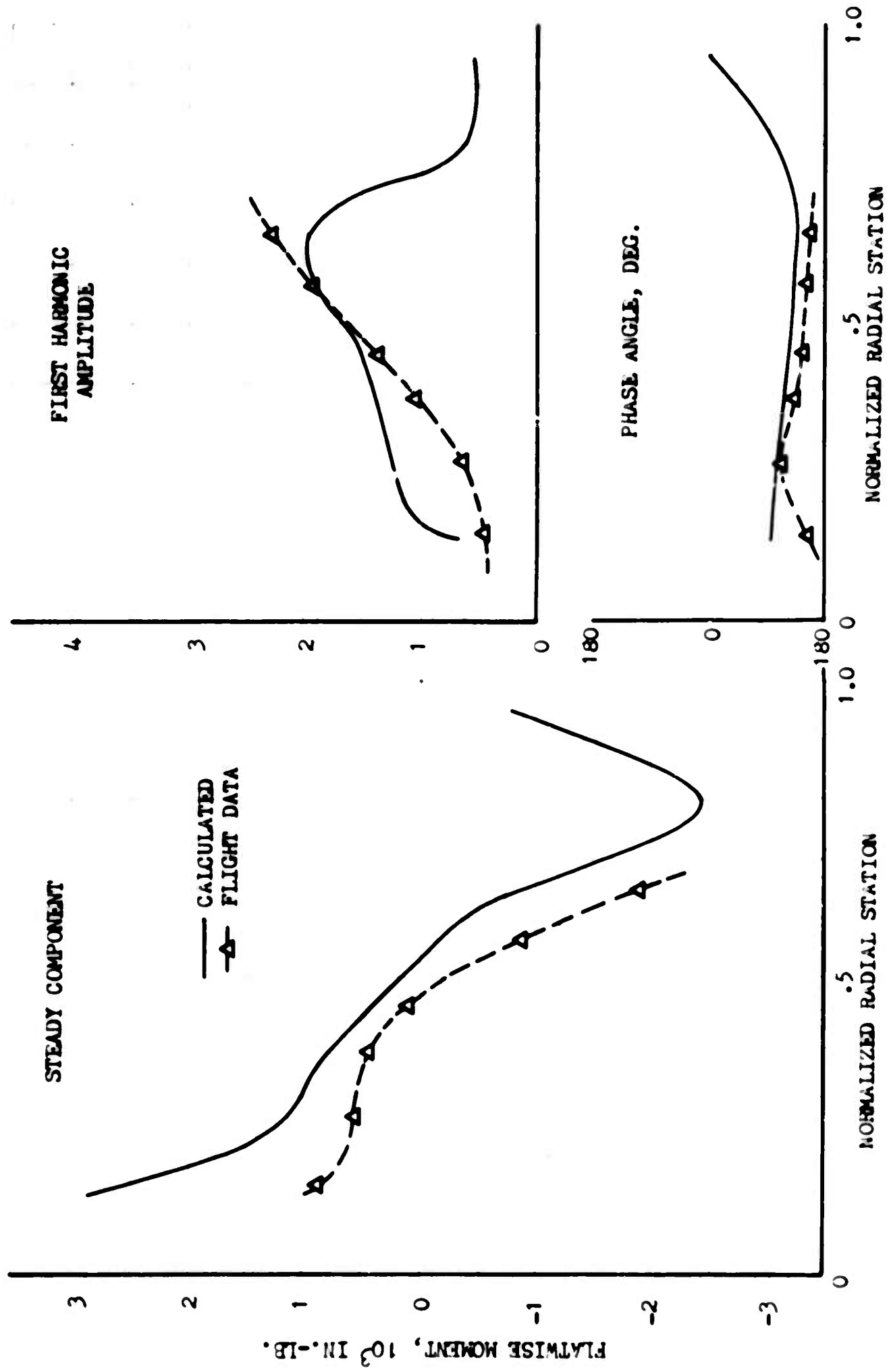
FIGURE 22. CASE 1: H-34 FLATWISE MOMENTS AT 41 KNOTS

86
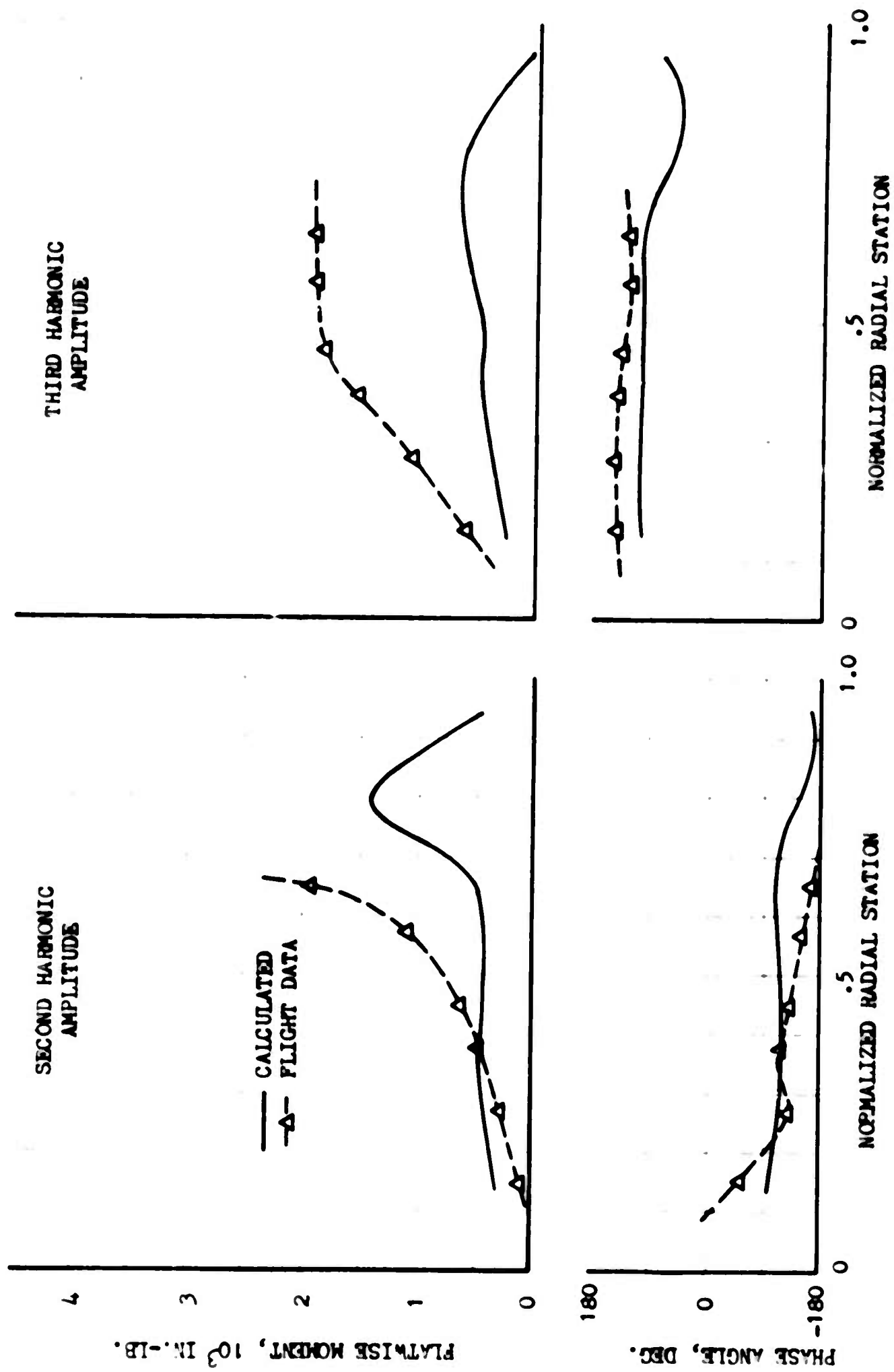
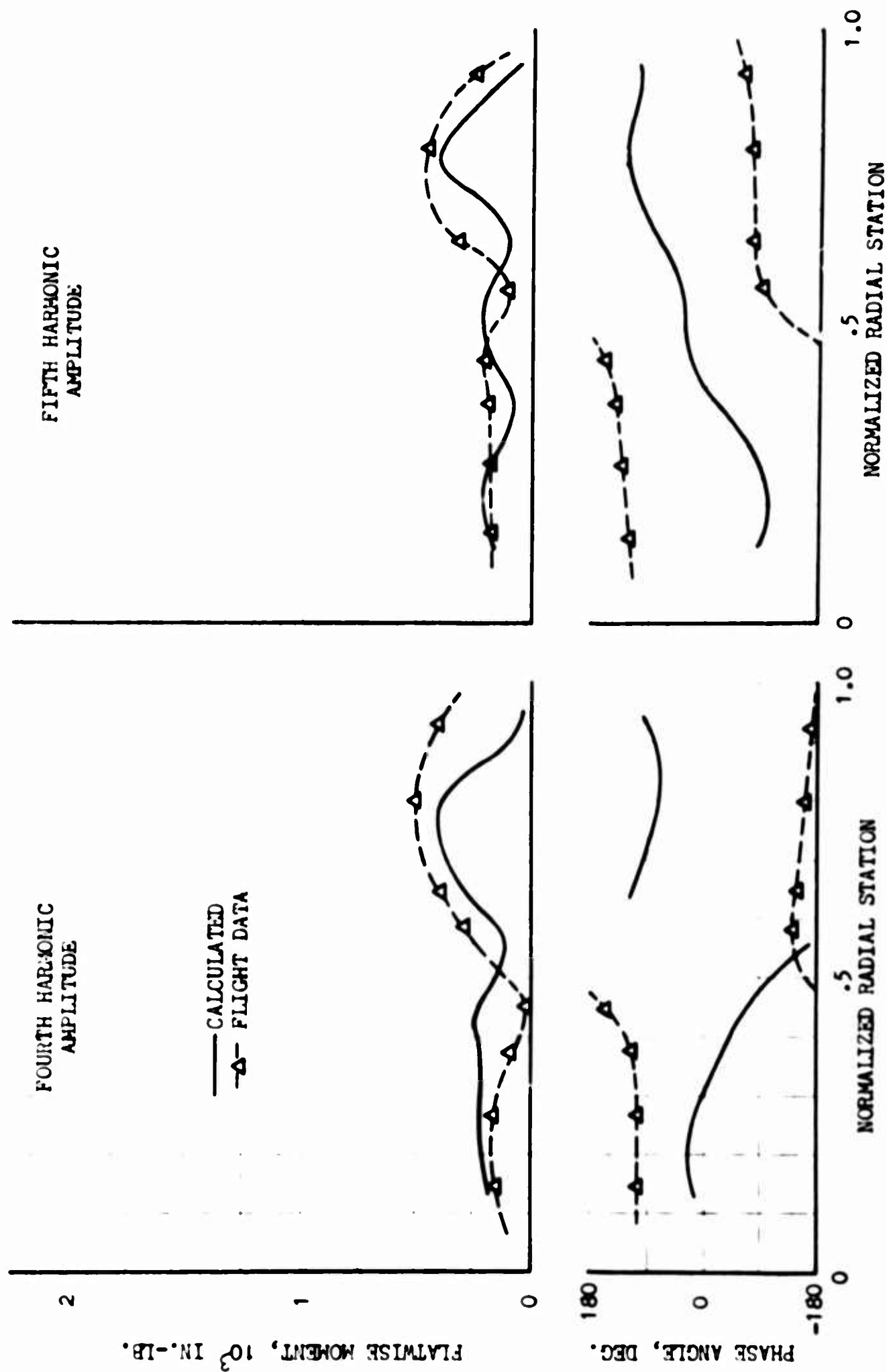FIGURE 23. CASE 1: H-34 FLATWISE MOMENTS AT 41 KNOTS

87
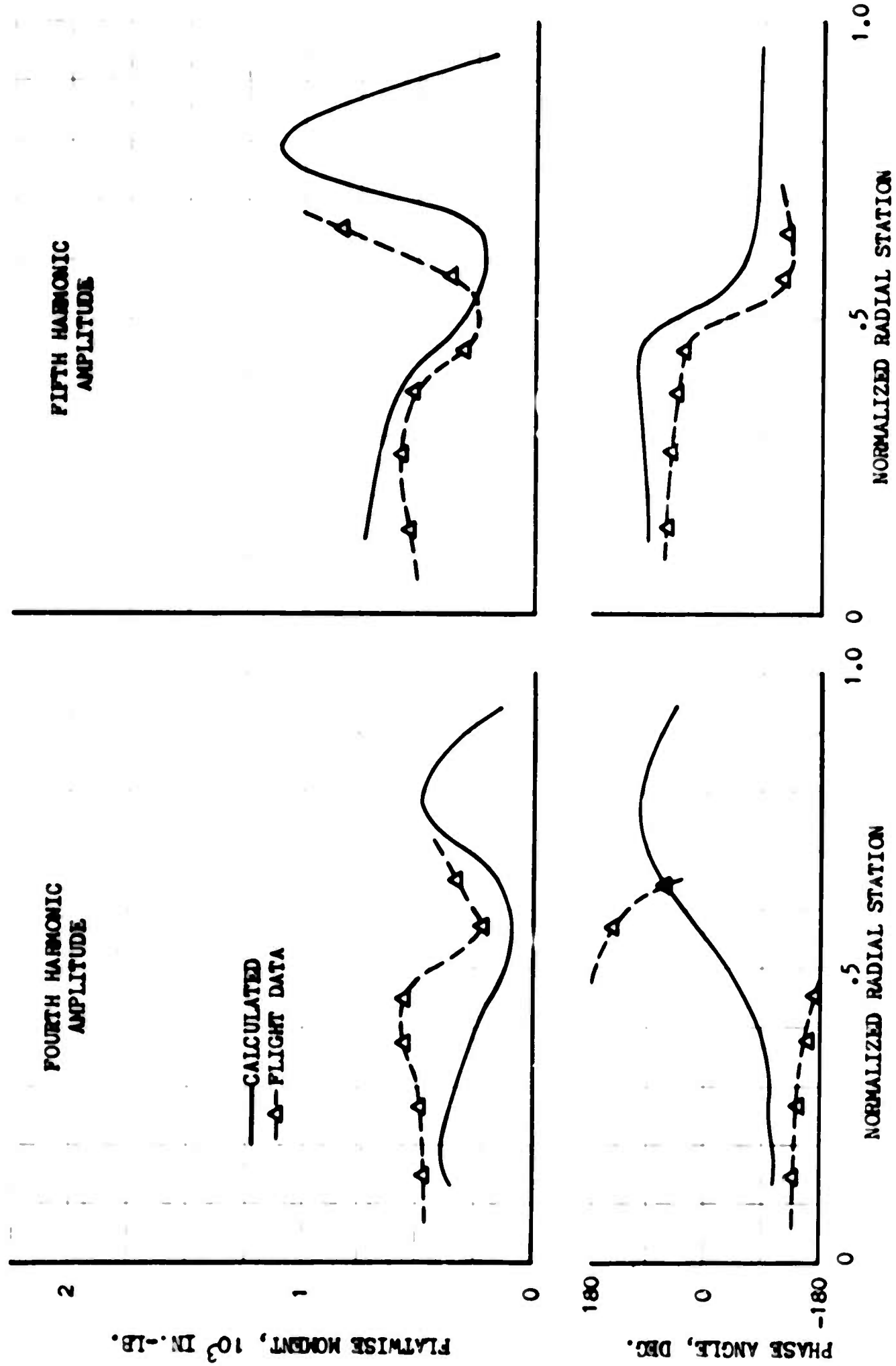
FIGURE 24. CASE 1: H-34 FLATWISE MOMENTS AT 41 KNOTS
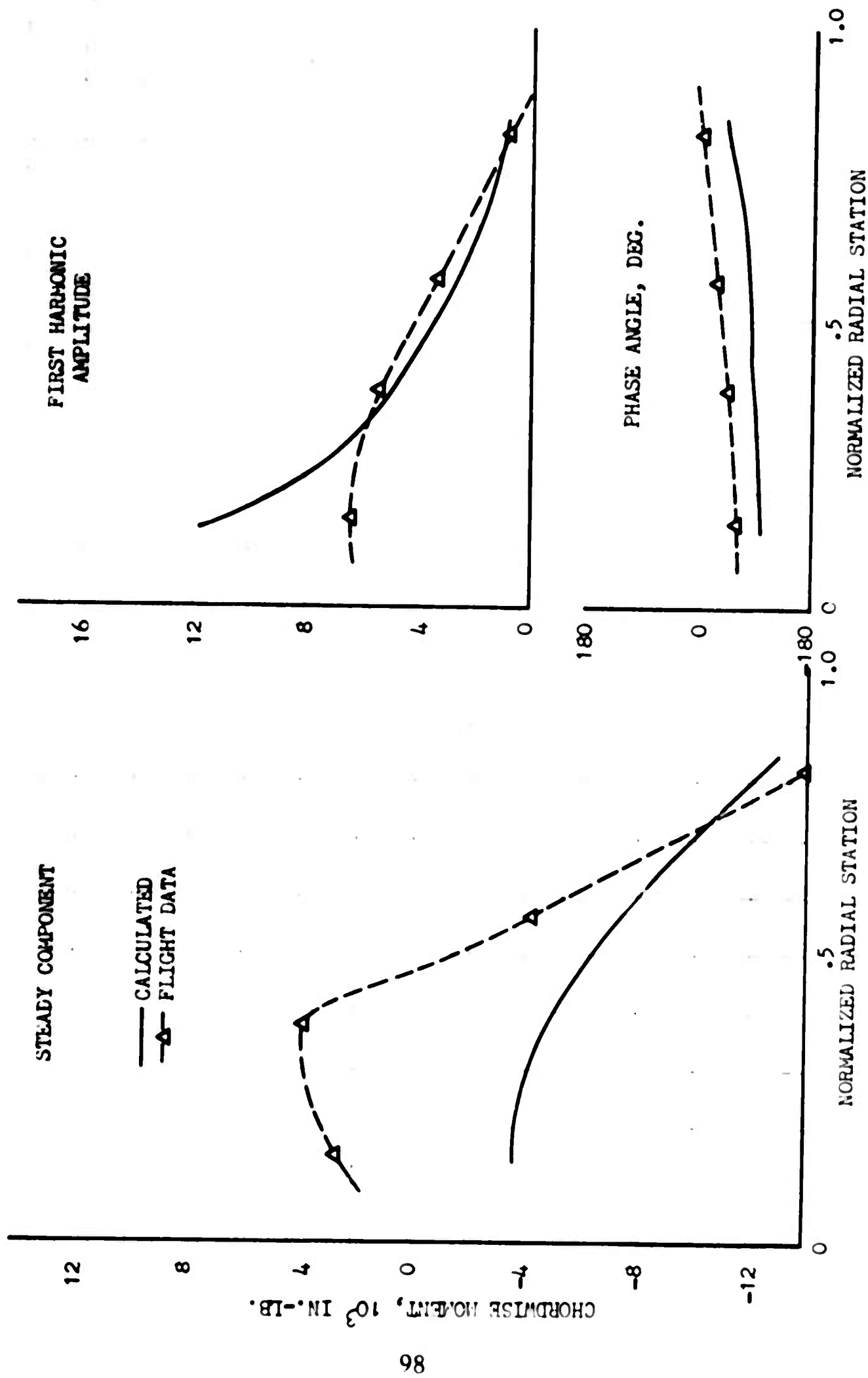
88
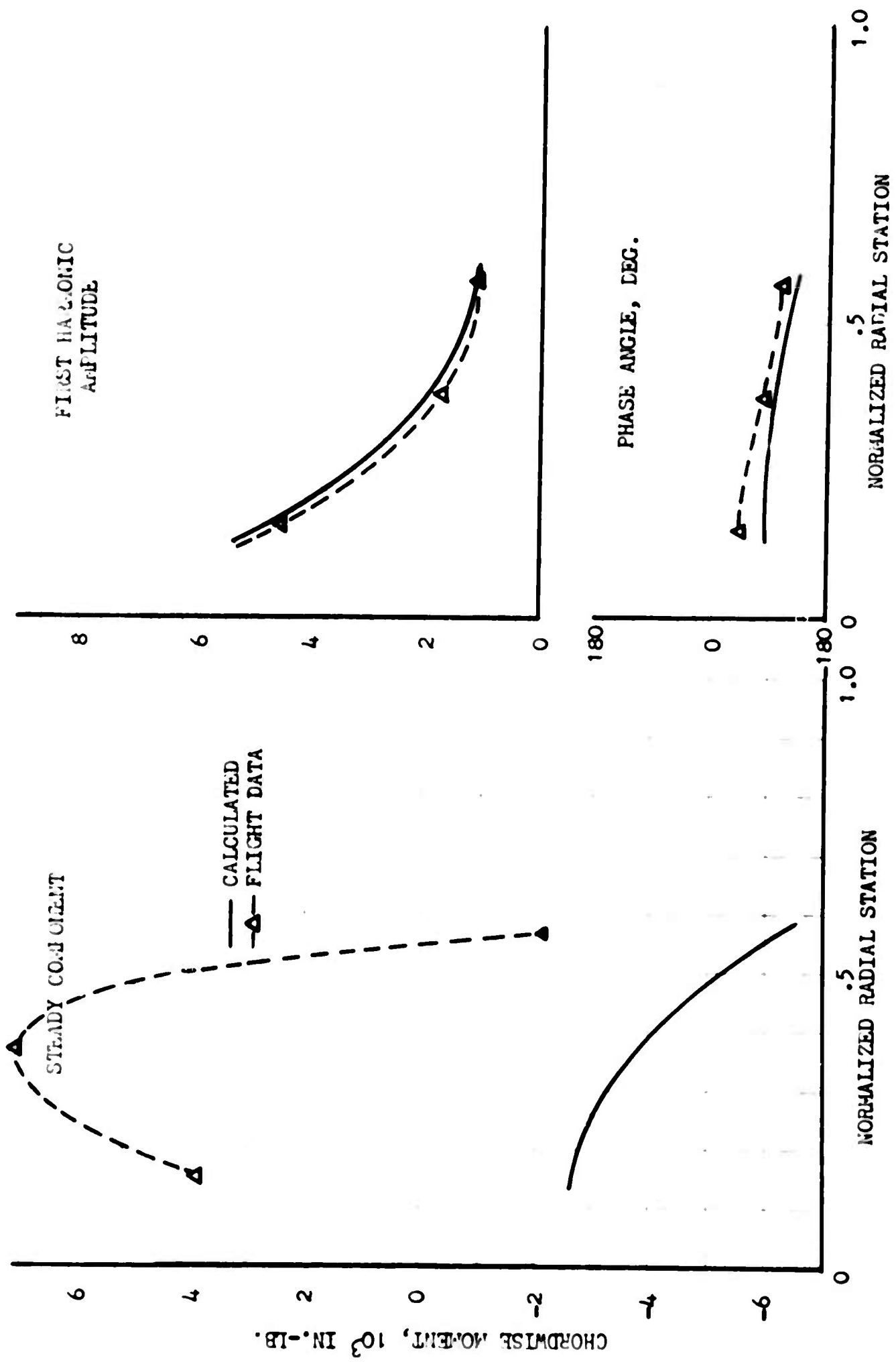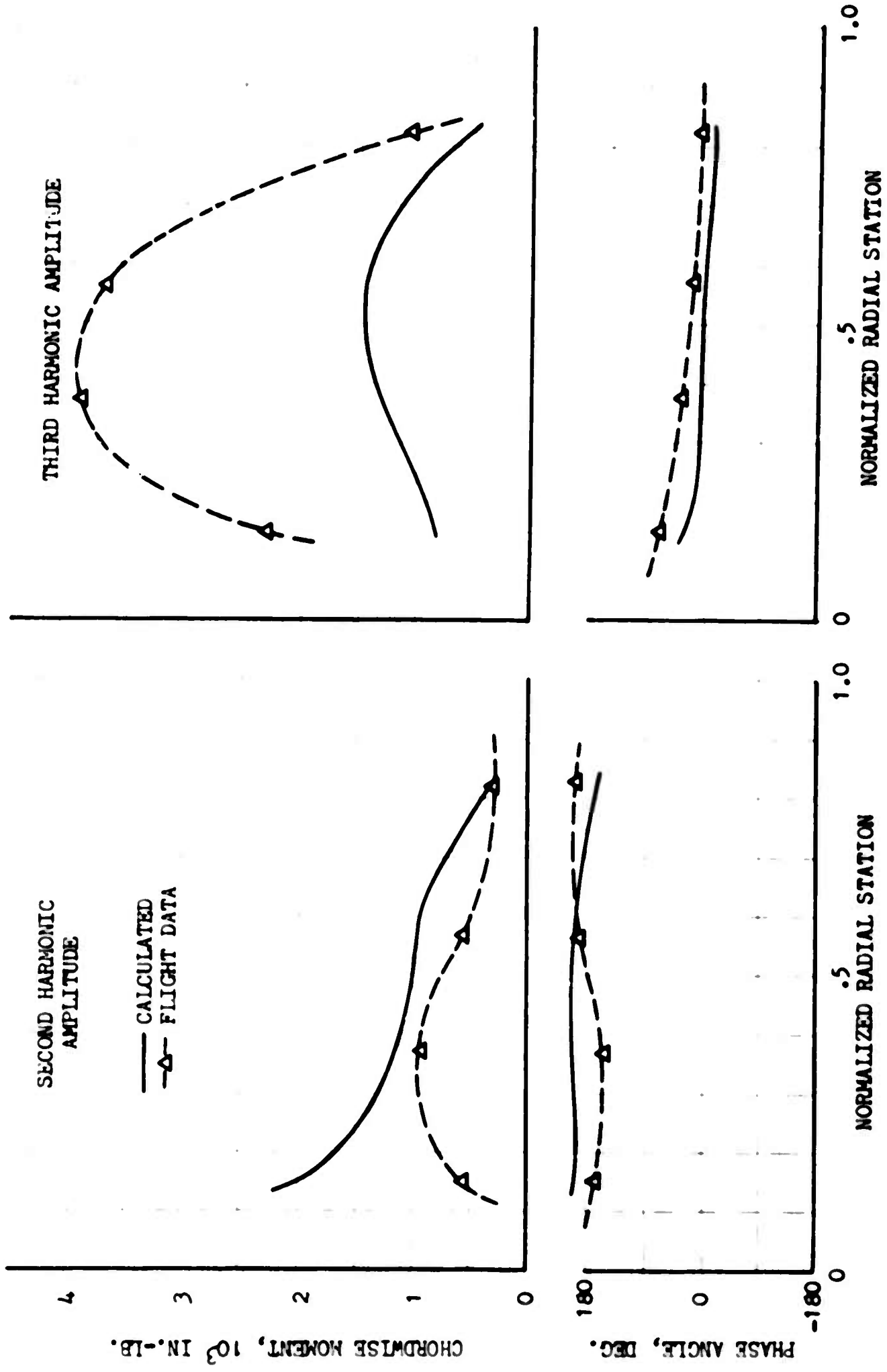
FIGURE 25. CASE 1: H-34 CHORDWISE MOMENTS AT 41 KNOTS

89
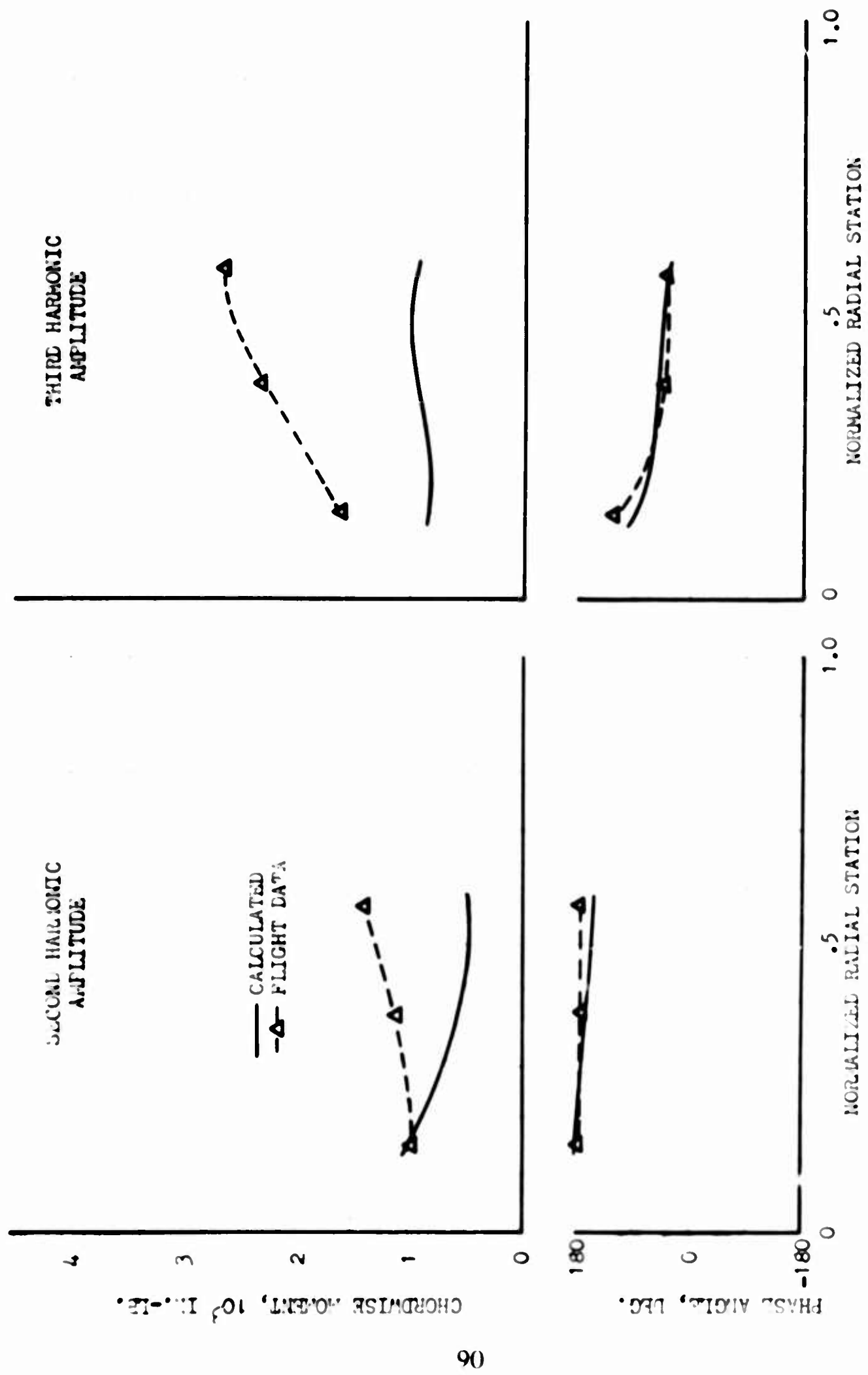
FIGURE 26. CASE 1: H-34 CHORDWISE MOMENTS AT 41 KNOTS
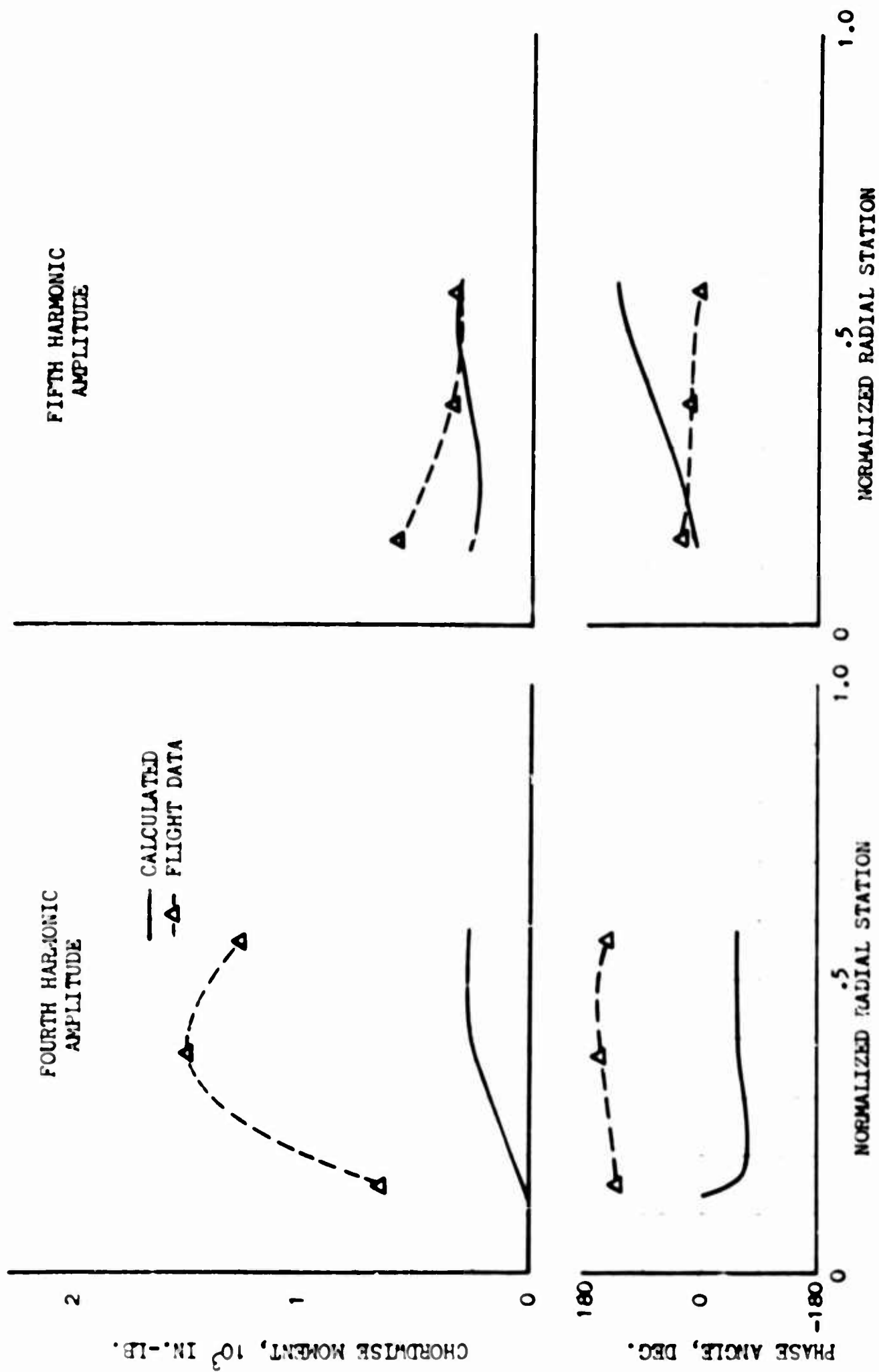
FIGURE 27. CASE 1: H-34 CHORDWISE MOMENTS AT 41 KNOTS

FIGURE 28. CASE 4: H-34 AIR LOADS AT 112 KNOTS
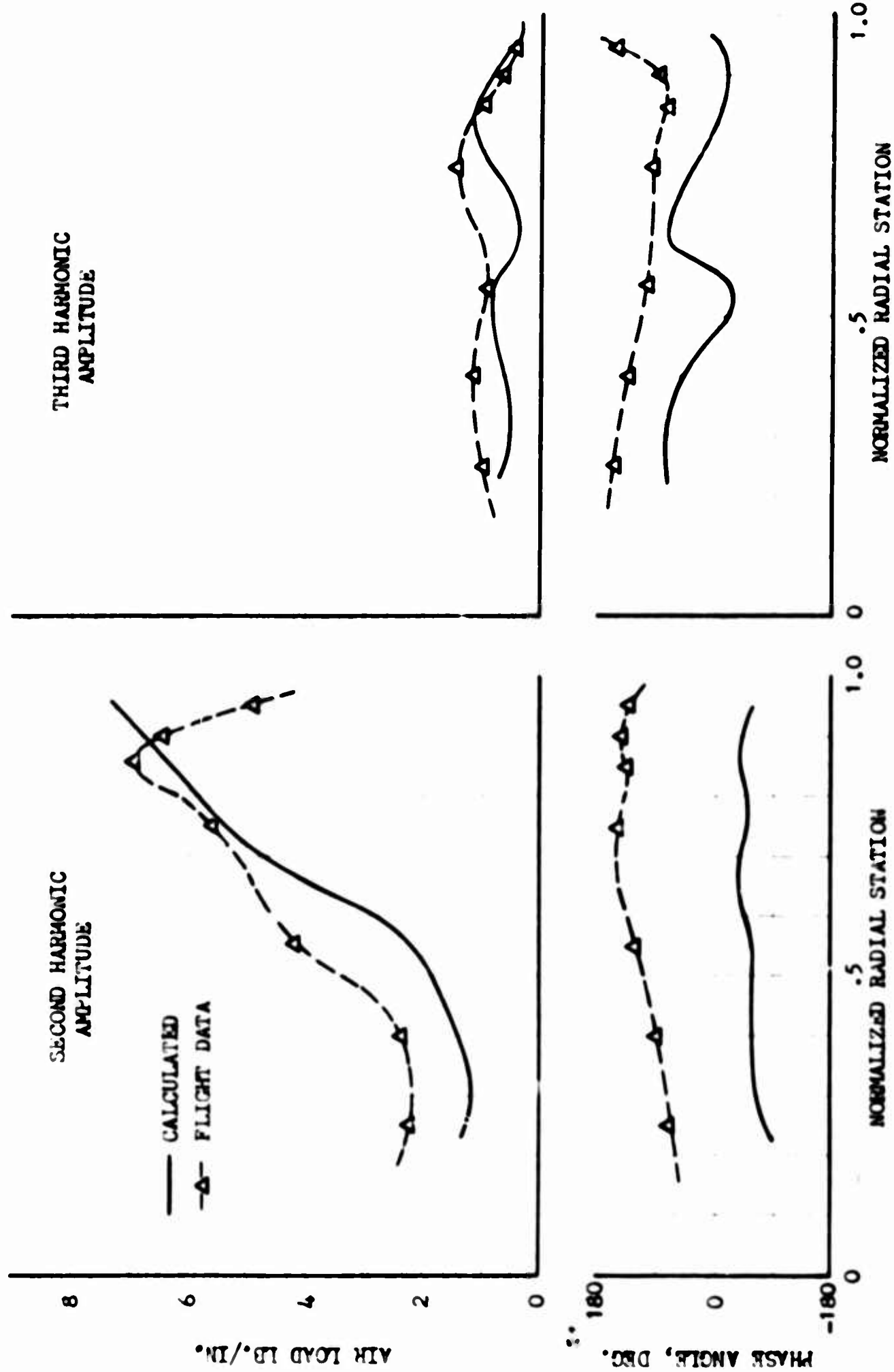
FIGURE 29. CASE 4: H-34 AIR LOADS AT 112 KNOTS

FIFTH HARMONIC
AMPLITUDE

FOURTH HARMONIC
AMPLITUDE

— CALCULATED
—△— FLIGHT DATA

NORMALIZED RADIAL STATION

NORMALIZED RADIAL STATION

NORMALIZED RADIAL STATION

AMPLITUDE, LB./IN.

PHASE ANGLE, DEG.

0   .5   1.0

2

1

0

180

0

-180
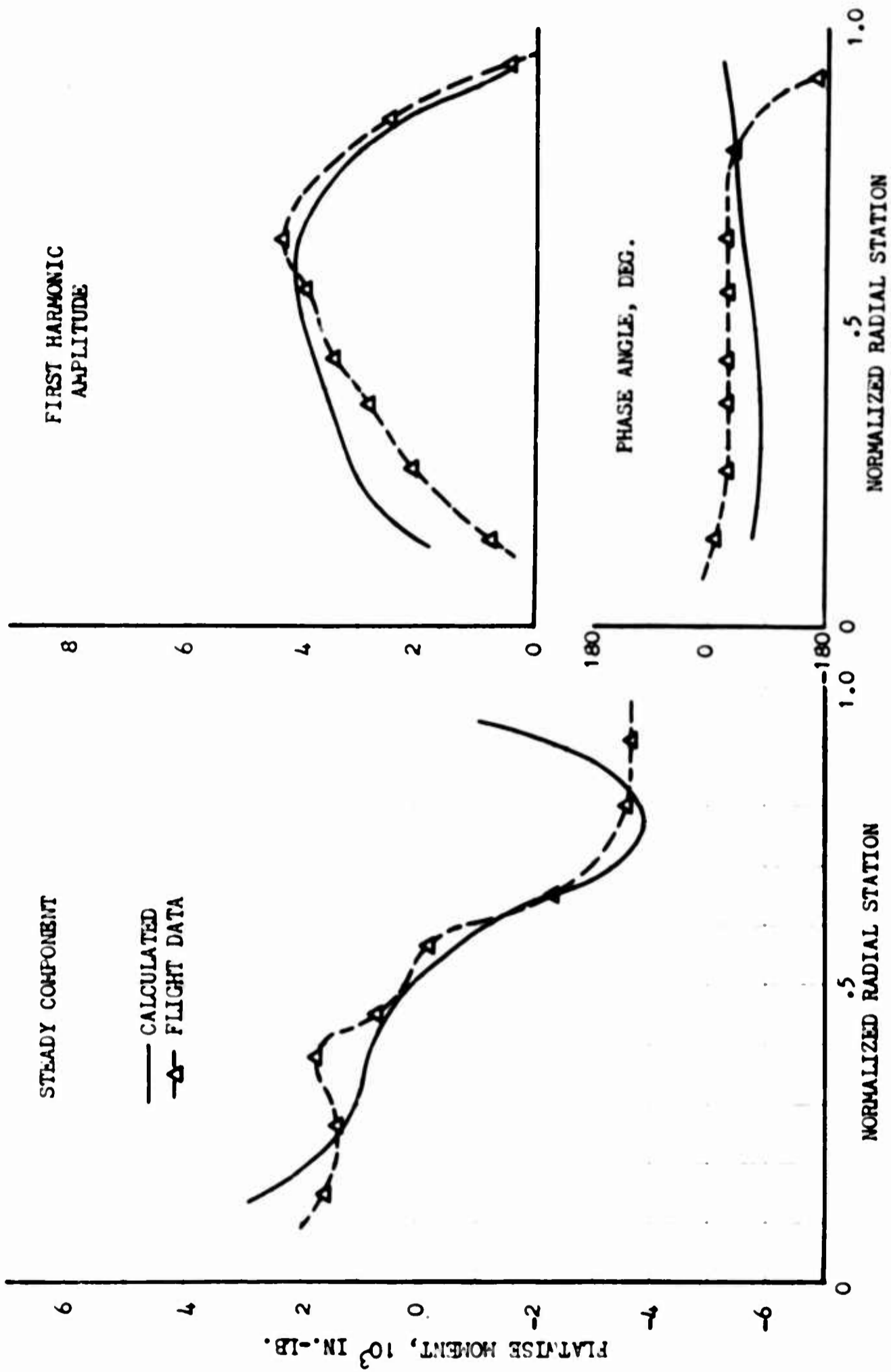
FIGURE 30.   CASE 4:   H-34

FIGURE 31. CASE 4: H-34 FLATWISE MOMENTS AT 112 KNOTS

95

FIGURE 32. CASE 4: H-34 FLATWISE MOMENTS AT 112 KNOTS
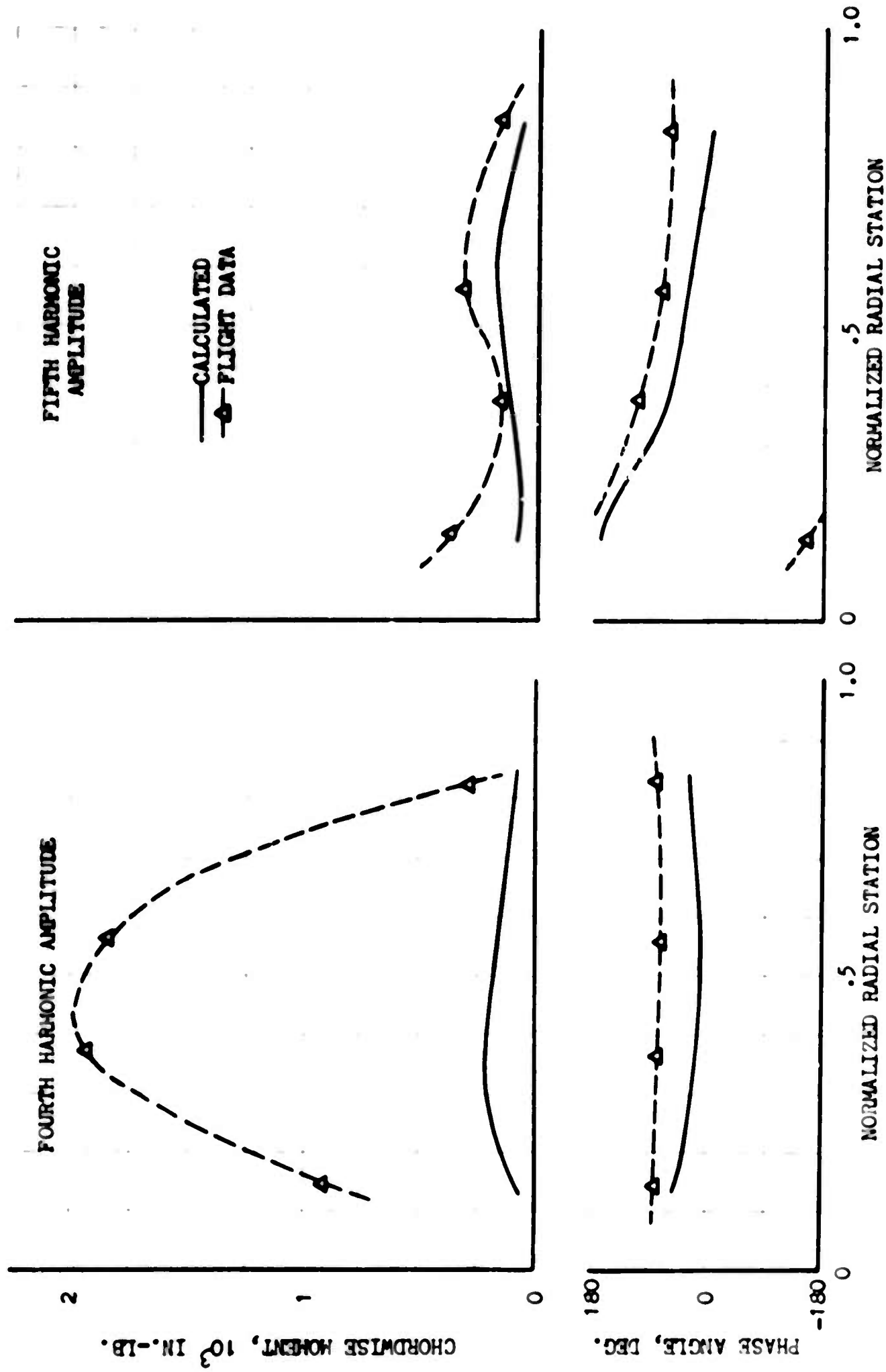
96

FIGURE 33. CASE 4: H-34 FLATWISE MOMENTS AT 112 KNOTS

97

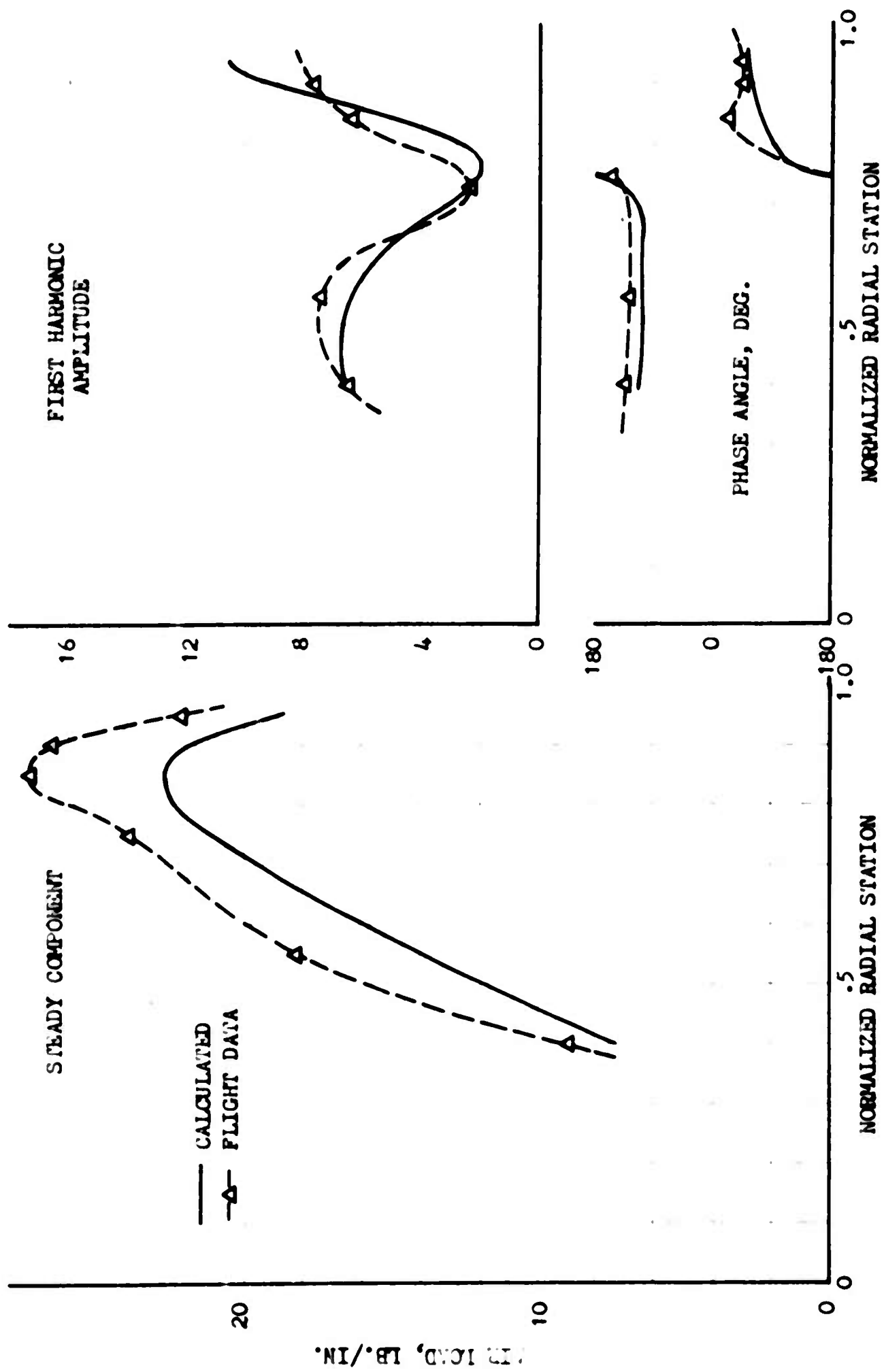FIGURE 34. CASE 4: H-34 CHORDWISE MOMENTS AT 112 KNOTS

THIRD HARMONIC AMPLITUDE

SECOND HARMONIC
AMPLITUDE

—— CALCULATED
–△– FLIGHT DATA

NORMALIZED RADIAL STATION

NORMALIZED RADIAL STATION

CHORDWISE MOMENT, 10³ IN.-LB.

PHASE ANGLE, DEG.

FIGURE 35. CASE 4: H-34 CHORDWISE MOMENTS AT 112 KNOTS

99

FIFTH HARMONIC AMPLITUDE

—— CALCULATED
-▵- FLIGHT DATA

NORMALIZED RADIAL STATION

FOURTH HARMONIC AMPLITUDE

NORMALIZED RADIAL STATION

CHORDWISE MOMENT, 10^3 IN.-LB.

PHASE ANGLE, DEG.

FIGURE 36. CASE 4: H-34 CHORDWISE MOMENTS AT 112 KNOTS

FIRST HARMONIC
AMPLITUDE

PHASE ANGLE, DEG.

NORMALIZED RADIAL STATION

STEADY COMPONENT

CALCULATED

FLIGHT DATA

NORMALIZED RADIAL STATION

FIGURE 37. CASE 5: HU-1A AIR LOADS AT 113 KNOTS

101
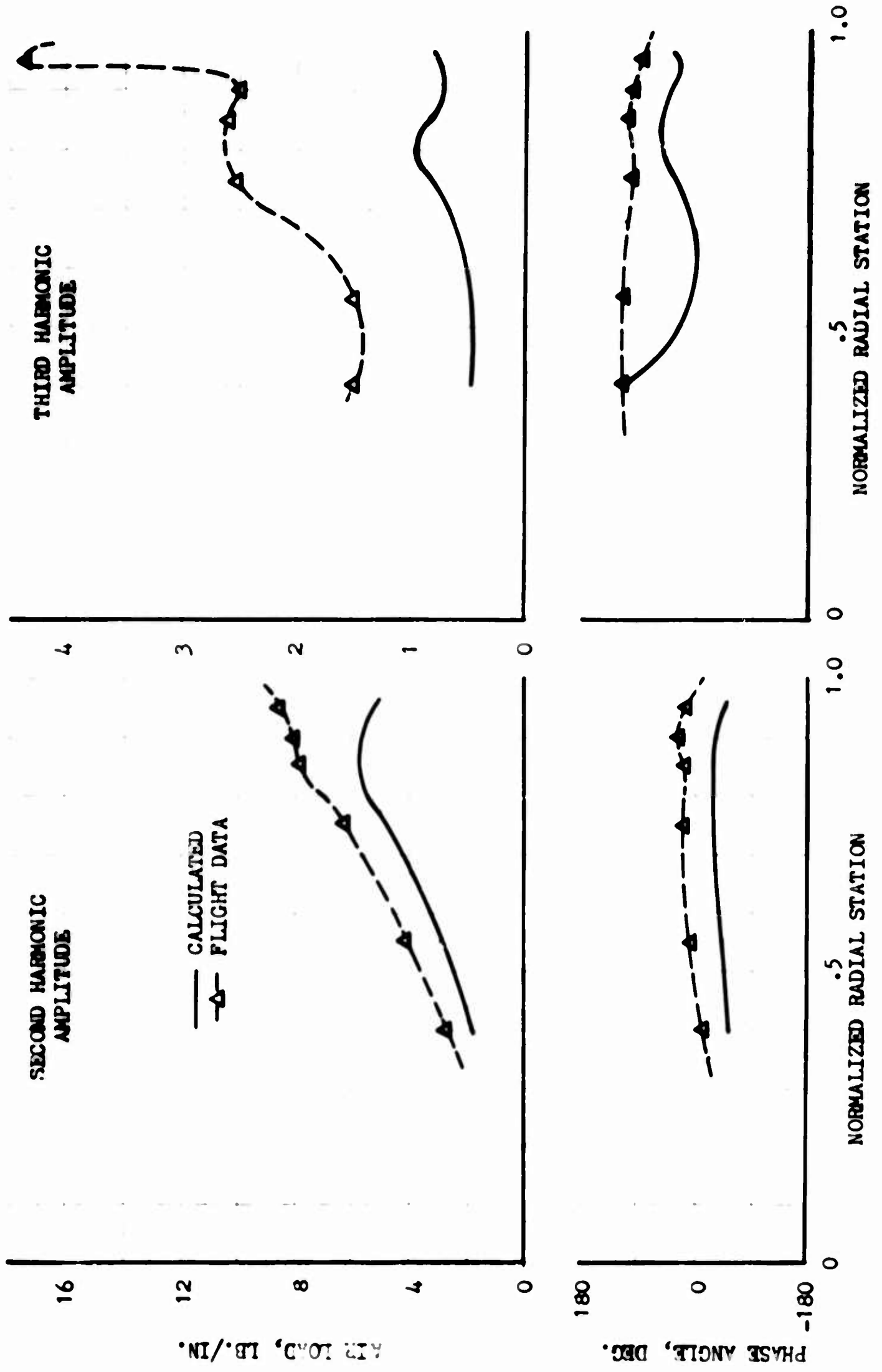
FIGURE 38. CASE 5. HU-1A AIR LOADS AT 112 KNOTS

102
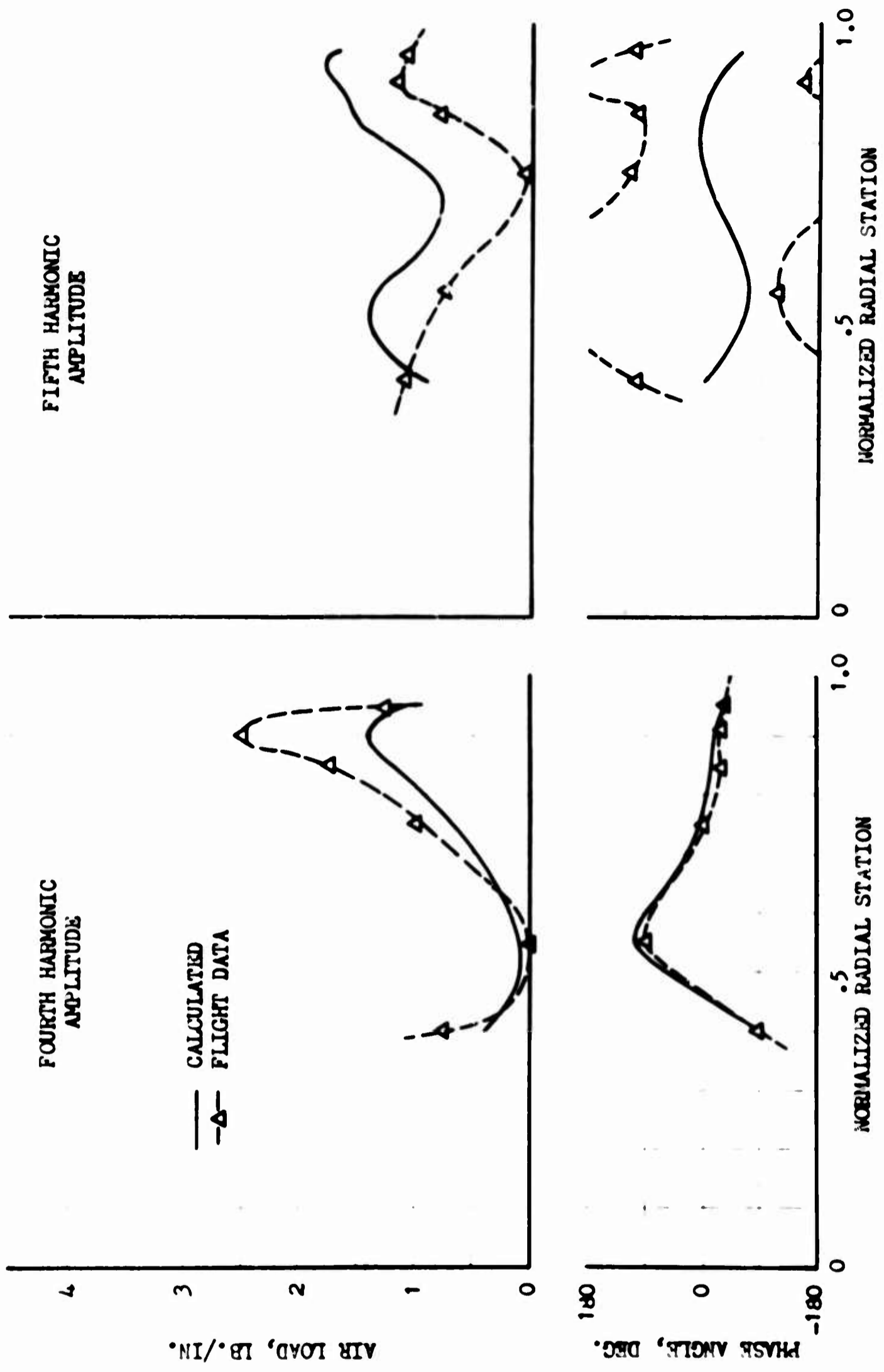
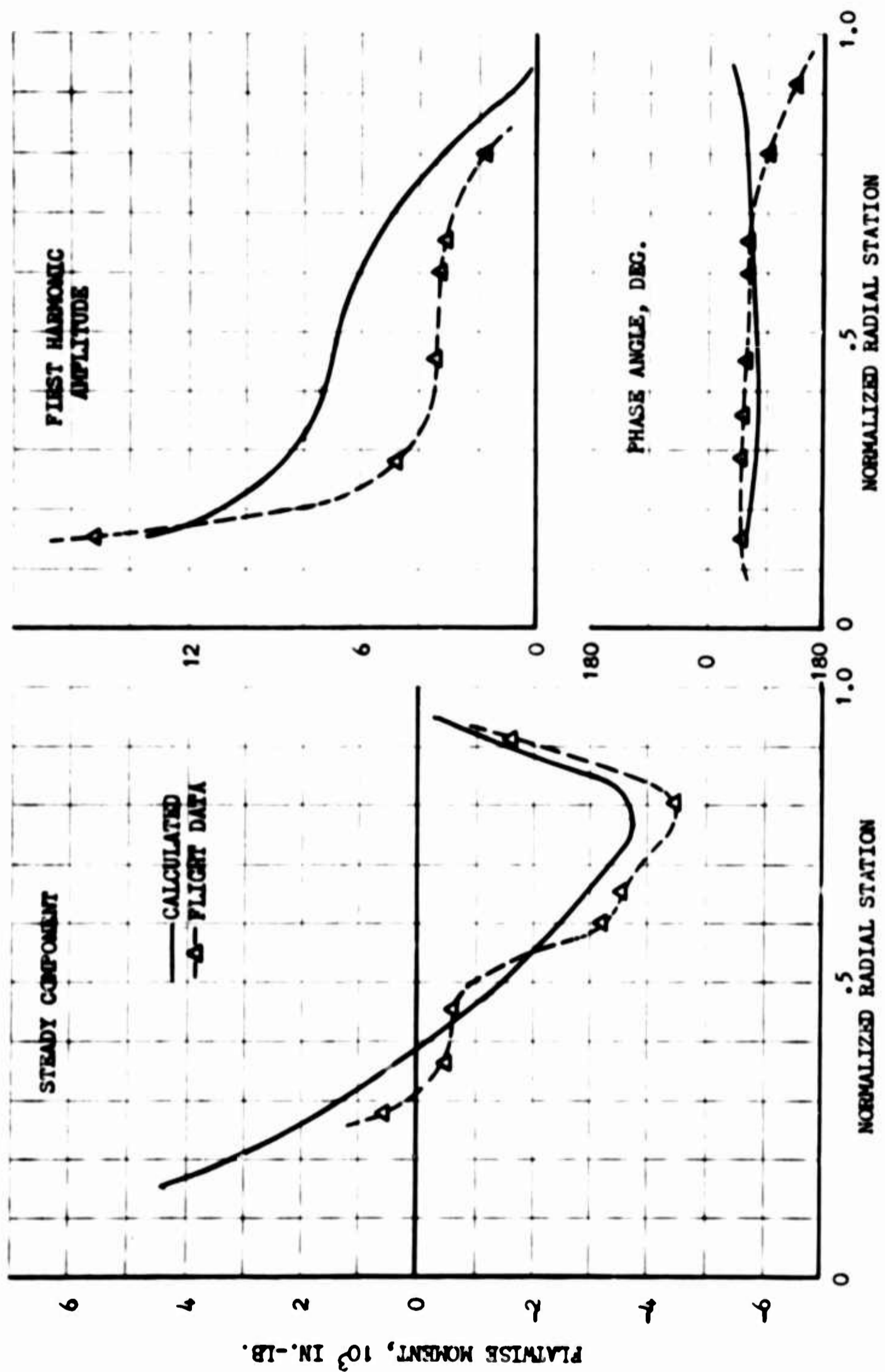FIGURE 39. CASE 5: HU-1A AIR LOADS AT 112 KNOTS

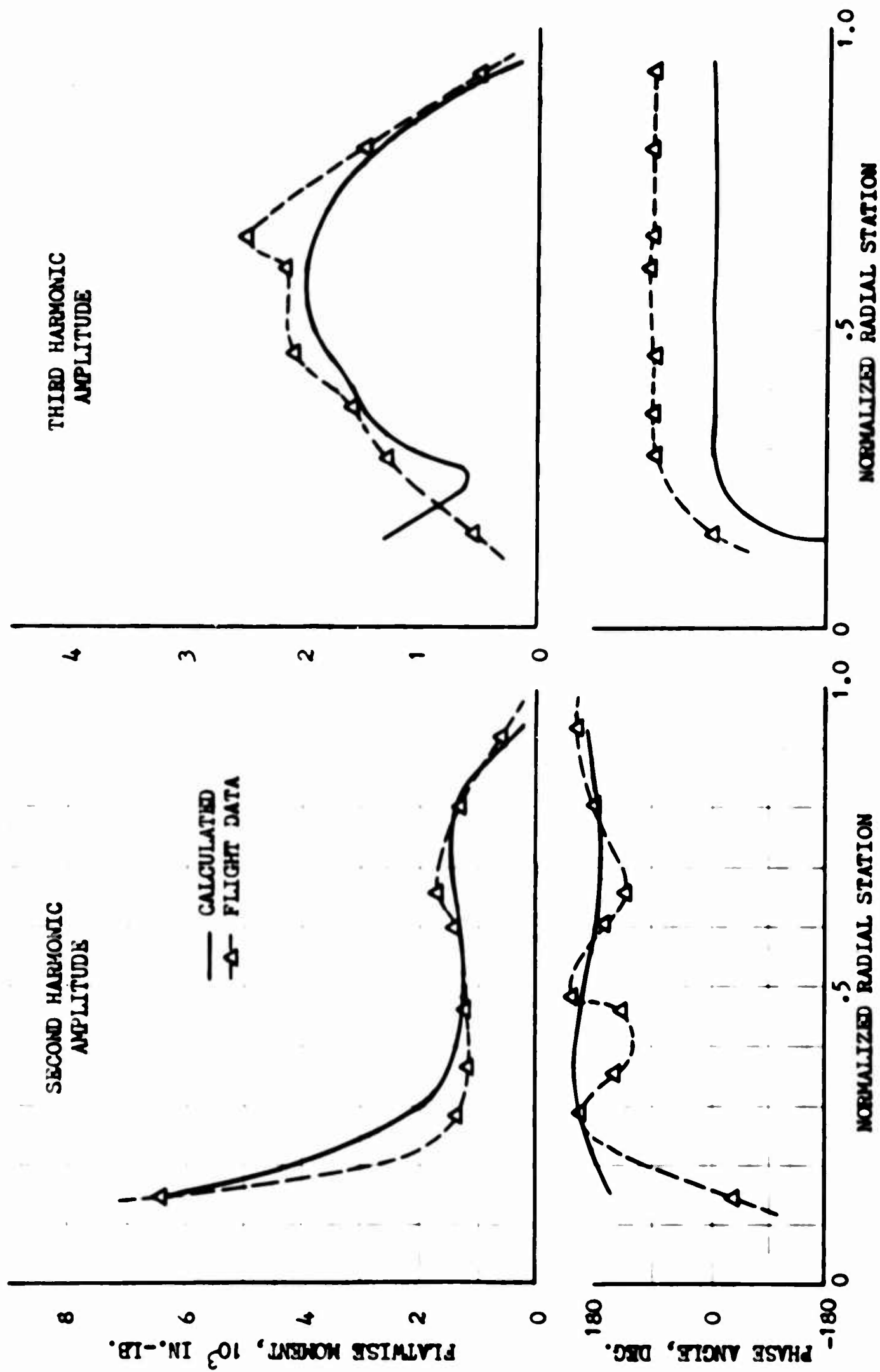FIGURE 40. CASE 5: HU-1A FLATWISE MOMENTS AT 113 KNOTS

104

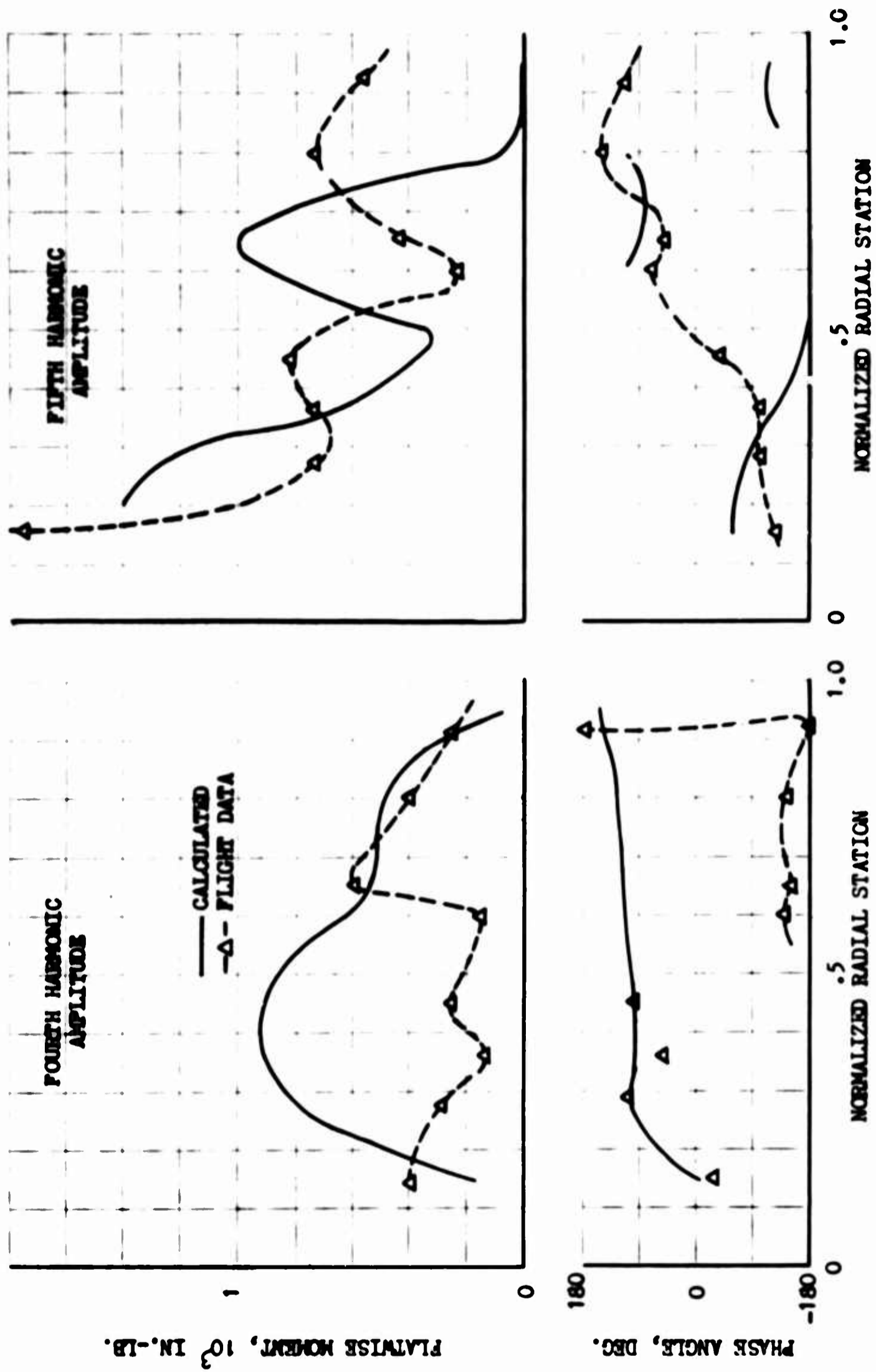FIGURE 41. CASE 5: HU-1A FLATWISE MOMENTS AT 113 KNOTS

105

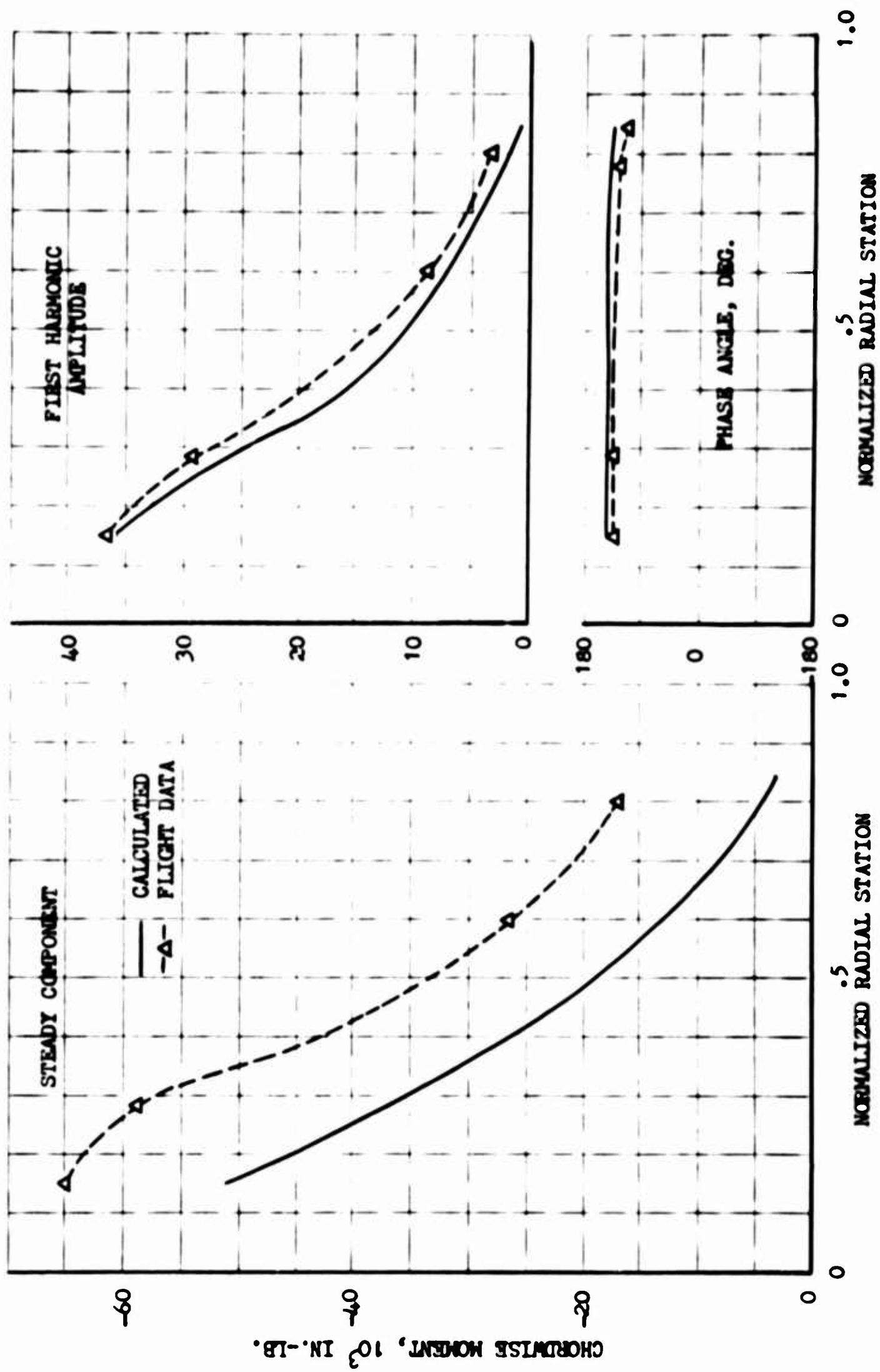FIGURE 42. CASE 5: HU-1A FLATWISE MOMENTS AT 113 KNOTS

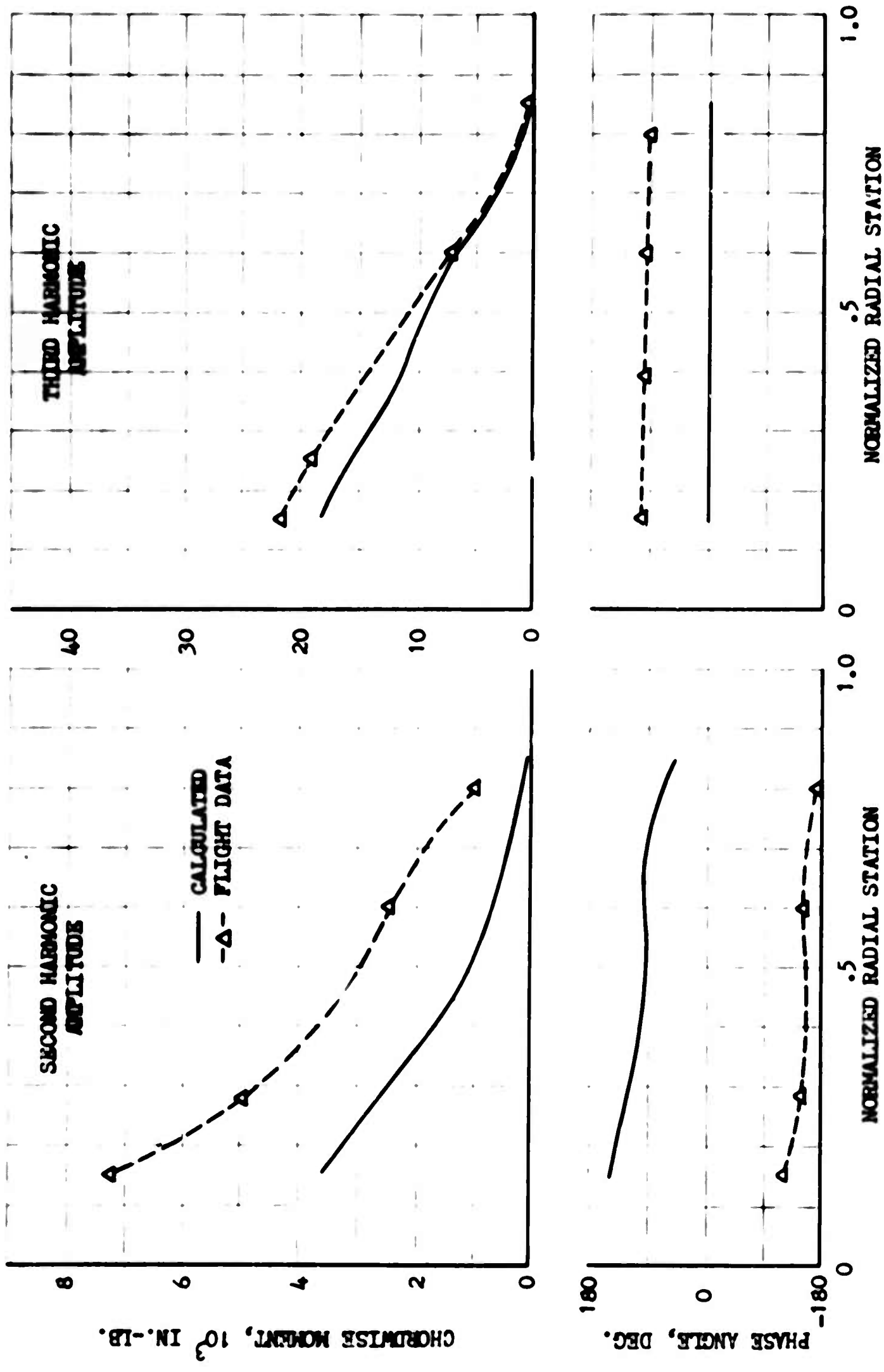FIGURE 43. CASE 5: HU-1A CHORDWISE MOMENTS AT 113 KNOTS

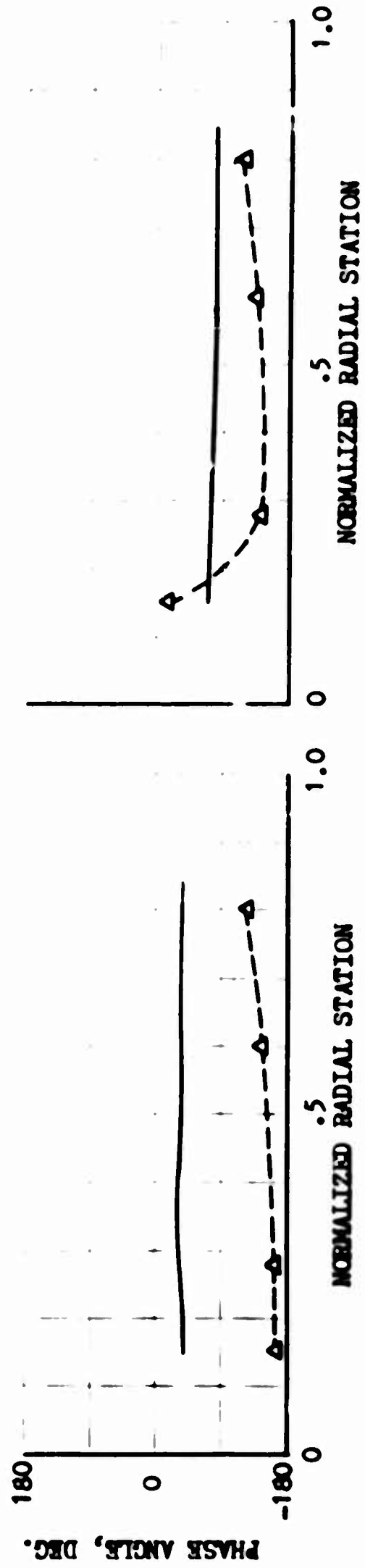FIGURE 44. CASE 5: HU-1A CHORDWISE MOMENTS AT 113 KNOTS
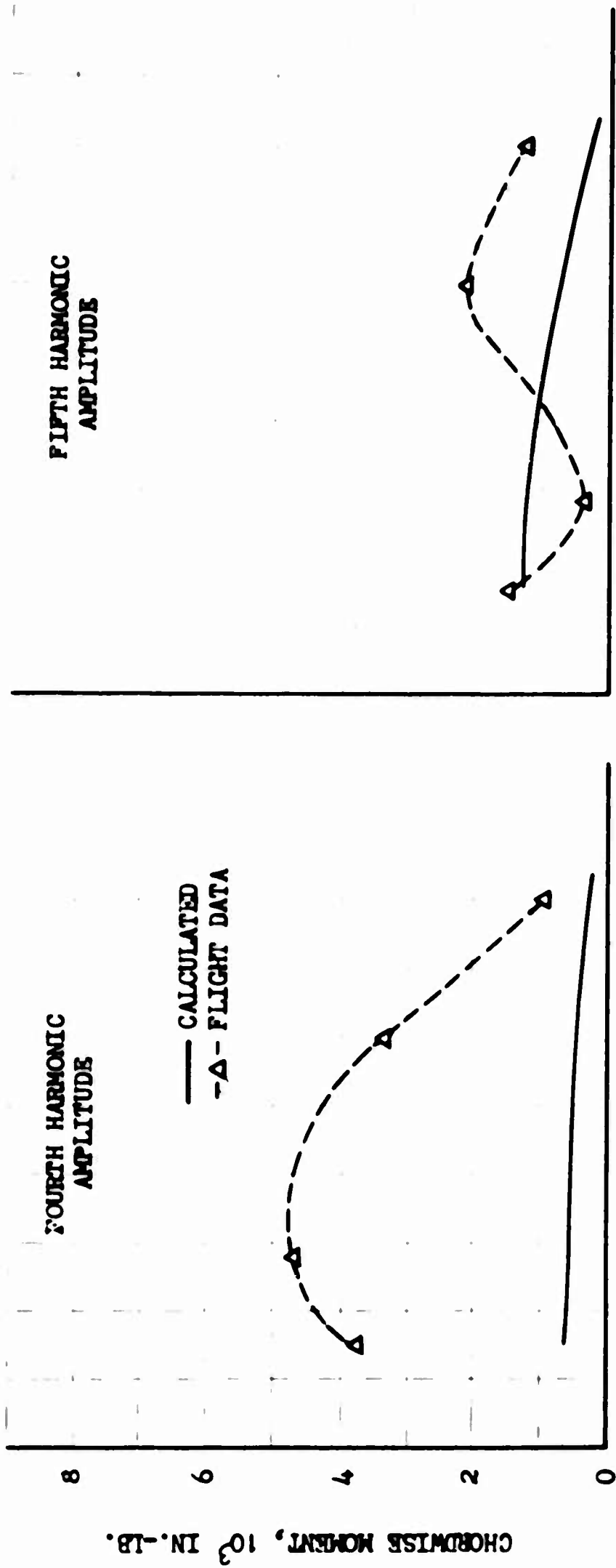
FIGURE 45. CASE 5: HU-1A CHORDWISE MOMENTS AT 113 KNOTS

DOCUMENT CONTROL DATA - R&D

(Security classification of title, body of abstract and indexing annotation must be entered when the overall report is classified)

1 ORIGINATING ACTIVITY *(Corporate author)*	2a REPORT SECURITY CLASSIFICATION
SIKORSKY AIRCRAFT DIVISION UNITED AIRCRAFT CORPORATION STRATFORD, CONNECTICUT	UNCLASSIFIED
	2b GROUP

3 REPORT TITLE

ANALYSIS AND CORRELATION OF HELICOPTER ROTOR BLADE RESPONSE IN A VARIABLE INFLOW ENVIRONMENT

4 DESCRIPTIVE NOTES *(Type of report and inclusive dates)*

FINAL

5 AUTHOR(S) *(Last name, first name, initial)*

CARLSON, RAYMOND G.
HILZINGER, KURT, D.

6 REPORT DATE	7a TOTAL NO OF PAGES	7b NO OF REFS
SEPTEMBER 1965	109	12

8a CONTRACT OR GRANT NO	9a ORIGINATOR'S REPORT NUMBER(S)
DA 44-177-AMC-87(t)	
b PROJECT NO	USAAVLABS Technical Report 65-51
c Task No. 1D121401A142	9b OTHER REPORT NO(S) *(Any other numbers that may be assigned this report)*
d	Ser-50405

10 AVAILABILITY LIMITATION NOTICES

Qualified requesters may obtain copies of this report from DDC. This report has been furnished to the Department of Commerce for sale to the public.

11 SUPPLEMENTARY NOTES	12 SPONSORING MILITARY ACTIVITY
	U.S. ARMY AVIATION MATERIEL LABORATORIES FORT EUSTIS, VIRGINIA

13 ABSTRACT

This program was conducted to determine the ability to predict Helicopter rotor response with a combined analysis based on the Sikorsky aeroelastic analysis and the Cornell Aeronautical Laboratory variable inflow analysis.

The Sikorsky analysis is a fully coupled flatwise-edgewise-torsional dynamic analysis modified to incorporate refinements in rotor trim and airload calculation and to adapt it for use with the variable inflow analysis. Analytical results were compared with available flight data for steady level flight of the H-34 at 41, 70, and 112 knots with a neutral center of gravity (C.G.), and 73 knots with aft C.G., as well as the HU-1A at 113 knots with neutral C.G. Fairly good correlation with test data was obtained. The analysis gave better correlation of blade air loads and bending moments than had been obtained from constant inflow analysis. In particular, more realistic values were obtained for the higher harmonic root-shear forces needed to define airframe response. While further improvement can be obtained by refinement of the variable inflow analysis, the combined analysis developed for this program provides an improved design tool for rotor blade evaluation.

DD FORM 1473

KEY WORDS	LINK A		LINK B		LINK C	
	ROLE	WT	ROLE	WT	ROLE	WT
1. Helicopter Rotors-Structural Analysis 2. Helicopter Rotors-Aerodynamic Characteristics						

INSTRUCTIONS

1. ORIGINATING ACTIVITY. Enter the name and address of the contractor, subcontractor, grantee, Department of Defense activity or other organization (corporate author) issuing the report.

2a. REPORT SECURITY CLASSIFICATION: Enter the overall security classification of the report. Indicate whether "Restricted Data" is included. Marking is to be in accordance with appropriate security regulations.

2b. GROUP: Automatic downgrading is specified in DoD Directive 5200.10 and Armed Forces Industrial Manual. Enter the group number. Also, when applicable, show that optional markings have been used for Group 3 and Group 4 as authorized.

3. REPORT TITLE. Enter the complete report title in all capital letters. Titles in all cases should be unclassified. If a meaningful title cannot be selected without classification, show title classification in all capitals in parenthesis immediately following the title.

4. DESCRIPTIVE NOTES: If appropriate, enter the type of report, e.g., interim, progress, summary, annual, or final. Give the inclusive dates when a specific reporting period is covered.

5. AUTHOR(S): Enter the name(s) of author(s) as shown on or in the report. Enter last name, first name, middle initial. If military, show rank and branch of service. The name of the principal author is an absolute minimum requirement.

6. REPORT DATE: Enter the date of the report as day, month, year, or month, year. If more than one date appears on the report, use date of publication.

7a. TOTAL NUMBER OF PAGES: The total page count should follow normal pagination procedures, i.e., enter the number of pages containing information.

7b. NUMBER OF REFERENCES: Enter the total number of references cited in the report.

8a. CONTRACT OR GRANT NUMBER: If appropriate, enter the applicable number of the contract or grant under which the report was written.

8b, 8c, & 8d. PROJECT NUMBER: Enter the appropriate military department identification, such as project number, subproject number, system numbers, task number, etc.

9a. ORIGINATOR'S REPORT NUMBER(S): Enter the official report number by which the document will be identified and controlled by the originating activity. This number must be unique to this report.

9b. OTHER REPORT NUMBER(S): If the report has been assigned any other report numbers (either by the originator or by the sponsor), also enter this number(s).

10. AVAILABILITY/LIMITATION NOTICES: Enter any limitations on further dissemination of the report, other than those imposed by security classification, using standard statements such as:

(1) "Qualified requesters may obtain copies of this report from DDC."

(2) "Foreign announcement and dissemination of this report by DDC is not authorized."

(3) "U. S. Government agencies may obtain copies of this report directly from DDC. Other qualified DDC users shall request through

_____."

(4) "U. S. military agencies may obtain copies of this report directly from DDC. Other qualified users shall request through

_____."

(5) "All distribution of this report is controlled. Qualified DDC users shall request through

_____."

If the report has been furnished to the Office of Technical Services, Department of Commerce, for sale to the public, indicate this fact and enter the price, if known.

11. SUPPLEMENTARY NOTES: Use for additional explanatory notes.

12. SPONSORING MILITARY ACTIVITY: Enter the name of the departmental project office or laboratory sponsoring (paying for) the research and development. Include address.

13. ABSTRACT: Enter an abstract giving a brief and factual summary of the document indicative of the report, even though it may also appear elsewhere in the body of the technical report. If additional space is required, a continuation sheet shall be attached.

It is highly desirable that the abstract of classified reports be unclassified. Each paragraph of the abstract shall end with an indication of the military security classification of the information in the paragraph, represented as (TS), (S), (C), or (U).

There is no limitation on the length of the abstract. However, the suggested length is from 150 to 225 words.

14. KEY WORDS: Key words are technically meaningful terms or short phrases that characterize a report and may be used as index entries for cataloging the report. Key words must be selected so that no security classification is required. Identifiers, such as equipment model designation, trade name, military project code name, geographic location, may be used as key words but will be followed by an indication of technical context. The assignment of links, rules, and weights is optional.